

RECENT ADVANCES IN VALORIZATION METHODS OF INORGANIC/ORGANIC SOLID, LIQUID, AND GAS WASTES

GUEST EDITORS: LICÍNIO M. GANDO-FERREIRA, FAÏÇAL LARACHI,
AND SANTIAGO ESPLUGAS





Recent Advances in Valorization Methods of Inorganic/Organic Solid, Liquid, and Gas Wastes

International Journal of Chemical Engineering

**Recent Advances in Valorization Methods of
Inorganic/Organic Solid, Liquid, and Gas Wastes**

Guest Editors: Licínio M. Gando-Ferreira, Faïçal Larachi,
and Santiago Esplugas



Copyright © 2012 Hindawi Publishing Corporation. All rights reserved.

This is a special issue published in “International Journal of Chemical Engineering.” All articles are open access articles distributed under the Creative Commons Attribution License, which permits unrestricted use, distribution, and reproduction in any medium, provided the original work is properly cited.

Editorial Board

Muthanna Al-Dahhan, USA
Miguel J. Bagajewicz, USA
Alfons Baiker, Switzerland
Jerzy Bądryga, Poland
Mostafa Barigou, United Kingdom
Gino Baron, Belgium
Hans-Jörg Bart, Germany
Raghunath V. Chaudhari, USA
Jean-Pierre Corriou, France
Donald L. Feke, USA
James J. Feng, Canada
Rafiqul Gani, Denmark
Jinlong Gong, China
Thomas R. Hanley, USA
Michael Harris, USA

Kus Hidajat, Singapore
Vladimir Hlavacek, USA
Xijun Hu, Hong Kong
M. G. Ierapetritou, USA
Dilhan M. Kalyon, USA
Kyung Aih Kang, USA
Iftekhar A. Karimi, Singapore
B. D. Kulkarni, India
Deepak Kunzru, India
Janez Levec, Slovenia
Jose C. Merchuk, Israel
Badie I. Morsi, USA
S. Murad, USA
Dmitry Murzin, Finland
Ahmet N. Palazoglu, USA

Fernando T. Pinho, Portugal
Peter N. Pintauro, USA
Doraiswami Ramkrishna, USA
Alírio Rodrigues, Portugal
Jose Alberto Romagnoli, USA
Adrian Schumpe, Germany
Moshe Sheintuch, Israel
Katsumi Tochigi, Japan
Evangelos Tsotsas, Germany
Toshinori Tsuru, Japan
Tapio Westerlund, Finland
Jaime Wisniak, Israel
King Lun Yeung, Hong Kong
Zhibing Zhang, United Kingdom

Contents

Recent Advances in Valorization Methods of Inorganic/Organic Solid, Liquid, and Gas Wastes,
Licínio M. Gando-Ferreira, Faïçal Larachi, and Santiago Esplugas
Volume 2012, Article ID 594683, 2 pages

High-Added Value Materials Production from OMW: A Technical and Economical Optimization,
E. C. Arvaniti, D. P. Zagklis, V. G. Papadakis, and C. A. Paraskeva
Volume 2012, Article ID 607219, 7 pages

Titanium Dioxide-Mediated Photocatalysed Degradation of Two Herbicide Derivatives Chloridazon and Metribuzin in Aqueous Suspensions, A. Khan, N. A. Mir, M. Faisal, and M. Muneer
Volume 2012, Article ID 850468, 8 pages

Valorization of Agroindustrial Wastes as Biosorbent for the Removal of Textile Dyes from Aqueous Solutions, Elsa Contreras, Luisa Sepúlveda, and Carolyn Palma
Volume 2012, Article ID 679352, 9 pages

Utilization of Agrowaste Polymers in PVC/NBR Alloys: Tensile, Thermal, and Morphological Properties,
Ahmad Mousa, Gert Heinrich, Bernd Kretzschmar, Udo Wagenknecht, and Amit Das
Volume 2012, Article ID 121496, 5 pages

Application of Chemically Modified and Unmodified Waste Biological Sorbents in Treatment of Wastewater, John Kanayochukwu Nduka
Volume 2012, Article ID 751240, 7 pages

Biofuels Production from Biomass by Thermochemical Conversion Technologies, M. Verma, S. Godbout, S. K. Brar, O. Solomatnikova, S. P. Lemay, and J. P. Larouche
Volume 2012, Article ID 542426, 18 pages

Use of Iron (II) Salts and Complexes for the Production of Soil Amendments from Organic Solid Wastes,
Amerigo Beneduci, Ilaria Costa, and Giuseppe Chidichimo
Volume 2012, Article ID 701728, 9 pages

Degradation of Abamectin Using the Photo-Fenton Process, Thiago Augusto de Freitas Matos, Alexandra Lemos Nunes Dias, Amanda Di Piazza Reis, Milady Renata Apolinário da Silva, and Márcia Matiko Kondo
Volume 2012, Article ID 915724, 7 pages

Editorial

Recent Advances in Valorization Methods of Inorganic/Organic Solid, Liquid, and Gas Wastes

Licínio M. Gando-Ferreira,¹ Faïçal Larachi,² and Santiago Esplugas³

¹ Department of Chemical Engineering, University of Coimbra, Silvio Lima street, 3030-790 Coimbra, Portugal

² Department of Chemical Engineering, Laval University, 1065 la Médecine Avenue, Québec, QC, Canada G1V 0A6

³ Departamento d'Enginyeria Química, Universitat de Barcelona, Martí i Franques 1, 08028 Barcelona, Spain

Correspondence should be addressed to Licínio M. Gando-Ferreira, lferreira@eq.uc.pt

Received 2 April 2012; Accepted 8 April 2012

Copyright © 2012 Licínio M. Gando-Ferreira et al. This is an open access article distributed under the Creative Commons Attribution License, which permits unrestricted use, distribution, and reproduction in any medium, provided the original work is properly cited.

The main goal of this special issue was to gather contributions dealing with the latest breakthrough methods for providing value compounds and energy/fuel from waste valorization. Valorization is a relatively new approach in the area of industrial wastes management, a key issue to promote sustainable development. In this field, the recovery of value-added substances, such as antioxidants, proteins, vitamins, and so forth, from the processing of agroindustrial byproducts, is worth mentioning. Another important valorization approach is the use of biogas from waste treatment plants for the production of energy. Several approaches involving physical and chemical processes, thermal and biological processes that ensure reduced emissions and energy consumptions were taken into account. The papers selected for this topical issue represent some of the mostly researched methods that currently promote the valorization of wastes to energy and useful materials. As such, they provide interesting and timely research results in that field that we have the pleasure to share with the readers. We would like to thank all the authors for submitting their nice papers and all the referees for their excellent feedback.

This special issue includes eight papers, where one paper is related to the production of energy from biomass, and four papers cover application of advanced oxidation processes and of biological sorbents for the treatment of wastewaters. One paper addresses the rapid stabilization of organic wastes during the composting process and another utilization of agrowastes for preparation of PCV-based composites. Finally, one paper presents a technoeconomic analysis for production of value-added compounds from wastewaters.

In the paper entitled “*Biofuels production from biomass by thermochemical conversion technologies*,” Verma et al. presents a brief review on various available technologies for thermochemical conversion of biomass into biofuels that can be used as alternatives to fossil fuels. Some advantages of utilizing biomass pyrolysis for production of sustainable energy in comparison to combustion and gasification are also reported in this paper.

In the paper “*Titanium dioxide-mediated photocatalysed degradation of two herbicide derivatives chloridazon and metribuzin in aqueous suspensions*,” Khan et al. propose the advanced oxidation process with TiO₂ photocatalyst for the degradation/mineralization of two herbicides in aqueous suspensions. They demonstrate that in the case of CHL the highest degradation efficiency is achieved at pH 3.2, whereas for MET better degradation conditions are attained under alkaline conditions.

In the work entitled “*Degradation of abamectin using the photo-fenton process*,” Thiago et al. investigate the application of photo-Fenton process for the degradation of abamectin that is the active principle of one of most commonly used pesticides in the cultivation of strawberries. Their experiments showed that 70% of the initial load of the compound existent in water samples is removed after 60 minutes of UV radiation.

In the paper “*Utilization of agrowaste polymers in pvc/nbr alloys: tensile, thermal, and morphological properties*,” Ahmad et al. examine tensile properties of poly(vinyl chloride)-PVC/nitrile butadiene-NBR formulations with wood flour (WF), a natural byproduct from olive oil extraction industry.

They concluded that WF loading improves the tensile modulus of the blend, whereas the tensile strength is kept approximately constant.

The research of Nduka entitled "*Application of chemically modified and unmodified waste biological sorbents in treatment of wastewater*" focuses on the removal of pollutants of the textile industry and heavy metals contained in wastewaters using protein and cellulosic wastes. He presents high efficiencies in the detoxification of wastewater as dependent on the particle size of cellulosic waste sorbents and contact time.

In the paper "*Valorization of agroindustrial wastes as biosorbent for the removal of textile dyes from aqueous solutions*," Contreras et al. study the technical feasibility of using agroindustrial wastes for adsorption of dyes. Their results based on equilibrium isotherms and kinetic tests have shown that those biosorbents have significant potential for removal of basic dyes from aqueous solutions.

In the paper "*Use of iron (II) salts and complexes for the production of soil amendments from organic solid wastes*," Beneduci et al. propose the use of iron (II) ions in the oxidative decomposition process of solid wastes. It was demonstrated that these ions significantly enhance the extent of the oxidation process as evaluated from the value C/N ratio.

In the paper entitled "*High-added value materials production from OMW: A technical economical optimization*," Arvaniti et al. present a technoeconomic analysis for the treatment of olive mill wastewater (OMW) using the integration of membranes processes, namely, ultrafiltration, nanofiltration and reverse osmosis. They have shown that the utilization of isolated OMW fractions in fertilizers or in ecological herbicides can depreciate the total cost for a period of approximately five years.

Acknowledgment

The guest editors are also sincerely thankful to the editorial staff for the support, guidance, and efforts in welcoming this series of papers on a timely subject.

Licínio M. Gando-Ferreira
Faïçal Larachi
Santiago Esplugas

Research Article

High-Added Value Materials Production from OMW: A Technical and Economical Optimization

E. C. Arvaniti,^{1,2} D. P. Zagklis,^{1,2} V. G. Papadakis,³ and C. A. Paraskeva^{1,2}

¹ Institute of Chemical Engineering and High Temperature Chemical Processes, Foundation for Research and Technology-Hellas (FORTH/ICE-HT), Stadiou Street, Platani, 26504 Patras, Greece

² Department of Chemical Engineering, University of Patras, 26504 Patras, Greece

³ Department of Environmental & Natural Resources Management, University of Western Greece, 30100 Agrinio, Greece

Correspondence should be addressed to C. A. Paraskeva, takisp@chemeng.upatras.gr

Received 17 October 2011; Revised 3 February 2012; Accepted 6 February 2012

Academic Editor: Licínio M. Gando-Ferreira

Copyright © 2012 E. C. Arvaniti et al. This is an open access article distributed under the Creative Commons Attribution License, which permits unrestricted use, distribution, and reproduction in any medium, provided the original work is properly cited.

The extraction of olive oil generates huge quantities of solids and of high organic wastewaters with toxic constituents that have a great impact on land and water environments. Based on a membrane process, authors proposed an alternative method for treatment of olive mill wastewaters (OMWs). In the present paper, a technoeconomic analysis for the implementation of the proposed method in the entire Region of Western Greece (RWG) is presented. This paper takes into account fixed and operational costs, costs for the infrastructure, equipment, land, maintenance, and so forth, considering the treatment of 50,000 tons per harvesting period in the area of RWG. The study showed that the establishment of only one central treatment manufacture could reduce the uncontrolled disposal of OMW. Exploitation of the isolated fractions as manure in fertilizers (nutrients components) or as components in ecological herbicides (phenolics) can depreciate the total cost in a period of about five years.

1. Introduction

Olive oil production has roughly increased worldwide in the last decades. Mediterranean countries produce 95% of the total world production of olive oil [1]. The largest producers of olive oil are Spain (42% of world production in 2007), Italy (19%), and Greece (13%), followed by Tunisia, Syria, Morocco and Turkey [1]. This makes olive oil extraction an agroindustrial activity of vital economic significance to many Mediterranean countries.

Despite the economic benefit, olive oil production is unfortunately associated with the generation of large quantities of wastewaters (olive mill wastewater—OMW) [2] and solid wastes, whose management, treatment, and safe disposal raise serious environmental concerns. A typical olive mill is currently producing on the average some 1,000 metric tons of toxic liquid wastes per harvesting season [3]. Olive mill wastewater (OMW) is a mixture of nutritious agents appropriate for fertilizing or animal feed (inorganic salts, proteins, fat substances, etc.), as well as phenolics, tannins, and other substances with phytotoxic action. The characteristic properties of OMW include its dark color, characteristic

odor, acidic pH, and high organic content mainly composed of classes of pollutants such as phenolics that may exhibit antimicrobial, ecotoxic, and phytotoxic properties [4, 5]. The BOD (biochemical oxygen demand) and COD (chemical oxygen demand) of these wastewaters are such that the environmental damage from each olive mill is serious in touristic and agricultural Mediterranean regions. Due to the high organic load of OMW, it may contribute significantly to eutrophication of recipients in which fluid exchange rates are low (closed gulfs, estuaries, lakes, etc.) [6–8]. An additional adverse impact of OMW on the environment is the aesthetic degradation caused by its strong odour and dark coloration. Problems arise also from the fact that olive oil production is seasonal, and so the treatment process should be flexible enough to operate in a noncontinuous mode; otherwise storage of the wastewater will be required [9]. Moreover, the olive mills are small enterprises, mostly family businesses, scattered around the olive production areas, making individual on-site treatment options unaffordable. Therefore, it is not surprising that OMW treatment has received enormous attention over the past several years, and various

decontamination technologies based on biological, advanced oxidation, chemical and separation processes have been proposed by several research groups as summarized in a recent review article [10].

OMW composition depends significantly on the olive type and the treatment procedure. Thus, it may be different from one region to another and among the olive mills of the same region. In general, these wastewaters contain the largest fraction of water-soluble components of olives, solid organics, and fats and lipids. The majority of olive oil mills in Greece use the three-phase decanter systems that produce huge quantities of liquid wastes. The solids (olive kernels) are sold to olive core companies to produce the well-known olive core oil which is of less nutritious value. The liquid OMW is produced by the liquid fraction of the olive juice and the water used during the different phases of olive mill processing. Essentially, it is an aqueous vegetable extract, containing a number of substances such as sugars, nitrogenous compounds, organic acids, polyalcohols, polyphenols, and oil residue.

It should be noted that the production of olive oil is a natural process, and thus the olive mill wastewater does not contain other substances that are highly toxic, such as heavy metals and synthetic organic compounds. The phenolic components are the various phenolic acids (caffeic, protocatechuic, α -hydroxycinnamic, vanillic), flavonoids, anthocyanes, and seleeprotein. Phenolics and tannins are the main components with phytotoxic action. The main components with nutritious value are hydrocarbons, inorganic salts, and so forth, depending on the application (animal feed or fertilizers).

A combination of appropriate physicochemical processes can be applied for the fractionation of the wastes into useful isolated by-products as fertilizers, herbicides, and so forth. It must be added that almost in the same season of olive harvest, the farmers spray the land under the olive trees with herbicides for weed control. These strong chemicals affect the environment negatively, putting in high risk the health of the farmers; they are also accumulated and may be introduced in the food chain. On the contrary, the development of an environmentally friendly herbicide as a fraction from OMW will offer an ecological solution to this severe problem. Thus, two targets could be achieved simultaneously; a sustainable solution for the disposal of olive mill wastes and the production of alternative ecological herbicides and other useful by-products.

Coping with the environmental pollution problem, created by wastes from olive mills, presents large difficulties, mainly due to the high cost of the treatment of residual waters using the various systems proposed so far. In recent years, only in Italy more than 100 companies have proposed relevant systems, but none of them constitutes a practical and low-priced solution to the problem. Thus, the present situation is more or less the same as in the past: these wastes are led to large pits or discharged into the sea, lakes, rivers, and so forth, causing destructive environmental implications. As the fixed cost for installing such systems seems not decreasing, a profit from possible useful by-products could contribute

significantly to the problem solution. The present work is oriented to this direction.

The management of OMW has been extensively investigated, and some extensive and detailed reviews, which focus mainly on its management, have been recently published [10–12]. Provided that the fixed cost for the installation of OMW treatment systems seems to be in-elastic, operational cost reduction may be attained through the exploitation of the waste by-products. The proposed separation techniques (prefiltration (filter press), ultrafiltration (UF), nanofiltration (NF), and reverse osmosis (RO)) of the OMW treatment using membranes filtration have already been presented in previous works by the authors [3, 13]. The idea is based on the exploitation of membrane filtration fractions to reduce the high fixed costs in order for a viable and sustainable solution to be obtained. In those studies a pilot plant was developed in an olive mill (1,000 t/yr) operating in Achaia region (Patras, Greece) during a full harvesting period [3, 13], and a technoeconomical solution was presented for the implementation of the proposed method in each olive mill enterprise. However, private olive mills are small family businesses and cannot afford the costs of the treatment of their own wastewaters. Thus, in the present study three new options were taken into account. The first refers to the creation of an OMW treatment unit in every 5–6 adjacent olive mills, and the second refers to the development of a mobile unit that can pass across the olive mill units to treat their wastes. The third proposed method, which sounds interesting for the local olive mill industry, was the development of a central unit (50,000 t/yr) which can handle all olive mill wastewaters from all olive mills, in the prefecture of Achaia. The last idea was evaluated as a successful solution and can be applied also in other areas, which face the same environmental problems. The feasibility-exploitation study for the third suggested method is presented in detail and shows that indeed the depreciation of the expensive investment can be done in a short period of time.

2. Proposed Method

Ultrafiltration (UF), nanofiltration (NF), and/or reverse osmosis (RO) (Figure 1) can be used for isolation of OMW fractions. These methods were investigated in previous work [3, 13] through a systematic parametric study changing accordingly the operational parameters, such as temperature, pressure, and initial pH of different source of OMW, type and size of membranes (pore diameter), and so forth, in order to obtain a higher separation of toxic fraction from the nutritious one. Different fractions were derived from the entire process: a nutritious fraction as pre- or post UF concentrate containing the larger components of the solution in terms of molecular size, a toxic fraction as NF and/or RO concentrate containing the main part of phenolics (ecological herbicide), a plant nutritious fraction as RO permeate containing the inorganic salts (fertilizer), and almost pure water for recycling/irrigation or for free disposal to aqueous acceptors (lakes, rivers, or sea).

One thing that is of primary importance is that UF provides a “clean” solution appropriate to feed next treatment

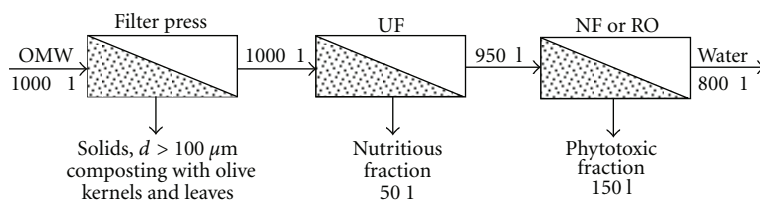


FIGURE 1: Separation structure of the flowsheet using ultrafiltration (UF), nanofiltration (NF), and/or reverse osmosis (RO) techniques.

TABLE 1: Physicochemical characterization of fractions of the various treatment stages.

Parameter	Raw	Perm prefilter = feed UF	Ultrafiltration		Nanofiltration		Reverse osmosis	
			Conc	Perm = feed NF	Conc	Perm = feed RO2	Conc	Perm
Salinity, %	0.66	0.66	0.67	0.59	1.11	0.01	0.02	0.0
TSS, g/L	21.5	18.56	46.98	2.36	5.32	0	0.0	0.0
t-COD, g/L	97.32	92.9	127.19	94.88	156.44	1	9.1	0.2
d-COD, g/L	85.68	72.24	61.92	77.64	131.32	1	7.56	0.16
Carbohydrates, g/L	28.75	20.51	18.8	24.1	51.827	0.310	3.2	0.1
Phenolics, g/L	5.91	5.08	4.16	5.04	10.6	0.1	0.9	0.01

processes (NF or RO). UF alone cannot isolate individual fractions (in terms of only toxic or only nutrient solutions) but without UF we cannot proceed for further purification with the NF and/or RO. Physicochemical analysis of the collected compounds in pretreatment procedure, ultrafiltration, nanofiltration, and reverse osmosis, is shown in Table 1. The permeate stream from each unit is used as feed stream for the next membrane unit. Treatment can be terminated after the implication of NF or RO since the permeate stream of NF (see Table 1) shows that the produced water can be safely used as irrigation water or to be disposed safely to aqueous receptors.

3. Technoeconomical Analysis

3.1. Proposed Technical Solution. Based on the suggested methods that should be followed for the efficient separation of the “nutritious” from the “toxic” fraction, an optimum, technical, and economical design of the process at industrial level was carried out. The target is a technically acceptable solution at the possible lowest fixed and operational cost. This goal was succeeded by applying a conceptual design to find the best process and estimate the optimum design conditions. After definition of the operational parameters, the process flowchart was constructed via a hierarchy of design decisions, namely, structure of input-output, recycling, separation, and thermal integration [3].

3.2. Preliminary Design. The technoeconomical study for the establishment of OMW treatment plant was done for the Region of Western Greece. The number of all olive mills for three regions (prefectures of Achaia, Ilia, Aitolokarnania) was recorded. There were three alternative scenarios: (a) the establishment of a central operation plant (e.g., one per region or a greater area), where OMW would be carried by

trucks. Profit will be made by the production of high-valued by-products. (b) The second was the establishment of more than one lower potential operation plants (one per five olive mills). In this case the transport expenses are diminished. (c) The third was a mobile OMW treatment unit.

The third case was rejected as olive mills work seasonally in the same period, and this constitutes several technical complications (size of the tanks on the truck, disposal of concentrated fractions, etc.). Therefore, the study was concentrated on the other two solutions. Taking into account the location, the distance and the number of olive mills per region, the cost and the time of transportation, the establishment of a central OMW treatment plant per region was considered to be more appropriate from both technical and economical point of view.

The most serious problems that could be faced are (a) the authorities permission for disposal and sale of by-products from the above OMW treatment that may be used as ecological herbicides and fertilizers for agriculture and (b) the possible denial of olive mills owners to bear the cost of their OMW storage, despite the fact that they are obliged to perform a kind of treatment.

Four actions took place (a) The first one was mapping of the olive mills that are active in Achaia and Ilia regions as first indicative areas, preliminary study of the cost and transferring time of OMW in a central place per region (e.g., Patras Industrial Area). (b) The second was examination of the legal framework that concerns the approval and sale of ecological herbicides and fertilizers for agriculture in Greek and European market. (c) The third was examination of the market demand for ecological herbicides and fertilizers for agriculture in the trade union and end users. (d) The last one was the examination of the use of OMW components for the production of biodiesel, bioplastic, or other alternative products of high value.

3.3. Case Study: Region of Western Greece. Region of Western Greece is the suggested area for the establishment of OMW pilot plant. It is an area with a tradition in olive oil production. Furthermore, Achaia is adjoining to several olive oil production areas. There are 50 active olive mills in Achaia and surroundings. Taking into account the distances among olive mills, the transportation costs (fuel and service expenses) are estimated to 0.25 €/km. All the olive mills are gathered close to Patras Industrial Area. There are available areas and the necessary infrastructures for the establishment of an OMW treatment unit. Investments incentives and tax reductions have been given to the Patras Industrial Area for the industrial development in Achaia, which increases depreciation of the investment. Therefore, the establishment of a central plant in the Industrial Area of Patras is suggested in the present work.

3.4. Capacity and Settlement of Production Process. The OMW treatment unit is designed to operate continuously 24 h/day, 7 days/week, 7 months/yr (period during oil production from October till April), 210 days/yr. The unit would have a capacity over 50,000 t/yr and will serve a number of about 50 olive mills of the surrounded area (an average production of 1,000 t/yr OMW per olive mill will give an average capacity of the unit which arises up to 50,000 tn/yr).

The technoeconomical study for the establishment of an OMW treatment unit has the following approximate characteristics:

- feed to the system: OMW,
- feed flow rate: 10,000 L/h (50,000 t/yr),
- permeate flow rate: 8,000 L/h,
- working temperature: 20–30 °C,
- working pressure: UF: 4 bar, RO: 70 bar max,
- COD removal: 99.5%,
- grease substances removal: 99.99%,
- dry matter removal: 99.5%,
- UF system:* feed pump, protective cartridge filter, loop pump, ceramic elements, structure, valves and piping, electrical part,
- RO system:* feed pump, protective cartridge filter, high pressure pump, filtering elements, structure, valves and piping, electrical part,
- utilities,*
 - air: 5/6 bar,
 - Water for membrane cleaning: demineralized/soft or osmotized,
 - power supply: 380 V, 50 Hz, three phases.

3.5. Fixed Cost and Initial Operating Capital. The establishment of an industrial unit demands costs for the designing study, for the building site purchasing and its modulation, for the purchasing and establishment of the equipment, and so forth. Cost for UF and RO systems, installed on site, feed tanks, any storage or peripheral tanks, prefilter system,

pumps and piping, hydraulic, electrical, and pneumatic connections, computers, vehicles, lab and office equipment, security equipment, offices, laboratories, storehouse and auxiliary equipment, land, and so forth are presented in Table 2. The method for ratio capacity units [14] has been used to estimate the fixed cost, initial networking capital, and investment capital. This method is based on the equation:

$$C_2 = C_1 \cdot \left(\frac{Q_2}{Q_1} \right)^n, \quad (1)$$

where Q_1 , Q_2 : capacity, C_1 : fixed cost for Q_1 , C_2 : fixed cost for Q_2 , and n parameter. For chemical industry exponent n is equal to 2/3, and the method is called method of 2/3.

A cost for the biodynamic experiments is calculated and included in the fixed cost. These experiments are needed for the investigation of the impact that produced herbicides, fertilizers, and water have on the human health.

3.6. Operational Cost. The operational cost (€/yr) includes a number of elements that are given in Table 3. In the same table information is given for the approximation of the cost of some of the elements in operational cost using coefficients. It is important to mention that when the taxes are negative (in the present case below 2,800 t/yr), the operational cost before taxes (OC') (Table 3) is taken into account. For the capacity of 50,000 t/yr, labor cost is about 28.79% of the operational cost and is the maximum percentage while the cost for the raw material (OMW) is zero. This percentage changes according to the capacity. Thus, if the capacity changes from 50,000 t/yr to 2,800 t/yr, then the depreciation cost reaches 5% of the operational cost while the labor cost drops at 4.29% of the operational cost. In any case the cost of OMW is zero because mill owners like to get rid of them. Furthermore, an income is more possible to arise from the OMW if the owners of the olive mill need to treat their wastes before disposing them to the soil; in order to avoid a penalty from the authorities.

A cost benefit analysis is presented in Figures 2 and 3 for two different capacities. Figure 4 shows the revenues of the investment for a capacity of 50,000 t/yr, which exhibits operational cost. On the other hand when the unit works with a capacity of 1000 t/yr, the operational cost is much higher than the revenues of the investment. Each element of the operational cost is changing according to the capacity changes. It has been calculated that in a capacity of 2,800 t/yr the revenues of the investment are equal to the operational cost.

4. Economical Potential: Assessment of the Investment

A production of 5% nutrition fraction which can be used as fertilizer and 15% of toxic fraction that can be used as herbicide can be expected. The rest is pure water which can be used for recycling and irrigation.

The value of the nutritious fraction, taking into account its concentration in nutritious components, (either as fertilizer or as animal feed integrator) is estimated to have an order of magnitude of 100 €/t UF concentrate that gives 250,000 €/yr (data from AGRO). The value of the

TABLE 2: Equipment, building, and operational costs for an OMW treatment unit of 50,000 t/yr capacity. Calculations of the fixed cost, initial networking capital cost, and investment capital cost in Euros.

Equipment for capacity Q1 = 50,000 t OMW/yr	Euro
Purchase and establishment of basic equipment (UF and RO units, mechanical and electrical parts, etc.)	1,000,000 €
Auxiliary settlement, environmental protection system, and equipment maintenance department (lifetime: 10 years)	78,000 €
Substation (lifetime: 15 years)	30,000 €
Quality control laboratory equipment (lifetime: 10 years)	21,000 €
Transportation unit and equipment store (lifetime: 10 years)	46,000 €
2 loading machines, clarks (lifetime: 10 years)	30,000 €
5 vehicles for OMW collection—product shell (lifetime: 10 years)	105,000 €
Safety equipment clothing (lifetime: 2 years)	5,000 €
Office equipment, PC, and furniture (lifetime: 10 years)	30,000 €
Total purchase and installation cost, CE1	1,345,000 €
Buildings cost	
Offices, laboratory, storage and building equipment	240,000 €
Fencing	5,000 €
Building site	100,000 €
Building total (depreciation in 25 years apart from building site)	345,000 €
General total (CE1 + building total)	1,690,000 €
Unexpectedly (10% direct cost)	169,000 €
Fixed cost, C_1 (general total + unexpectedly)	1,859,000 €
Biodynamic experiments, C_2	1,000,000 €
Total fixed cost, $C [C_1 + C_2]$	2,859,000 €
Initial networking capital cost, IC [$0.18 * C$]	334,620 €
Investment capital cost [$C + IC$]	3,193,620 €

TABLE 3: Operational costs for an OMW treatment unit of 50,000 t/yr capacity.

Operational cost	Euro/yr
(1) Feedstock, cleaning chemicals (114 €/day)	30,200 €
(2) Energy (UF: 260 kW, RO: 90 kW) (29.7 €/hr)	149,700 €
(3) Labor costs	329,000 €
(4) Maintenance ($0.05 * C$)	67,250 €
(5) Administration costs (usually 50% labor costs)	274,000 €
(6) Insurance (establishment and products) [$1\% * C$]	13,450 €
(7) Depreciation (linear depreciation zero residual value)	148,300 €
(8) Interest [$0.05 * C$]	67,250 €
(9) General costs	63,750 €
Operational cost before taxes (OC')	1,142,900 €
(10) Taxes (T) [$0.4 * (R-OC')$]	392,840 €
Operational cost after taxes (OC'')	1,535,740 €

“toxic fraction” as herbicide is estimated as much higher (data from AGRO), due to the higher value of phytotoxic constituents (herbicides) in the market. Taking into account the concentration of the RO concentrate, a modest value

of 250 €/t RO concentrate is estimated that gives about 1,875,000 €/yr.

Thus, an economical potential of 2,125,000 €/yr is expected annually if the capacity is 50,000 t/yr. Taking into account that taxes are 40%, a net profit of 589,260 €/yr is estimated. From the above analysis, the rate of return on investment, i_r , is estimated:

$$i_r = \frac{K}{(C + IC)}, \quad (2)$$

where K : the annual net profit, C : total fixed cost, and IC : the initial working capital. Between two or more alternative investments the one with the highest i_r will be chosen. When an investment is examined separately, the i_r of the investment should be higher than a minimum acceptable rate of return that has been determined by the company (possibly the bank interest). This method does not take into account the time value of money.

Thus, $i_r = 589,260 / (2,859,000 € + 334,620 €) \times 100\% = 18\%$.

In Figure 4 the return of the investment has been plotted as a function of the capacity. As it can be seen from the diagram the capacity that the i_r is zero is 2,800 t/yr, and this is the breakeven point of the investment. This capacity corresponds to wastes from 2-3 typical olive mills, and thus

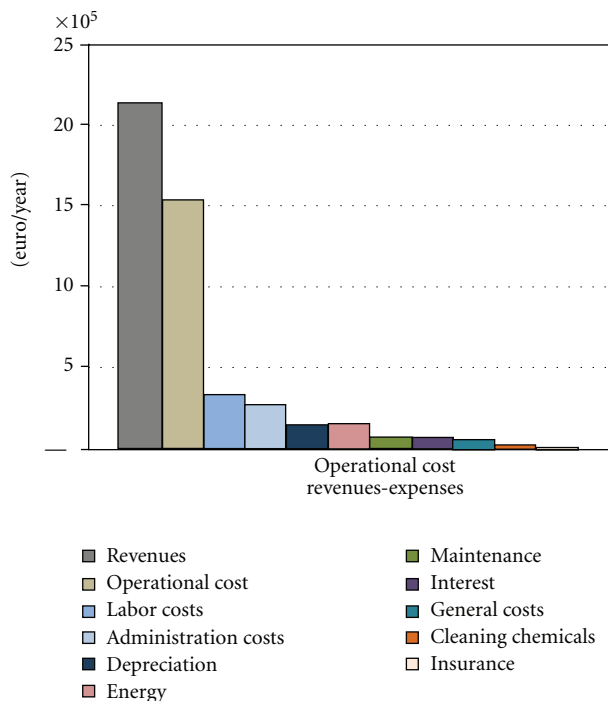


FIGURE 2: Cost-benefit analysis for a capacity of 50,000 t/yr.

when a plant is designed only at a local level in order to treat the OMW from 2-3 typical olive mills and less, it operates with deficits. Below this capacity the i_r is negative. Above this value the i_r is positive, and it does not increase proportionally to the capacity. For a capacity lower than 10,000 t/yr (capacity of 10 typical olive mills) the investment is not recommended to be undertaken as it gives a return on investment less than 5% (which it is supposed as a current “safe” bank interest). For the targeted capacity of 50,000 t/yr (capacity of 50 typical olive mills) the return on investment is considered as very satisfactory (18%).

The time needed to rebound the establishment capital cost from incomes during the operation period of the OMW treatment unit, that is, the mean payout period, τ , is estimated as follows:

$$\tau = \frac{(C + IC)}{K}. \quad (3)$$

The total cost of the investment can be replaced by the fixed cost, and the depreciation can be added to the net profit. Between two or more alternative investments the one with the lowest τ will be chosen. In Western Greece Region case, the mean payout period for the investment is estimated to $\tau = 5.42$ years. This is a very encouraging result, taking into account that a rather low value for the toxic fraction was considered (only 250 €/t). The above result is characterized as positive and indicates to undertake the investment.

5. Conclusions

The management of produced OMW constitutes a long-term and particularly unsolved problem, because of their

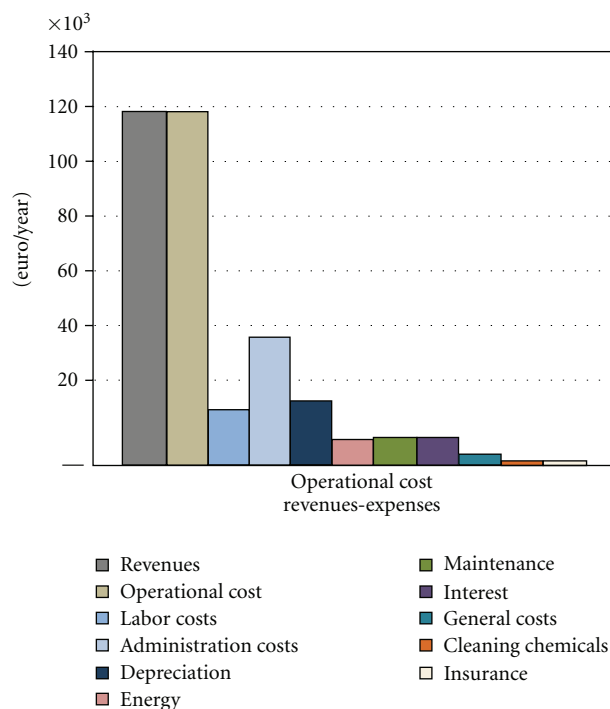
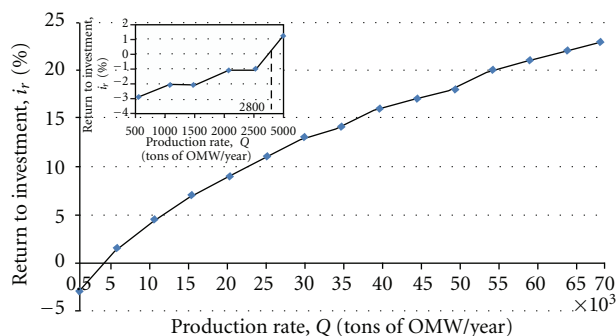


FIGURE 3: Cost-benefit analysis when the unit is working in a capacity of 2,800 t/yr (breakeven point).

FIGURE 4: Return of the investment as a function of the capacity. Breakeven point (2,800 t/yr) of the investment when i_r equals to zero.

high organic load, their particular physicochemical composition, the potentially toxic attributes, the intense of short time interval of production, and the high-cost investment requirements. The present work presents a technoeconomic analysis of the OMW treatment using membranes filtration. The idea of using membrane technology is presented by authors [13] in a previous work in which a new cost-effective system for complete exploitation of OMW is suggested, offering a viable solution to the problem of OMW disposal. A pilot plant was designed, constructed, and installed in a typical olive mill, where OMW quantities were treated at larger volumes. The efficiency of the proposed method for separation and exploitation of the OMW useful constituents was demonstrated.

In the present work, a feasibility study of the proposed method at a regional level was performed, indicating very positive financial results for a future exploitation. The successful integration of this work establishes the basis for a complete and profitable solution of one of the most important Mediterranean environmental problems, providing as main achievements the following. (a) The first is the development of a new cost-effective system for complete exploitation of OMW, which offers a viable solution to the problem of OMW disposal. The introduction of the proposed new integrated technology reduces dramatically the environmental damage and provides a profitable alternative to the olive mills due to utilization of all by-products. (b) The second is the development and production of alternative ecological herbicides and other useful by-products. It is expected that these new products will be highly accepted from the farmers and will enhance the agriculture sustainability.

The rate of return on the investment is acceptable (18%) for the targeted capacity of 50,000 t/yr (capacity of 50 typical olive mills), and the investment is considered viable. Nevertheless, when the capacity is 2,800 t/yr (breakeven point), the return of the investment is zero. Considering that this capacity corresponds to wastes from 2-3 typical olive mills, the investment is unaffordable for a plant that is designed only at a local level (2-3 typical olive mills and less). Moreover, the mean payout period can be considered as satisfactory, taking into account that the whole equipment of the investment is new, and the total cost of the investment has been considered; thus the depreciations have been added to the net profit. This is a very encouraging result, taking into account that a rather low value for the toxic fraction was also considered. The above result is characterized as positive and indicates to undertake the investment.

Acknowledgment

The authors wish to thank the European Commission for financial support for dissemination of their results under FP7-Regions-2009-1, STInno project (245405) and SWAM project (245427).

References

- [1] M. A. Mohammad, "World and Syrian Trade in Olive Oil And Related Agricultural Policy," COMMODITY BRIEF No 11, 2009.
- [2] N. Hytiris, I. E. Kapellakis, R. de la Roij, and K. P. Tsagarakis, "The potential use of olive mill sludge in solidification process," *Resources, Conservation and Recycling*, vol. 40, no. 2, pp. 129–139, 2004.
- [3] C. A. Paraskeva, V. G. Papadakis, D. G. Kanellopoulou, P. G. Koutsoukos, and K. C. Angelopoulos, "Membrane filtration of olive mill wastewater and exploitation of its fractions," *Water Environment Research*, vol. 79, no. 4, pp. 421–429, 2007.
- [4] J. Cegarra, C. Paredes, A. Roig, M. P. Bernal, and D. García, "Use of olive mill wastewater compost for crop production," *International Biodeterioration and Biodegradation*, vol. 38, no. 3-4, pp. 193–203, 1996.
- [5] C. Paredes, J. Cegarra, A. Roig, M. A. Sánchez-Monedero, and M. P. Bernal, "Characterization of olive mill wastewater (alpechin) and its sludge for agricultural purposes," *Biore-source Technology*, vol. 67, no. 2, pp. 111–115, 1999.
- [6] M. J. Paredes, E. Moreno, A. Ramos-Cormenzana, and J. Martinez, "Characteristics of soil after pollution with waste waters from olive oil extraction plants," *Chemosphere*, vol. 16, no. 7, pp. 1557–1564, 1987.
- [7] M. DellaGreca, P. Monaco, G. Pinto, A. Pollio, L. Previtera, and F. Temussi, "Phytotoxicity of low-molecular-weight phenols from olive mill wastewaters," *Bulletin of Environmental Contamination and Toxicology*, vol. 67, no. 3, pp. 352–359, 2001.
- [8] G. Rana, M. Rinaldi, and M. Introna, "Volatilisation of substances alter spreading olive oil waste water on the soil in a Mediterranean environment," *Agriculture, Ecosystems & Environment*, vol. 96, pp. 49–58, 2003.
- [9] P. Paraskeva and E. Diamadopoulos, "Technologies for olive mill wastewater (OMW) treatment: a review," *Journal of Chemical Technology and Biotechnology*, vol. 81, no. 9, pp. 1475–1485, 2006.
- [10] M. Niaounakis and C. P. Halvadakis, *Olive-Mill Waste Management: Literature Review and Patent Survey*, Typothito-George Dardanos Publications, Athens, Greece, 2006.
- [11] A. Roig, M. L. Cayuela, and M. A. Sánchez-Monedero, "An overview on olive mill wastes and their valorisation methods," *Waste Management*, vol. 26, no. 9, pp. 960–969, 2006.
- [12] N. Azbar, A. Bayram, A. Filibeli, A. Muezzinoglu, F. Sengul, and A. Ozer, "A review of waste management options in olive oil production," *Critical Reviews in Environmental Science and Technology*, vol. 34, no. 3, pp. 209–247, 2004.
- [13] C. A. Paraskeva, V. G. Papadakis, E. Tsarouhi, D. G. Kanellopoulou, and P. G. Koutsoukos, "Membrane processing for olive mill wastewater fractionation," *Desalination*, vol. 213, no. 1–3, pp. 218–229, 2007.
- [14] K. Kyriazis and V. G. Papadakis, *Technoeconomical Study*, Tziolas Publications, 2009.

Research Article

Titanium Dioxide-Mediated Photocatalysed Degradation of Two Herbicide Derivatives Chloridazon and Metribuzin in Aqueous Suspensions

A. Khan,¹ N. A. Mir,¹ M. Faisal,² and M. Muneer¹

¹ Department of Chemistry, Aligarh Muslim University, Aligarh 202002, India

² Centre of Advanced Materials and Nano-Engineering (CAMNE), Najran University, P.O. Box 1988, Najran 11001, Saudi Arabia

Correspondence should be addressed to M. Muneer, readermuneer@gmail.com

Received 9 October 2011; Revised 20 February 2012; Accepted 7 March 2012

Academic Editor: Licínio M. Gando-Ferreira

Copyright © 2012 A. Khan et al. This is an open access article distributed under the Creative Commons Attribution License, which permits unrestricted use, distribution, and reproduction in any medium, provided the original work is properly cited.

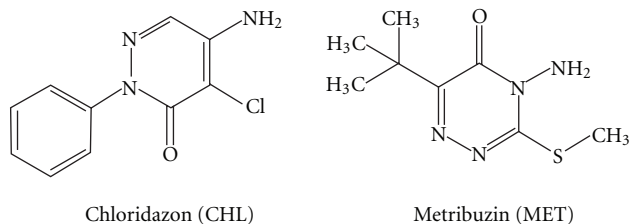
The aim of this paper is to find out the optimal degradation condition for two potential environmental pollutants, chloridazon and metribuzin (herbicide derivatives), employing advanced oxidation process using TiO₂ photocatalyst in aqueous suspensions. The degradation/mineralization of the herbicide was monitored by measuring the change in pollutant concentration and depletion in TOC content as a function of time. A detailed degradation kinetics was studied under different conditions such as types of TiO₂ (anatase/anatase-rutile mixture), catalyst concentration, herbicide concentration, initial reaction pH, and in the presence of electron acceptors (hydrogen peroxide, ammonium persulphate, potassium persulphate) in addition to atmospheric oxygen. The photocatalyst, Degussa P25, was found to be more efficient catalyst for the degradation of both herbicides as compared with two other commercially available TiO₂ powders like Hombikat UV100 and PC500. Chloridazon (CHL) was found to degrade more efficiently under acidic condition, whereas metribuzin (MET) degraded faster under alkaline medium. All three electron acceptors tested in this study were found to enhance the degradation rate of both herbicides.

1. Introduction

Clean and safe drinking water is vital for human health, wildlife, and also for a stable environment. Yet, water is being polluted at alarming rates, with chemicals, nutrients, metals, pesticides, and other contaminants from industrial effluents, chemical spills, and agricultural runoffs [1, 2]. A wide variety of herbicides and other chemicals are applied to agricultural field and lawns mainly to control undesirable vegetation. A fraction of herbicides applied to these sites end up as runoff. This runoff goes into the streams, rivers, and lakes. Some of the herbicides also end up in groundwater systems by percolating down through the soil. As a result, herbicides are widely found in rivers, streams, lakes, and even in drinking water [3]. These chemicals due to their toxicity, stability to natural decomposition, and persistence in the environment have been the cause of much concern to the

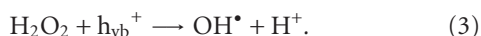
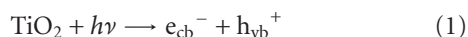
societies and regulatory authorities around the world [4]. The development of appropriate methods to treat these contaminated water is necessary before it is used for any useful purpose.

The photocatalysed degradation of various organic systems employing irradiated TiO₂ is well documented in the literature [5–14]. Briefly, when a semiconductor such as TiO₂ absorbs a photon of energy equal to or greater than its band gap energy, an electron may be promoted from the valence band to the conduction band (e_{cb}^-) leaving behind an electron vacancy or “hole” in the valence band (h_{vb}^+), as shown in (1). If charge separation is maintained, and the reaction is carried out in water and oxygen, the electron and hole may migrate to the catalyst surface where they participate in redox reactions with sorbed species. Specially, h_{vb}^+ may react with surface-bound H₂O to produce the hydroxyl radical and e_{cb}^- is picked up by oxygen to



SCHEME 1

generate superoxide radical anion ($\text{O}_2^{\bullet-}$), as indicated in the following equations (1)–(3)



It has been suggested that the hydroxyl radicals and superoxide radical anions are the primary oxidizing species in the photocatalytic oxidation processes. These oxidative reactions would result in the degradation of the pollutants.

CHL is a herbicide currently used for selective control in beets. It belongs to the class of Hill reaction inhibitors, whereas MET is used primarily to discourage growth of broadleaf weeds and annual grasses among vegetable crops and turf grass [15, 16]. CHL and MET possess high mobility in soil and thus have great potential to leach and pollute surface and groundwater [17]. Few studies relating to the degradation of chloridazon and metribuzin in UV and sunlight have been reported recently in the literature [18–20]. No major efforts have been made to study the detailed degradation kinetics of these two herbicide derivatives. Therefore, in this paper we present a detailed degradation of these compounds as shown in Scheme 1 in aqueous suspensions of TiO_2 under a variety of conditions such as different types of TiO_2 , reaction pH, catalyst and substrate concentration, and also in the presence of electron acceptors like hydrogen peroxide, potassium persulphate, and ammonium persulfate besides atmospheric oxygen.

2. Experimental

2.1. Reagents and Chemicals. Laboratory grade chloridazon was kindly supplied by Parijat Industries India Pvt. Ltd., Ambala whereas, the pesticide derivative metribuzin was obtained from Rallis India Ltd., and they were used as such for our studies without any further purification. All the solutions were made in double-distilled water for the irradiation experiments. Degussa P25 was used as catalyst in most of the experiments performed to carry out the photocatalytic degradation of these two model compounds. Other catalyst powders, namely, Hombikat UV100 (Sachtleben Chemie GmbH) and PC500 (Millennium Inorganic Chemicals), were used for comparative study. Degussa P25 contains 80% anatase and 20% rutile with a specific BET surface area

of $50 \text{ m}^2 \text{ g}^{-1}$ and a primary particle size of 20 nm [21]. Hombikat UV100 consists of 100% pure anatase with a specific BET surface area of $250 \text{ m}^2 \text{ g}^{-1}$ and a primary particle size of 5 nm [22]. The photocatalyst PC500 has a BET-surface area of $287 \text{ m}^2 \text{ g}^{-1}$ with 100% anatase and primary particle size of 5–10 nm [23]. All other chemicals such as sodium hydroxide, nitric acid, hydrogen peroxide, potassium persulphate, and potassium bromate were obtained from Merck.

2.2. Procedure. An immersion well photochemical reactor consisting of inner and outer jacket made of Pyrex glass was used for the irradiation experiments. The detailed design of the photoreactor has been illustrated elsewhere [24]. Prior to illumination, stock solutions of CHL and MET were prepared in double-distilled water with desired concentration. The irradiation experiments were carried out in aqueous suspensions of TiO_2 using a pyrex-filtered output of 125 W medium pressure mercury lamp (Philips). The light intensity was measured by UV light intensity detector (Lutron UV-340) and was found to be in the range of 4.86–4.88 mW/cm^2 . The experimental runs were carried out by using the following procedure for both the herbicide derivatives: firstly 125 mL solution of the herbicide derivative was taken into the reactor and required amount of photocatalyst was added. The suspension was magnetically stirred and purged with atmospheric oxygen in the dark for 10 min to attain adsorption-desorption equilibrium between herbicide derivatives and TiO_2 . The zero time reading was obtained from blank solution kept in the dark. Samples (5 mL) were taken at regular time intervals from the reactor and analysed after centrifugation. The pH of the reaction mixture was adjusted by adding dilute NaOH and HNO_3 .

2.3. Analysis. The analysis was carried out after removal of photocatalyst by centrifuging the samples at 4000 rpm for 1 h using Remi centrifuge (model R24). The degradation of CHL and MET was followed by measuring the change in absorption intensity at their respective λ_{max} 238 nm (CHL) and 295 nm (MET) using Shimadzu UV-Vis Spectrophotometer (Model 1601), and mineralization was monitored by measuring the depletion in Total Organic Carbon (TOC) content with a Shimadzu TOC_{VCSH} Analyzer. The pH of the reaction mixture was measured using HI 2210 pH meter.

3. Results and Discussion

3.1. Photolysis of CHL and MET in Aqueous Suspensions of TiO_2 . Irradiation of an aqueous suspensions of CHL (0.18 mM, 125 mL, pH 6.2) and MET (0.30 mM, 125 mL, pH 6.5) in the presence of TiO_2 (Degussa P25, 1 g L^{-1}) using 125 W medium pressure mercury lamp in an immersion well photochemical reactor with constant stirring and bubbling of air led to a decrease in absorption intensity as a function of time as shown in the inset of Figures 1(a) and 1(b), respectively. The change in the concentration of the pollutant was calculated from standard calibration curve obtained from the absorption intensity of the herbicide derivatives at different

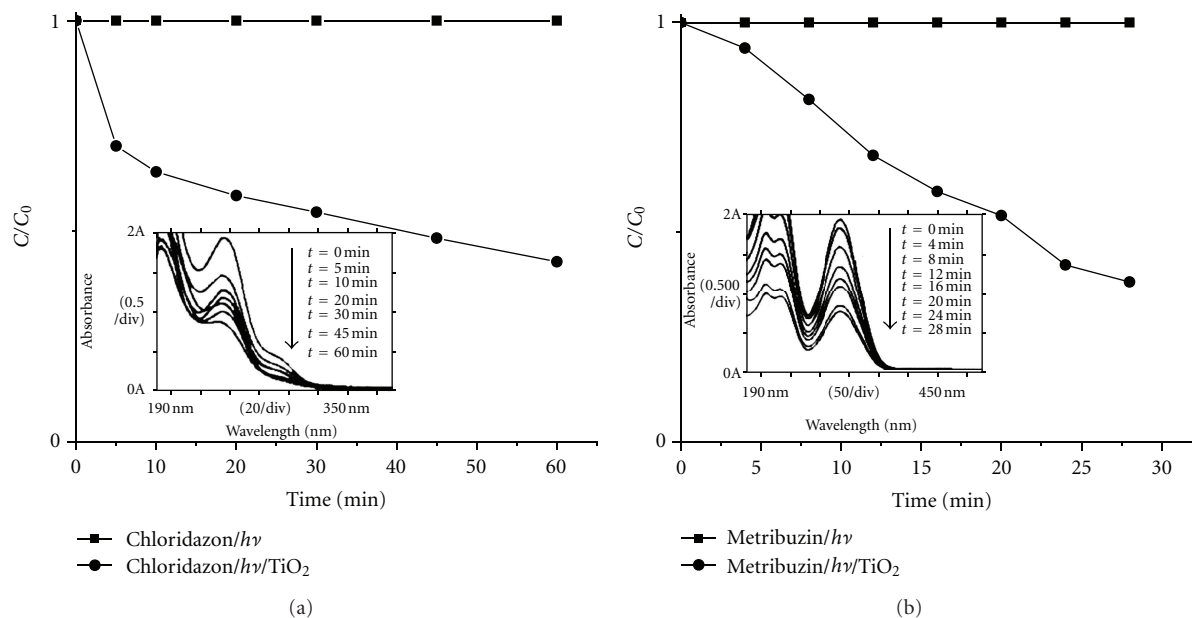


FIGURE 1: (a) Change in concentration as a function of time on irradiation of an aqueous solution of CHL in the presence and absence of photocatalyst. Inset: Change in absorption intensity at 238 nm on irradiation of aqueous suspension of CHL containing TiO_2 . Experimental conditions: CHL (0.18 mM), $V = 125$ mL, 125 W medium pressure mercury lamp, light intensity: 4.88 mW/cm^2 , irradiation time: 60 min. (b) Change in concentration as a function of time on irradiation of an aqueous suspension of MET in the presence and absence of photocatalyst. Inset: Change in absorption intensity at 295 nm on irradiation of aqueous suspension of MET containing TiO_2 . Experimental conditions: MET (0.30 mM), $V = 125$ mL, 125 W medium pressure mercury lamp, light intensity: 4.88 mW/cm^2 , Irradiation time: 28 min.

concentration. The change in concentration in the presence and absence of photocatalyst as a function of time is shown in Figures 1(a) and 1(b), for herbicide derivatives, CHL and MET, respectively. The results demonstrate that 62% degradation of CHL and 55% degradation of MET could be achieved in 60 min and 28 min, respectively, whereas in the absence of photocatalyst no significant degradation was observed as shown in the Figure 1. Control experiments were carried out to show that there was no appreciable loss of the compound in unirradiated blank solutions and also due to adsorption on the surface of the photocatalyst. In order to see the effect of change in initial volume, experiments were carried out (data not shown), where samples were withdrawn initially at zero min and then directly after 60 min (CHL) and 28 min, (MET). There was no significant effect of volume alteration on the reaction rate.

For each experiment, the degradation rate constant of the compound was calculated from the linear regression of a plot of the natural logarithm of the compound concentration as a function of irradiation time. The degradation rate of the herbicide derivatives was calculated using the formula given below

$$-\frac{d[c]}{dt} = kc^n, \quad (4)$$

k equals rate constant (min^{-1}), c equals concentration (mol L^{-1}) of the pollutant, n is order of reaction.

The degradation rate for both the herbicides was found to follow pseudo-first-order reaction kinetics, and the degradation rate was calculated in terms of $\text{mmol L}^{-1} \text{ min}^{-1}$.

3.2. Comparison of Photocatalytic Activity of Different TiO_2 Powders. Titanium dioxide is the most widely used photocatalyst in heterogeneous photocatalysis due to its low cost, high photocatalytic activity, nontoxic nature, photostability, and chemical and biological inertness [14]. The photocatalytic activity of three commercially available TiO_2 powders, namely, Degussa P25, Hombical UV100, and PC500, was tested on the degradation kinetics of herbicide derivatives CHL and MET. The rates obtained for the degradation of CHL and MET in the presence of different types of TiO_2 powders by continuous purging of air are shown in Table 1. It has been observed that the degradation of CHL and MET proceeds much more rapidly in the presence of Degussa P25 as compared to other TiO_2 powders. The photocatalysts UV100 and PC500 showed a comparable photocatalytic activity for the degradation of MET.

The photocatalyst Degussa P25 has been found to be a better photocatalyst for the degradation of a large number of compounds reported earlier [25–27]. The reason for the better photocatalytic activity of Degussa P25 is attributed to its anatase/rutile mixture as reported earlier [28, 29]. In all following experiments, Degussa P25 was used since this material exhibited the highest photocatalytic activity as compared to other photocatalyst tested for the degradation of herbicides under investigation.

3.3. Effect of pH. The pH of the reaction mixture in surface reactions significantly influences the physicochemical properties of titanium dioxide, including the charge on its

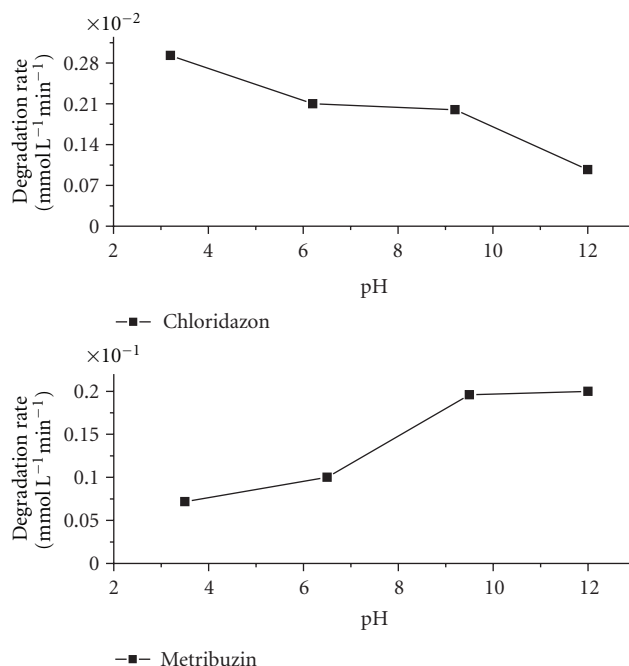


FIGURE 2: Influence of pH on the degradation rate of CHL and MET. *Experimental conditions:* CHL (0.18 mM), MET (0.30 mM), initial reaction pH of CHL (3.2, 6.2, 9.2, and 12), initial reaction pH of MET (3.5, 6.5, 9.5, and 12), $V = 125$ mL, photocatalyst: TiO_2 Degussa P25 (1 gL^{-1}), irradiation time: 60 min (CHL), 28 min (MET).

TABLE 1: (a) Comparison of degradation rate of CHL and MET in the presence of different types of TiO_2 samples. *Experimental conditions:* CHL (0.18 mM), MET (0.30 mM), $V = 125$ mL, photocatalysts: Degussa P25 (1 gL^{-1}), Sachtleben Hombikat UV100 (1 gL^{-1}), PC500 (1 gL^{-1}), irradiation time: 60 min (CHL), 28 min (MET). (b) Comparison of mineralization rate of CHL and MET in the presence of TiO_2 and $\text{TiO}_2/\text{H}_2\text{O}_2$. *Experimental conditions:* CHL (0.55 mM), MET (0.11 mM), $V = 125$ mL, photocatalysts: Degussa P25 (1 gL^{-1}), irradiation time: 60 min (CHL), 28 min (MET).

	(a) Rate of photodegradation ($\text{mmol L}^{-1} \text{ min}^{-1}$)			(b) Rate of photomineralization ($\text{mmol L}^{-1} \text{ min}^{-1}$)	
	P25	UV100	PC500	$h\nu/\text{P25}$	$h\nu/\text{P25}/\text{H}_2\text{O}_2$
Chloridazon	0.0021	0.0018	0.0011	0.0003	0.0022
Metribuzin	0.036	0.025	0.025	0.0003	0.0008

surface, the aggregation numbers of particles it forms, and the position of the conductance and valence bands [30]. The effect of pH on the degradation of CHL and MET employing Degussa P25 was studied in the pH range between 3 and 12. The rate obtained for the degradation of herbicide derivatives CHL and MET as a function of reaction pH is shown in Figure 2. It is interesting to note that in the case of compound CHL, the highest degradation rate was observed at pH 3.2, which slowly decreases with the increase in reaction pH, whereas in the case of MET, the degradation rate was found to increase with the increase in reaction pH.

The zero point of charge (pH_{zpc}) of Degussa P25 has been reported as 6.25 [31]; hence, at more acidic pH values, the TiO_2 particle surface is positively charged; while at pH values above pH_{zpc}, it is negatively charged. The pK_a for CHL and MET has been reported as 2.96 and 7.0, respectively [32, 33]. The higher degradation rate for CHL at lower pH

values and MET at higher pH values could be explained on the basis of the fact that the structural orientation of the compound at these pH values are favoured for the reactive species.

3.4. Effect of TiO_2 Concentration. The optimal amount of TiO_2 has to be found out in order to avoid unnecessary excess catalyst and also to ensure total absorption of light for efficient photodegradation. In order to find out the optimal catalyst concentration, we have investigated the influence of different concentrations of Degussa P25 (0.5 to 4 gL^{-1}) on the degradation kinetics of CHL and MET, and the results are shown in Figure 3. As expected, the rate of degradation for the model compound CHL was found to increase with the increase in catalyst concentration up to 2 gL^{-1} after which a further increase in catalyst concentration led to a decrease in degradation rate. The degradation rate for MET

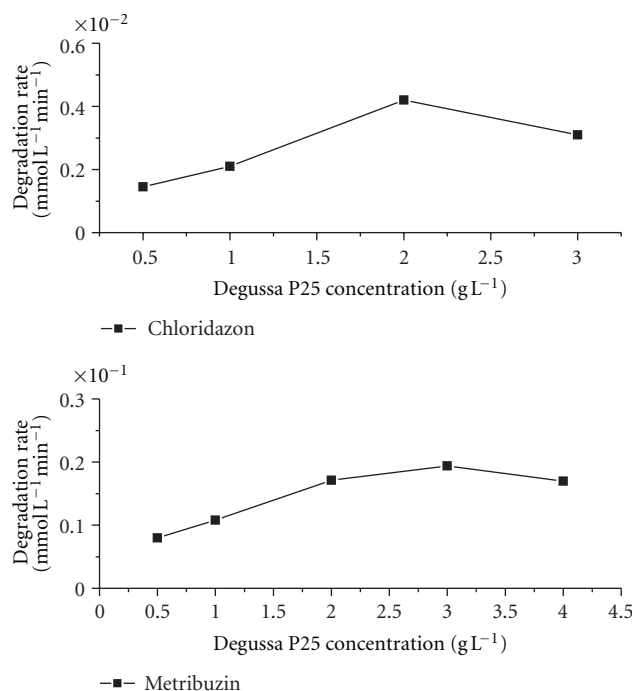


FIGURE 3: Influence of Degussa P25 concentration on the degradation rate of CHL and MET. *Experimental conditions:* CHL (0.18 mM), MET (0.30 mM), TiO₂ Degussa P25 (0.5, 1, 2, and 3 and 4 g L⁻¹), V = 125 mL, irradiation time: 60 min (CHL), 28 min (MET).

was found to increase linearly up to 3 g L⁻¹ followed by a decrease in degradation rate on further increase in catalyst concentration.

The decrease in degradation rate at a higher catalyst concentration may be due to the fact that when the catalyst concentration is very high, after traversing a certain optical path, turbidity impedes further penetration of light in the reactor (incidence of the combined phenomena of particle masking and scattering), lowering the efficiency of the catalytic process. The results are in agreement with the studies reported earlier by our group [34].

3.5. Effect of the Initial Herbicide Concentrations. The study of the dependence of the photocatalytic degradation rate on the substrate concentration is very important for the application of the photocatalytic process to waste-water treatment. Hence the effect of initial herbicide concentration, varying from 0.14 to 0.20 for CHL and 0.24–0.33 for MET on the photocatalytic degradation was studied, and the results, are shown in Figure 4.

As expected, the rate of degradation of CHL was found to increase gradually with the increase in substrate concentration from 0.14 to 0.18 mM. Further increase in substrate concentration led to a slight decrease in the rate of the reaction. Similar results were obtained for the degradation of MET, that is, the rate was found to increase with the increase in substrate concentration from 0.24 to 0.30 mM, and a further increase in the concentration led to more or less

same degradation rate within experimental error limits. The results are in agreement with earlier reported studies [35].

3.6. Effect of Electron Acceptors. Charge recombination of the photogenerated electron hole pairs is the major bottleneck in semiconductor photocatalysis. Due to the process of electron-hole recombination, both charge carriers annihilate each other. As a result, the rates of the photocatalytic transformations are limited by the rates of electron-hole recombination in the bulk of TiO₂ or at the surface. In order to enhance the formation of hydroxyl radicals and also inhibit undesired electron/hole pair recombination, electron acceptors such as hydrogen peroxide (10 mM), ammonium per sulphate (3 mM), and potassium per sulphate (3 mM) were used in addition to Degussa P25 in order to see their effect on the degradation kinetics of the herbicide derivative CHL and MET. The rate obtained for the decomposition of herbicide derivatives in the presence and absence of additives is shown in Figure 5.

All employed additives were found to enhance the degradation of both compounds, CHL and MET. The highest degradation rate for the decomposition of MET was observed in the presence of hydrogen peroxide as an electron acceptor in the presence of Degussa P25. In addition, the effect of different concentrations of hydrogen peroxide on the degradation kinetics of both herbicides have also been studied, and the rates are shown in the inset of Figure 5. In both compounds, the rates were found to increase as the H₂O₂ concentration increases from 5 to 15 mM (markedly in the

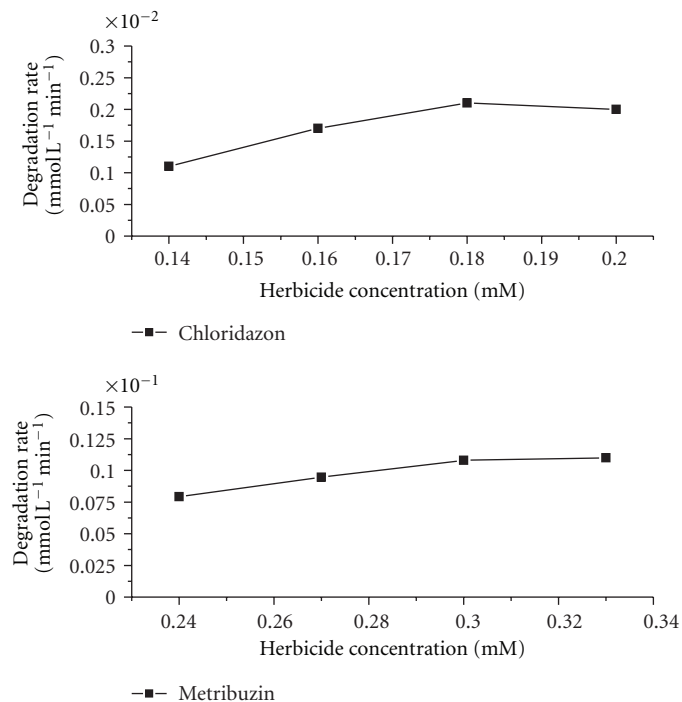


FIGURE 4: Effect of initial herbicide concentration on the degradation rate. *Experimental conditions:* Herbicide concentration: CHL (0.14, 0.16, 0.18, and 0.20 mM), MET (0.24, 0.27, 0.30, and 0.33 mM), $V = 125$ mL, photocatalyst: TiO_2 Degussa P25 (1 g L^{-1}), irradiation time: 60 min (CHL), 28 min (MET).

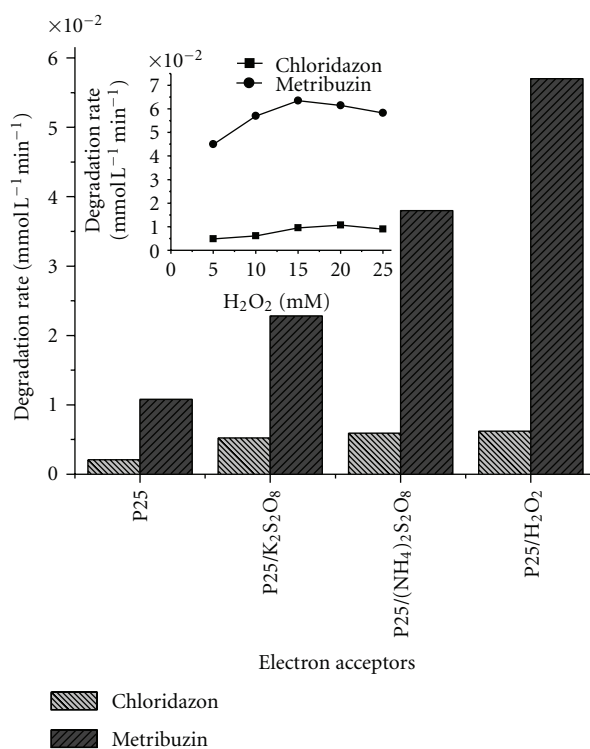
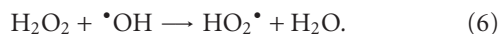
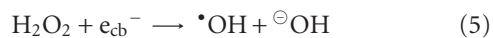


FIGURE 5: Influence of electron acceptors on the the degradation rate of CHL and MET. *Experimental conditions:* CHL (0.18 mM), MET (0.30 mM), electron acceptors, $\text{K}_2\text{S}_2\text{O}_8$ (3 mM), $(\text{NH}_4)_2\text{S}_2\text{O}_8$ and H_2O_2 (10 mM), $V = 125$ mL, photocatalyst: TiO_2 Degussa P25 (1 g L^{-1}), irradiation time: 60 min (CHL), 28 min (MET).

case of MET). A further increase in the H_2O_2 concentration leads to a slight decrease in the degradation rate of MET and more or less same in the case of CHL.

The rate enhancement by H_2O_2 addition could be attributed to its better electron acceptance (5), thereby reducing electron hole recombination. Above the optimum value, the competitive reactions between hydroxyl radical and peroxide lead to the generation of less reactive hydroperoxide radicals, which does not contribute to the oxidative degradation of CHL (6)



3.7. Photomineralization of CHL and MET in Aqueous Suspension of TiO_2 . The photocatalytic mineralization of CHL and MET was studied in aqueous suspensions of TiO_2 in the presence and absence H_2O_2 . Table 1 shows the mineralization rate of CHL and MET in aqueous suspension of Degussa P25 in the presence and absence of H_2O_2 . Blanks experiments were carried out by irradiating the pesticide solutions in the absence of TiO_2 containing H_2O_2 where no appreciable loss of the compounds was observed (data not shown). It is obvious from the table that the mineralization rate was enhanced in the presence of TiO_2 containing hydrogen peroxide due to the efficient generation of hydroxyl radicals with the addition of H_2O_2 .

4. Conclusion

TiO_2 can efficiently catalyze the degradation and mineralization of herbicide derivatives chloridazon, and metribuzin in the presence of UV light. All parameters have been found to markedly influence the overall efficiency of degradation. Degussa P25 showed greater photocatalytic activity for the degradation of both herbicides, CHL and MET. In the case of chloridazon the highest efficiency was observed at pH 3.2, whereas metribuzin showed better degradation under alkaline condition. All the electron acceptors markedly enhanced the degradation of MET, and the highest rate was achieved with H_2O_2 , whereas in the case CHL all acceptors enhanced the degradation at comparable rate. The observations of these investigations clearly demonstrate the importance of choosing the optimum degradation conditions to obtain high degradation and mineralisation, which is essential for any practical application of photocatalytic oxidation processes.

Acknowledgments

Financial support for the research projects from CSTUP, Lucknow, UGC, New Delhi, India, and DRS-1 (SAP) to the Department of Chemistry, AMU Aligarh, is gratefully acknowledged. Total Organic Carbon analyzer (TOC) used for the analysis of the samples was a gift instrument from the Alexander von Humboldt foundation, Bonn, Germany.

References

- [1] G. D. Agrawal, "Diffuse agricultural water pollution in India," *Water Science and Technology*, vol. 39, pp. 33–47, 1999.
- [2] S. Mukherjee and P. Nelliya, *Groundwater Pollution and Emerging Environmental Challenges of Industrial Effluent Irrigation in Mettupalayam Taluk*, Tamil Nadu International Water Management Institute, Colombo, Sri Lanka, 2007.
- [3] D. Muszkat, M. Raucher, M. Mogařitz, and D. Ronen, "Groundwater contamination by organic pollutants," in *Groundwater Contamination and Control*, M. Dekker and U. Zoller, Eds., pp. 257–272, Amer Society of Civil Engineer, New York, NY, USA, 1994.
- [4] J. A. Graham, "Monitoring groundwater and well water for crop protection chemicals," *Analytical Chemistry*, vol. 63, no. 11, pp. 631–622, 1991.
- [5] C. Shifu and L. Yunzhang, "Study on the photocatalytic degradation of glyphosate by TiO_2 photocatalyst," *Chemosphere*, vol. 67, no. 5, pp. 1010–1017, 2007.
- [6] S. Han, J. Li, H. Xi, D. Xu, Y. Zuo, and J. Zhang, "Photocatalytic decomposition of acephate in irradiated TiO_2 suspensions," *Journal of Hazardous Materials*, vol. 163, no. 2–3, pp. 1165–1172, 2009.
- [7] M. M. Haque and M. Muneer, "Photodegradation of norfloxacin in aqueous suspensions of titanium dioxide," *Journal of Hazardous Materials*, vol. 145, no. 1–2, pp. 51–57, 2007.
- [8] M. N. Abellán, B. Bayarri, J. Giménez, and J. Costa, "Photocatalytic degradation of sulfamethoxazole in aqueous suspension of TiO_2 ," *Applied Catalysis B*, vol. 74, no. 3–4, pp. 233–241, 2007.
- [9] H. K. Singh, M. Saquib, M. M. Haque, and M. Muneer, "Heterogeneous photocatalysed decolorization of two selected dye derivatives neutral red and toluidine blue in aqueous suspensions," *Chemical Engineering Journal*, vol. 136, no. 2–3, pp. 77–81, 2008.
- [10] J. C. Garcia, J. I. Simionato, A. E. C. da Silva, J. Nozaki, and N. E. D. Souza, "Solar photocatalytic degradation of real textile effluents by associated titanium dioxide and hydrogen peroxide," *Solar Energy*, vol. 83, no. 3, pp. 316–322, 2009.
- [11] W. Bahnemann, M. Muneer, and M. M. Haque, "Titanium dioxide-mediated photocatalysed degradation of few selected organic pollutants in aqueous suspensions," *Catalysis Today*, vol. 124, no. 3–4, pp. 133–148, 2007.
- [12] E. Evgenidou, E. Bizani, C. Christophoridis, and K. Fytianos, "Heterogeneous photocatalytic degradation of prometryn in aqueous solutions under UV-Vis irradiation," *Chemosphere*, vol. 68, no. 10, pp. 1877–1882, 2007.
- [13] E. Kusvuran, A. Samil, O. M. Atanur, and O. Erbatur, "Photocatalytic degradation kinetics of di- and tri-substituted phenolic compounds in aqueous solution by TiO_2/UV ," *Applied Catalysis B*, vol. 58, no. 3–4, pp. 211–216, 2005.
- [14] C. C. Chen, C. S. Lu, Y. C. Chung, and J. L. Jan, "UV light induced photodegradation of malachite green on TiO_2 nanoparticles," *Journal of Hazardous Materials*, vol. 141, no. 3, pp. 520–528, 2007.
- [15] EPA, "Health effects support document for metribuzin U.S. Environmental Protection Agency Office of Water (4304T)," Tech. Rep. 822-R-03-004, Health and Ecological Criteria Division, Washington, DC, USA, February 2003.
- [16] R. Cremllyn, "Pesticides—preparation and mode of action," in *Herbicides*, R. Cremllyn, Ed., pp. 140–172, John Wiley and Sons, Chichester, UK, 1978.
- [17] M. F. Pérez, M. V. Sánchez, F. F. Céspedes, S. P. García, and I. D. Fernández, "Prevention of chloridazon and metribuzin

- pollution using lignin-based formulations," *Environmental Pollution*, vol. 158, no. 5, pp. 1412–1419, 2010.
- [18] D. M. Fouad and M. B. Mohamed, "Photodegradation of chloridazon using Coreshell Magnetic Nanocomposites," *Journal of Nanotechnology*, vol. 2011, 7 pages, 2011.
 - [19] E. M. Scherer, Q. Q. Wang, A. G. Hay, and A. T. Lemley, "The binary treatment of aqueous metribuzin using anodic fenton treatment and biodegradation," *Archives of Environmental Contamination and Toxicology*, vol. 47, pp. 154–161, 2004.
 - [20] L. Muszkat, L. Feigelson, L. Bir, and K. A. Muszkat, "Photocatalytic degradation of pesticides and bio-molecules in water," *Pest Management Science*, vol. 58, no. 11, pp. 1143–1148, 2002.
 - [21] R. I. Bickley, T. G. Carreno, J. S. Lees, L. Palmisano, and R. J. D. Tilley, "A structural investigation of titanium dioxide photocatalysts," *Journal of Solid State Chemistry*, vol. 92, no. 1, pp. 178–190, 1991.
 - [22] M. Lindner, D. W. Bahnemann, B. Hirthe, and W. D. Griebler, "Solar water detoxification: Novel TiO₂ powders as highly active photocatalysts," *Journal of Solar Energy Engineering, Transactions of the ASME*, vol. 119, no. 2, pp. 120–125, 1997.
 - [23] S. Rauer, *Untersuchung von kommerziell erhältlichen Titan-dioxidien hinsichtlich ihrer photokatalytischen Aktivität, Diplomarbeit, Fachhochschule Hannover, Fachbereich Maschinenbau Vertiefung Umwelt-und Verfahrenstechnik*, Ph.D. thesis, University of Hannover, Hannover, Germany, 1998.
 - [24] M. Qamar and M. Muneer, "Comparative photocatalytic study of two selected pesticide derivatives, indole-3-acetic acid and indole-3-butyric acid in aqueous suspensions of titanium dioxide," *Journal of Hazardous Materials*, vol. 120, no. 1-3, pp. 219–227, 2005.
 - [25] H. K. Singh, M. Saquib, M. M. Haque, and M. Muneer, "Heterogeneous photocatalysed degradation of 4-chlorophenoxyacetic acid in aqueous suspensions," *Journal of Hazardous Materials*, vol. 142, no. 1-2, pp. 374–380, 2007.
 - [26] M. Muneer, J. Theurich, and D. Bahnemann, "Titanium dioxide mediated photocatalytic degradation of 1,2-diethyl phthalate," *Journal of Photochemistry and Photobiology A*, vol. 143, no. 2-3, pp. 213–219, 2001.
 - [27] M. M. Haque, M. Muneer, and D. W. Bahnemann, "Semiconductor mediated Photocatalysed degradation of a herbicide derivative chlorotoluron in aqueous suspensions," *Environmental Science & Technology*, vol. 40, pp. 4765–4770, 2006.
 - [28] D. C. Hurum, A. G. Agrios, K. A. Gray, T. Rajh, and M. C. Thurnauer, "Explaining the enhanced photocatalytic activity of Degussa P25 mixed-phase TiO₂ using EPR," *Journal of Physical Chemistry B*, vol. 107, no. 19, pp. 4545–4549, 2003.
 - [29] D. C. Hurum, K. A. Gray, T. Rajh, and M. C. Thurnauer, "Recombination pathways in the degussa P25 formulation of TiO₂: Surface versus lattice mechanisms," *Journal of Physical Chemistry B*, vol. 109, no. 2, pp. 977–980, 2005.
 - [30] C. Kormann, D. W. Bahnemann, and M. R. Hoffmann, "Photolysis of chloroform and other organic molecules in aqueous TiO₂ suspensions," *Environmental Science and Technology*, vol. 25, no. 3, pp. 494–500, 1991.
 - [31] J. Augustynski, *Structural Bonding*, chapter 1, Springer, Berlin, Germany, 1988.
 - [32] M. Zimpl, M. Kotouček, K. Lemr, J. Veselá, and J. Skopalová, "Electrochemical reduction of chloridazon at mercury electrodes, and its analytical application," *Analytical and Bioanalytical Chemistry*, vol. 371, no. 7, pp. 975–982, 2001.
 - [33] D. C. Peek and A. P. Appleby, "Effect of pH on Phytotoxicity of Metribuzin and Ethyl-metribuzin," *Weed Technology*, vol. 3, pp. 636–639, 1989.
 - [34] A. Khan, M. M. Haque, N. A. Mir, M. Muneer, and C. Boxall, "Heterogeneous photocatalysed degradation of an insecticide derivative acetamiprid in aqueous suspensions of semiconductor," *Desalination*, vol. 261, no. 1-2, pp. 169–174, 2010.
 - [35] W. Bahnemann, M. Muneer, and M. M. Haque, "Titanium dioxide-mediated photocatalysed degradation of few selected organic pollutants in aqueous suspensions," *Catalysis Today*, vol. 124, no. 3-4, pp. 133–148, 2007.

Research Article

Valorization of Agroindustrial Wastes as Biosorbent for the Removal of Textile Dyes from Aqueous Solutions

Elsa Contreras,¹ Luisa Sepúlveda,¹ and Carolyn Palma²

¹ Engineering Department, Santiago de Chile University, Avenida Libertador Bernardo O'Higgins 3363, Estación Central, Santiago, CP 9160000, Chile

² Chemical and Environmental Engineering Department, Federico Santa Maria Technical University, Avenida Vicuña Mackenna 3939, San Joaquín, Santiago, CP 8940897, Chile

Correspondence should be addressed to Carolyn Palma, carolyn.palma@usm.cl

Received 31 October 2011; Revised 12 February 2012; Accepted 20 February 2012

Academic Editor: Licínio M. Gando-Ferreira

Copyright © 2012 Elsa Contreras et al. This is an open access article distributed under the Creative Commons Attribution License, which permits unrestricted use, distribution, and reproduction in any medium, provided the original work is properly cited.

The goal is to determinate the technical feasibility of using agroindustrial wastes for adsorption of dyes. The pH_{pzc} of Brewer's spent grains and Orange peel is 5.3 and 3.5, respectively. The equilibrium isotherms of Basic Blue 41, Reactive Black 5, and Acid Black 1 were carried out without pHs control which ranging between 4 and 5.5. The equilibrium concentrations for both adsorbents were fitted by the Freundlich and Langmuir models. The maximum adsorption capacity measured for Basic Blue 41, Reactive Black 5, and Acid Black 1 was 32.4, 22.3, and 19.8 mg g^{-1} for Brewer's spent grains; and 157, 62.6, and 45.5 for orange peel, respectively. The kinetic of process was fitted by the model of pseudo-second order. The constant rate for orange peel decreased to extend the initial concentration of dye increased, obtaining $4.08 \times 10^{-3} - 0.6 \times 10^{-3}$ (Basic Blue 41), $2.98 \times 10^{-3} - 0.36 \times 10^{-3}$ (Acid Black 1), and $3.40 \times 10^{-3} - 0.46 \times 10^{-3} \text{ g mg}^{-1} \text{ min}^{-1}$ (Reactive Black 5). The best removal efficiency was obtained in orange peel with values started from 63% to 20%. Consequently, according the results obtained there are two positive effects, the reuse of agricultural wastes and its use as low-cost adsorbent of the dyes.

1. Introduction

The discharges of industrial wastewater containing dyes cause serious environmental problems, because their chemical structure gives them a persistent and recalcitrant nature. The released dye in water streams represents a risk of ecotoxicity and a potential danger of bioaccumulation. The transport of these contaminants through the food chain could even affect the human health. In the last two decades, the elimination of dyes from industrial textile waste waters has been one of the major challenges for researchers.

Adsorption has received special attention as a treatment for colorized wastewater because it produces an effluent of better quality and comparatively can become more effective and less expensive than conventional treatments. Granular-activated carbon has been designated by the Environmental Protection Agency (EPA) of USA as the best available technology (BAT) for organic chemicals removal. In fact, activated carbon adsorption is an effective treatment for removing varied organic contaminants and, particularly, textile

dyes of different ionic nature [1, 2]. However, the high volume of effluents generated in the textile wet process involves a high cost for regeneration of the activated carbon [3, 4].

On the other hand, as a consequence of industrial development, enormous quantities of agroindustrial wastes are generated annually that can be used like supplies for other processes in order to give added value. An alternative is the application in processes of wastewater treatment, promoting in this way a sustainable and environmentally friendly development. Recently, it has been evaluated the performance of different low-cost adsorbents, which can be used only once to avoid the costly stage of regeneration. These studies have included some types of biomass such as agroindustrial or forest wastes, namely, rice husk [5], coconut [6], spent coffee grounds, a byproducts of instant coffee industry [7], wood bark [8], among others. Although the removal efficiency that is achieved is less than using the activated carbon, the application to industrial scale can be economically attractive [9].

The adsorption capacity of these nonconventional adsorbents is due to the presence of biopolymers such as polysaccharides, lignin, hemicelluloses, and cellulose [9, 10]. Brewers' spent grains, a lignocellulosic residual biomass from the brewing industry, are the major solid waste generated during the production process. The potential use of this waste as raw material in food industry, energy production, and biotechnological processes is currently being investigated [11]. Brewer's spent grains also have showed a significant potential as a biosorbent for application in the remediation of wastewater contaminated with metal and dye [12–14]. Besides other cellulose-based wastes such as banana peel have been used in the removal of dyes by adsorption [15, 16]. The biomass residual of the citrus juice industry, peel, pulp, and seed represents 50% of the processed fruit mass. The efficient management of these agroindustrial wastes should not only promote but diversify its use. The utilization of citrus peel, orange, lemon, mandarin, and grapefruit, as a low-cost adsorbent, has recently been studied [17–20].

The aim of this research is to explore the technical feasibility of use the waste biomass such as Brewer's spent grains and orange peel for the biosorptive removal of textile dyes.

2. Materials and Methods

2.1. Agroindustrial Wastes. Brewer's spent grains (BSG,) were obtained from the local brewery. Orange peel (OP) from fruit purchased from a local market. These residual biomasses were dried at room temperature until they reached the equilibrium moisture content, around 10% (wt). The dry solids were crushed and later the mesh cut $[-18 + 60]$, which corresponds to particles larger than 0.25 mm and smaller than 1 mm, was selected.

2.2. Dyes. The adsorbates evaluated in this study were the cationic dye Basic Blue 41 (C.I. 11105) and the anionic dyes, Acid Black 1 (C.I. 20470) and Reactive Black 5 (C.I. 20505). Methylene Blue (Basic Blue 9, C.I. 52015) was used for the determination of adsorptive properties of the agroindustrial wastes. Dyes are analytical grade supplied by Sigma Aldrich Co. The structure and properties of the dyes are shown in Table 1.

2.3. Physical and Chemical Characterization

Morphologic Characterization. It was realized by a Scanning Electron Microscopy analysis of the agroindustrial wastes, using JSPM-5410 Scanning Probe Microscope (JEOL Ltda) implemented with Anaglyph Maker 1.08 software. The images were obtained with a magnification of 1000x.

Surface Acidity and Basicity. The concentrations of acidic and basic sites in the adsorbents were determined by acid-base titration method proposed by Boehm [21]. 0.5 g of agroindustrial waste was contacted with 50 mL of NaOH 0.01 M (acidity) or 50 mL of 0.1 M HCl (basicity) until the equilibrium was reached. An aliquot of 20 mL filtrate obtained from the contact assay (24 h) was then titrated with 0.01 M HCl or 0.1 M NaOH to neutralize the sodium hydroxide or hydrochloric acid in excess, respectively.

Point of Zero Charge (pH_{pzc}). 10, 7.5, 5, 2.5, and 1.25 mL of 0.1 M HCl were added to 1 g of agroindustrial wastes. Similarly, there was prepared another set of suspensions with 0.1 M NaOH. Next, in all the flasks was added 5 mL of KCl 0.1 M and was then completed with distilled water until 100 mL. The flasks were maintained in a shaker with thermal control (20°C, 150 rpm) for 1 h and pH values (pH_1) were recorded. Subsequently 5 mL of KCl 1 M was added to each sample, maintaining the agitation during 1 h. The final pH of each sample (pH_2) was measured. The pH_{pzc} for each waste was estimated as the final pH value, for which the difference between pH_1 and pH_2 was equal to zero [22].

pH of Adsorbent ($pH_{KCl\ 1\ M}$, $pH_{CaCl_2\ 0.01\ M}$). 50 mL of solution KCl 0.1 M or $CaCl_2$ 0.01 M was added in a flask containing 0.2 g of agroindustrial waste. The flasks were maintained in a shaker with thermal control (25°C, 220 rpm) for 2 h; after that, the pH was measured for each suspension.

2.4. Adsorptive Properties

Methylene Blue Index. There was evaluated the adsorptive power of each waste by the Methylene Blue. Brewer's spent grains and Orange peel were place in contact with solution of Methylene Blue until equilibrium was reached. Solutions of dyes with an initial concentration between 50 and 500 mg L⁻¹ and a dose of 3 g of Brewer's spent grains or 2 g of Orange peel per liter of solution were used. These suspensions were continuously stirred in a shaker with temperature controlled at 20°C for 24 h. Finally the equilibrium concentration of dye in the solution was determined. The experimental equilibrium concentrations in the liquid and solid phase were correlated using the Langmuir isotherm model.

2.5. Biosorption of Dyes

Adsorption Equilibrium of Dyes. 100 mL of solutions with different initial concentrations in the range 50–500 mg L⁻¹ were place in contact with 0.2 g of BSG or OP in Erlenmeyer flasks which were kept with agitation and temperature control (200 rpm, 25 ± 2°C) until the equilibrium was achieved. Finally, the equilibrium concentration of dye in the solution was determined.

Adsorption Kinetic of Dyes. 100 mL of dye solution with different initial concentrations (50, 200, and 500 mg L⁻¹) was placed in contact with 0.2 g of agroindustrial waste (BSG and OP), in Erlenmeyer flasks which were agitated and kept with controlled temperature (200 rpm, 25 ± 2°C). The dynamic process was identified through the evolution of residual concentration of dye in solution at different contact times, until the variation between two successive measurements was not significant.

pH of Adsorbent. 50 mL of solution KCl 1 M or of $CaCl_2$ 0.01 M was added to 0.2 g of agroindustrial wastes, and then, the flasks were maintained in a shaker with thermal control (25°C, 220 rpm) for 2 h. Finally the pH of each suspension was measured.

TABLE 1: Structure and properties of dyes.

Dye	Molecular weight g mol ⁻¹	Wavelength of maximum absorption nm	Structure
Basic Blue 41 (BB41)	482.57	617	
Acid Black 1 (AB1)	616.49	620	
Reactive Black 5 (RB5)	991.82	597	
Basic Blue 9 (Methylene Blue)	319.86	665	

2.6. *Parameter Estimation of Equilibrium and Kinetic Model.* The function was fitted by the method of Nonlinear-Least-Squares using the algorithm of Levenberg-Marquardt that minimizes the sum of the squares of the errors between the data points and the function. The statistical indicators used to assess convergence were the determination coefficient (R^2) and the quadratic sum of the residues ($\sum e^2$) by

$$R^2 = \frac{\sum_1^n (q_{\text{exp}} - \bar{q})^2 - \sum_1^n (q_{\text{exp}} - q_{\text{model}})^2}{\sum_1^n (q_{\text{exp}} - \bar{q})^2}, \quad (1)$$

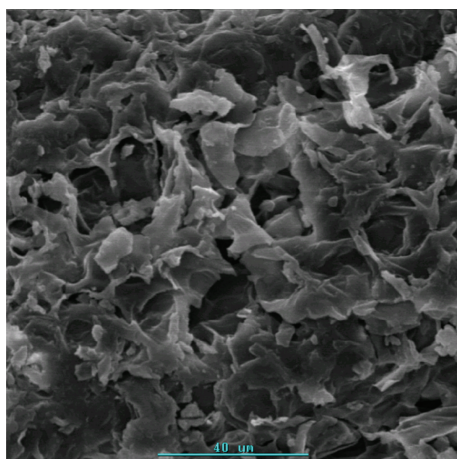
$$\sum e^2 = \sum_1^n (q_{\text{exp}} - q_{\text{model}})^2.$$

The resolution of algorithm was realized by Statistic 7.0 software.

2.7. *Analytical Assays.* The samples were centrifuged and the residual dye concentration in the supernatant was determined by measuring absorbance at maximum wavelength of each dye in a Helios Gamma UV-Vis spectrophotometer (UK).

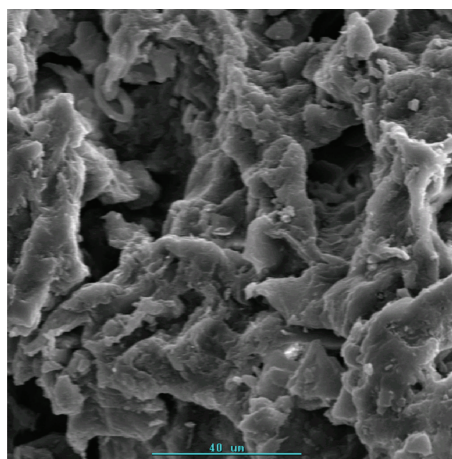
The adsorption capacity was determined using mass balance, applied to solid and liquid phases in accordance with the following:

$$q = \frac{V(C_0 - C)}{m}, \quad (2)$$



Accelerating voltage: 20Kev
Resolution: 1024x1024
Magnification: 1000
Pixel size: 0.118515 microns

(a) Brewer's spent grains



Accelerating voltage: 20Kev
Resolution: 1024x1024
Magnification: 1000
Pixel size: 0.118515 microns

(b) Orange peel

FIGURE 1: Analysis SEM of agroindustrial wastes.

TABLE 2: Chemical and physical characterization of adsorbents.

	Brewer's spent grains	Orange peel
Point of zero charge	5.3	3.5
pH_{water}	—	4.98 ± 0.00
$\text{pH}_{\text{KCl } 1.0 \text{ M}}$	4.80 ± 0.08	4.21 ± 0.04
$\text{pH}_{\text{CaCl}_2 \text{ } 0.01 \text{ M}}$	4.55 ± 0.10	4.67 ± 0.01
Surface acidity (NaOH) mmol g^{-1}	3.37 ± 0.02	2.58 ± 0.19
Surface basicity (HCl) mmol g^{-1}	3.16 ± 0.01	0.25 ± 0.07
Methylene Blue Index mg g^{-1}	64.9	178.7

where q is the adsorption capacity (mg g^{-1}), V is the solution volume (L), C_0 is the initial dye concentration (mg L^{-1}), and C is the dye concentration on time (mg L^{-1}).

3. Results and Discussion

3.1. Physical and Chemical Characterization of Adsorbent. The surface morphology of the particle wastes, Brewer's spent grains (Figure 1(a)) and Orange peel (Figure 1(b)), was analyzed by scanning electron microscopy. The micrographs revealed that the particles of Brewer's spent grains showed a rigid structure and higher density of macropores, while the particles of Orange peel are rather nonporous. The particles of both wastes have irregular shape and the textures of its surface are microrough.

The acid-base behavior of functional groups of the adsorbent surface plays a crucial role in interactions occurring during the process. The surface charge of the agroindustrial waste can be explained in terms of its pH_{pzc} value and of the concentration of acidic and basic sites at the particles surface. The acidic characteristic of activated carbon surface,

for example, is caused by the presence of carboxyl groups, lactones, and of phenolic hydroxyl groups [21]. Similarly the cellulose, one of the major components of agroindustrial waste, has a predominantly acid character because the hydrogen atoms of the hydroxyl groups act as electron acceptors [23]. Furthermore the principal components of the Orange peel, addition of the soluble material (41%) and other minor compounds, are cellulose (16%), hemicellulose (13.8%), pectin (14%), and protein (7.9%) [24, 25]. These components contain carboxyl and hydroxyl groups, causing the acid behavior of its surface. Brewer's spent grains contain principally cellulose (16–25%), hemicellulose (30%), lignin (7–27%), and protein (2.4–24%), its acid character being determined principally by phenolic hydroxyl groups present in the lignin [12]. The basic behavior of BSG is caused by the amine groups present in the protein.

Table 2 shows the value of pH_{pzc} and the basicity and acidity surface of Brewer's spent grains and Orange peel. The magnitude of these properties agrees with the values presented by other authors for this same type of wastes [25]. It can be seen that Orange peel has acid character higher than

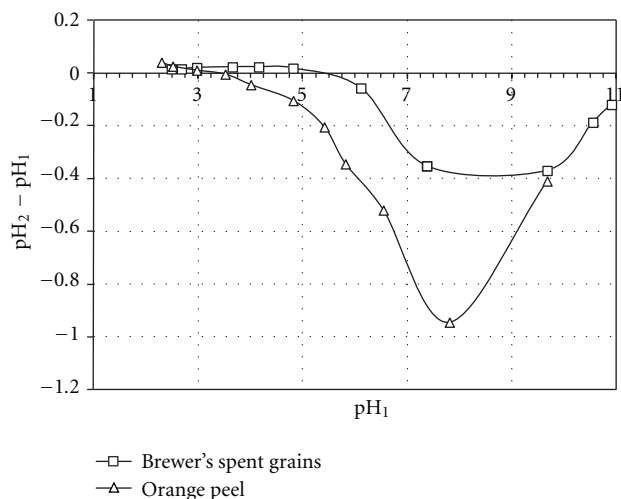


FIGURE 2: Zero charge point of agroindustrial wastes.

Brewer's spent grains. The acidic sites concentration of OP is 10 times higher than the sites with basic behavior while in BSG this relation is scarcely higher than one.

Consequently the zero-charge point of OP is less than BSG and corresponds to pH value of 3.5 (Figure 2). Then OP is classified as a biosorbent of acid type so that, when the pH of a solution is higher than the value of pH_{pzc} , the acid groups of pectin (galacturonic acid) are in the deprotonated form. Under this condition OP interacts preferentially with cationic species.

The complex structure of the agrowaste has similitude with the soil organic matter; that is, their functional groups contain electron pairs nonbinding that can interact with the protons present in the liquid phase in equilibrium; therefore in this case, the evaluation of surface acidity by measurement of pH can also show any fluctuation. This effect can be evaluated measuring the pH of suspensions in different saline solutions. The protocols of characterization of soils indicate to use KCl 1 M and $CaCl_2$ 0.01 M [26]. The results of pH drop between both measures ($pH_{water} - pH_{KCl\ 1.0\ M} = 0.77$ and $(pH_{water} - pH_{CaCl_2\ 0.01\ M}) = 0.31$, which were obtained for OP confirming that this is a biosorbent with strongly acidic character, coincide with the low value of pH_{pzc} (Table 2). In the first measurement, the pH drop is a consequence of the replacement of the hydrogen ions of the surface functional groups by the potassium from the solution, causing a decrease in the pH. Since $CaCl_2$ is a weak base, it causes an impoverishment in hydroxyl ions whose, although has an effect similar to increased of protons produced in the previous case, magnitude is lower.

The concentration of surface groups present in this type of lignocellulosic adsorbents is significantly higher than that found in commercial activated carbons. For example, commercial activated carbon F-400 (Calgon Carbon) exhibits a functional group concentration between 0.4 and 0.6 meq g^{-1} , with a slightly basic feature, which provides a zero charge point between 7.3 and 7.9 [2, 27].

The quality of adsorbents, activated carbons particularly, is evaluated in terms of their adsorptive power and superficial area. The Methylene Blue Index that quantifies the amount of dye necessary to cover the total surface of the particles is widely used to evaluate the active carbon and other alternative adsorbents. The nonpolar nature of the Methylene Blue molecule and its molecular size (8.4 Å) (Table 1) suggests that the adsorption occurs at the macropores and mesopores.

The Methylene Blue Index of Brewer's spent grains and the Orange peel is shown in Table 2. The values obtained confirm the observations of morphological analysis; that is, BSG has a mesoporous structure. These results are comparable with the Index of the active carbons prepared from sugarcane bagasse and coconut shell (79.6 and 10.5 $mg\ g^{-1}$, resp.) and less than the value of cellulose materials such as cotton [28, 29]

The estimation of specific surfaces of BSG and OP using the adsorption of Methylene Blue was 206.2 $m^2\ g^{-1}$ and 567.3 $m^2\ g^{-1}$, respectively. Both values obtained for other low-cost biosorbents, such as peanut shells, olive stones, bamboo cane, and date stones, have the same order of magnitude (368–394 $m^2\ g^{-1}$) [30].

3.2. Equilibrium Isotherm. The most widely models used to describe the adsorption equilibrium are the Langmuir [31] and Freundlich [32] isotherms, which are shown in (3) and (4), respectively:

$$q_e = \frac{q_{max} b C_e}{(1 + b C_e)}, \quad (3)$$

where q_{max} is the maximum adsorption capacity (complete monolayer) ($mg\ g^{-1}$) and b is associated with interaction energy between adsorbate and adsorbent ($L\ g^{-1}$):

$$q_e = k_F C_e^{1/n}, \quad (4)$$

where k_F is the equilibrium constant ($mg\ g^{-1}\ (L\ mg^{-1})^{1/n}$) and n is a parameter associated with the affinity between adsorbate and adsorbent.

Figures 3 and 4 show the dependence between equilibrium concentrations of both phases for adsorption of BB41, RB5, and AB1 dyes on Brewer's spent grains and Orange peel, respectively.

Additionally, the parameters and their standard deviations, obtained by fitting the Langmuir and Freundlich models, are shown in Tables 3 and 4. The experimental data adsorption equilibrium of dyes on BSG can be interpreted adequately by the Freundlich model ($R^2 > 0.96$), whereas with the Langmuir model a better quality of fit was obtained for the BB41 and RB5 adsorption on Orange peel ($R^2 > 0.97$). The values of maximum adsorption capacity of the dyes on OP are higher than BSG, 5, 2.5, and 2-fold for BB41, RB5, and AB1, respectively.

The magnitudes of b parameters of the Langmuir isotherm indicate that the interaction energies between the dyes and adsorption sites of the BSG, are greater than those obtained with BSG (Table 3), probably due to the acidic nature of this latter provided by the carboxylic functional groups. In the case of adsorption of RB5 on OP this

TABLE 3: Langmuir model parameters.

Dye	Brewer's spent grains				Orange peel			
	q_{\max} (mg g ⁻¹)	b (L mg ⁻¹)	R^2	$\sum e^2$	q_{\max} (mg g ⁻¹)	b (L mg ⁻¹)	R^2	$\sum e^2$
BB41	32.4 ± 2.3	0.021 ± 0.007	0.772	66.5	157.2 ± 4.2	0.021 ± 0.002	0.992	108.4
RB5	22.3 ± 1.9	0.0077 ± 0.0019	0.911	12.2	62.6 ± 14.8	0.0012 ± 0.0004	0.977	8.2
AB1	19.8 ± 0.3	0.019 ± 0.001	0.985	1.26	45.3 ± 7.5	0.0086 ± 0.0042	0.737	102.2

TABLE 4: Freundlich model parameters.

Dye	Brewer's spent grains				Orange peel			
	k_F (mg g ⁻¹)(mg L ⁻¹) ^{-1/n}	N	R^2	$\sum e^2$	k_F (mg g ⁻¹)(mg L ⁻¹) ^{-1/n}	n	R^2	$\sum e^2$
BB41	5.54 ± 0.70	3.51 ± 0.28	0.962	11.4	15.72 ± 3.06	2.50 ± 0.25	0.951	625.9
RB5	1.46 ± 0.26	2.42 ± 0.19	0.967	4.6	0.21 ± 0.06	1.31 ± 0.09	0.980	7.0
AB1	3.67 ± 0.43	3.77 ± 0.30	0.962	3.4	3.08 ± 1.39	2.42 ± 0.48	0.822	130.3

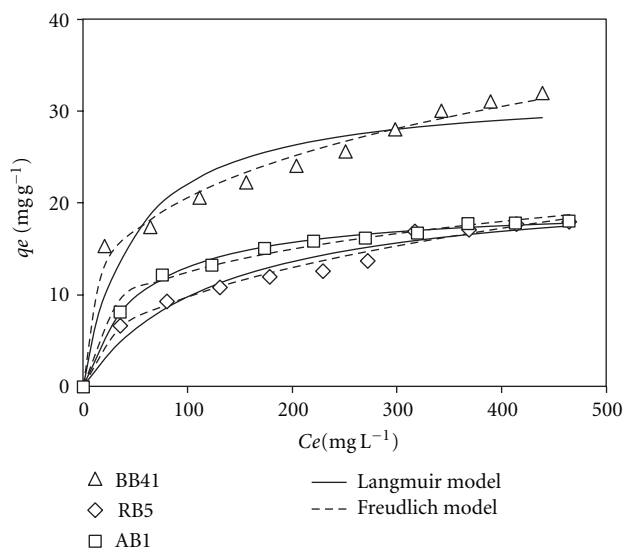


FIGURE 3: Adsorption isotherms of dyes on Brewer's spent grains. Experimental conditions: temperature: 25°C; pH (natural): 4.0 (BB41), 5.0 (RB5), 5.3 (AB1); particle size; 0.25–1.00 mm.

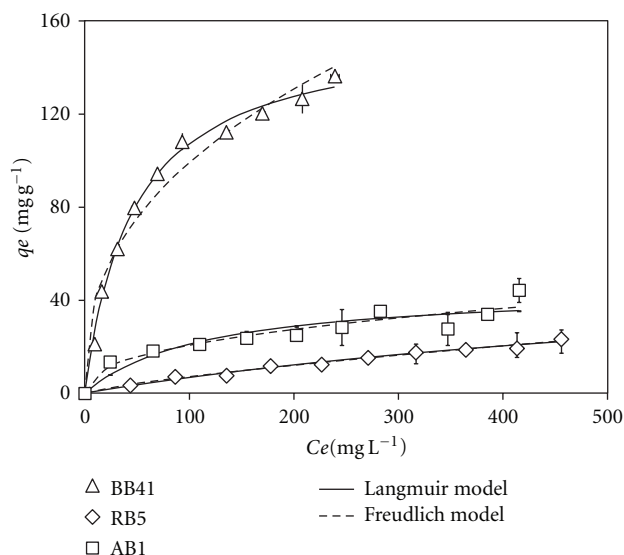


FIGURE 4: Adsorption isotherms of dyes on Orange peel. Experimental conditions: temperature 25°C; pH (natural): 4.4 (BB41), 5.5 (RB5), 4.9 (AB1); particle size: 0.25–1.00 mm.

parameter is 20 times lower with respect to the one obtained for the basic dye, whereby the isotherm is almost linear. The partition constant was estimated in 0.0528 with a correlation coefficient of 0.96. This means that the removal of dye by OP is only caused by a phenomenon of partition and the interactions occur primarily with adsorption sites existing on the outer surface of this waste. This result also is originated for the lower hydrophobicity and higher charge density that has RB5 in respect to the other dyes.

In another study performed with the orange peel, reported similar results for the adsorption of basic and acid dyes. The maximum adsorption capacity of acid dyes is between 40 and 65 mg g⁻¹, and the magnitude of the interaction parameters is equal to that obtained in this study (0.001–0.008 L mg⁻¹) [33]. On the other hand, the maximum adsorption capacity of malachite green on OP was determined in 483 mg g⁻¹ [34]. Similarly, the maximum

adsorption capacity reported for the acid dyes uptake (Acid Yellow 17 and Acid Blue 25) on Brewer's spent grains is equivalent to that obtained in this work [35].

Although both adsorbents have an adsorption capacity of dyes, of different ionic behavior, significantly lower than those reported for commercial activated carbon and that their interaction energies are also lower, they have a higher density of functional groups [1, 2, 26, 36]. In particular it has been reported that the adsorption capacity of RB5 by activated carbon is 175 mg g⁻¹ [37]. Despite this, the adsorption capacities obtained with the Orange peel indicate that its use in the removal of dyes from waste water can be an attractive option, especially for those of basic type.

3.3. Kinetic Modeling. The pseudo-second-order rate expression has been used to describe adsorption that involves valence forces through electrons shared or exchanged between

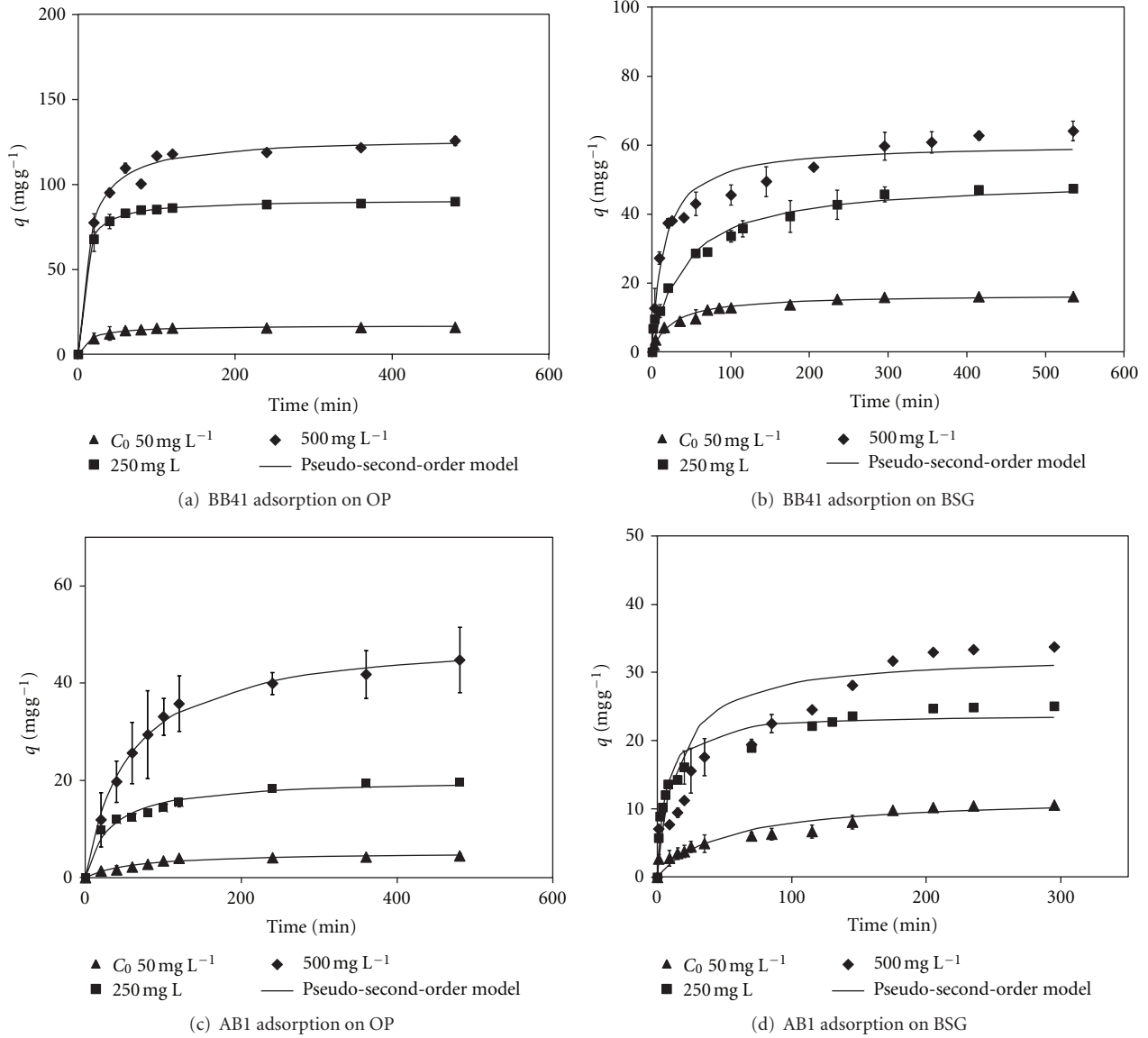


FIGURE 5: Kinetic modeling of dye adsorption on agroindustrial wastes.

the adsorbent and adsorbate, such as covalent interactions and ion exchange [38]. Recently this kinetic model (5) has been successfully applied to the adsorption of pollutants from aqueous solutions:

$$\frac{dq}{dt} = k_2 (q_e - q)^2, \quad (5)$$

where k_2 is the pseudo-second-order rate constant ($\text{g mg}^{-1} \text{min}^{-1}$), q_e is the amount of dye adsorbed at equilibrium (mg g^{-1}), and q is the amount of dye adsorbed at time t (mg g^{-1}).

Equation (6) is obtained by integrating (5) using the boundary conditions $t = 0$ to $t = t$ and $q = 0$ to $q = q$:

$$q = q_e \left[1 - \frac{1}{(1 + k_2 q_e t)} \right]. \quad (6)$$

The progress curve of the adsorption capacity (6) was properly interpreted by the pseudo-second-order model (Figure 5); the coefficients of determination are in the range 0.90–0.99. The results indicate that the adsorption capacity was increasing to the extent that the initial concentration of dye was higher because the driving force has been enhanced. However, for the adsorption of dyes onto BSG using the greater initial concentration (500 mg L^{-1}), the intraparticle diffusion restriction appears very early, which is consistent with the porous morphology of this adsorbent. The diffusive control intraparticle is more notable to the extent that the molecular weight increases. Figures 5(b) and 5(d) show the adsorption of BB41 and AB1 whose ratio of molecular weights is 1 : 1.3 (Table 1). Therefore this effect is manifested most significantly with the dye RB5.

TABLE 5: Parameters of pseudo second order model.

Basic Blue 41					
C_0 (mg L ⁻¹)		q_e (mg g ⁻¹)	$k_2 * 10^3$ (g mg ⁻¹ min ⁻¹)	R^2	$\sum e^2$
50	BSG	16.67 ± 0.51	2.30 ± 0.39	0.979	8.23
	OP	16.87 ± 0.29	4.08 ± 0.51	0.992	1.75
250	BSG	49.88 ± 2.06	0.51 ± 0.11	0.972	97.03
	OP	91.15 ± 0.33	1.67 ± 0.68	0.999	2.89
500	BSG	60.38 ± 2.09	1.08 ± 0.23	0.952	225.96
	OP	127.46 ± 2.60	0.61 ± 0.09	0.989	143.81
Acid Black 1					
50	BSG	11.85 ± 1.02	1.68 ± 0.59	0.904	14.52
	OP	5.21 ± 0.33	2.98 ± 0.76	0.961	0.78
250	BSG	23.87 ± 0.80	6.97 ± 1.35	0.948	44.95
	OP	20.26 ± 0.82	1.57 ± 0.32	0.971	8.66
500	BSG	32.65 ± 1.77	2.04 ± 0.62	0.920	135.85
	OP	49.85 ± 1.05	0.36 ± 0.03	0.995	9.15
Reactive Black 5					
50	BSG	10.07 ± 0.46	7.30 ± 0.13	0.990	1.18
	OP	3.18 ± 0.10	3.40 ± 0.39	0.993	0.05
250	BSG	17.38 ± 0.61	0.62 ± 0.09	0.991	3.32
	OP	20.03 ± 0.34	1.87 ± 0.17	0.994	1.67
500	BSG	97.5 ± 35.10	0.01 ± 0.00	0.975	81.73
	OP	40.32 ± 2.37	0.46 ± 0.11	0.958	47.89

The decay curves of RB5 concentration (C/C_0 against t) obtained for adsorption on OP at different initial concentrations of dye, overlap. This result indicates the absence of diffusion intraparticle, and therefore, the process is governed only by the external mass transfer. The high molecular weight of RB5 and the structure nonporous of OP are the causes of this behavior.

The parameters of pseudo-second-order model, q_e and k_2 , and their standard deviations are shown in Table 5. The equilibrium adsorption capacity of OP was higher than BSG; specifically the values for BB41, RB5 and AB1, are respectively, 6-, 2.5- and 2-fold higher. The equilibrium capacities for both adsorbents increase as the initial dye concentration is increased. The kinetic parameter k_2 , obtained for Orange peel, decreases steadily to the extent that the initial dye concentration increased, while for BSG it does not show a clear trend as a consequence of the restrictions imposed by the diffusion intraparticle.

4. Conclusion

The present study shows that the agroindustrial wastes biomass such Orange peel and Brewer's spent grains has significant potential as biosorbents for the removal of basic dyes from its aqueous solution, because their surfaces are predominantly negatively charged. The results indicated that the Orange peel presented a higher maximum capacity of adsorption than Brewer's spent grains for the cationic dye, Basic Blue 41, as well as for the anionic dyes, Acid Black 1, and Reactive Black 5.

Acknowledgment

This work was funded by Chilean Agency Fondecyt, Project 1090098.

References

- [1] P. C. C. Faria, J. J. M. Orfão, and M. F. R. Pereira, "Adsorption of anionic and cationic dyes on activated carbons with different surface chemistries," *Water Research*, vol. 38, no. 8, pp. 2043–2052, 2004.
- [2] Y. S. Al-Degs, M. I. El-Barghouthi, A. H. El-Sheikh, and G. M. Walker, "Effect of solution pH, ionic strength, and temperature on adsorption behavior of reactive dyes on activated carbon," *Dyes and Pigments*, vol. 77, no. 1, pp. 16–23, 2008.
- [3] R. Kant and V. K. Rattan, "Adsorption of dye Green B from a textile industry effluent using two different samples of activated carbon by static batch method and continuous process," *Indian Journal of Chemical Technology*, vol. 16, no. 3, pp. 240–244, 2009.
- [4] Y. S. Al-Degs, M. A. M. Khraisheh, S. J. Allen, and M. N. Ahmad, "Adsorption characteristics of reactive dyes in columns of activated carbon," *Journal of Hazardous Materials*, vol. 165, no. 1–3, pp. 944–949, 2009.
- [5] V. Vadivelan and K. Vasanth Kumar, "Equilibrium, kinetics, mechanism, and process design for the sorption of methylene blue onto rice husk," *Journal of Colloid and Interface Science*, vol. 286, no. 1, pp. 90–100, 2005.
- [6] B. H. Hameed, D. K. Mahmoud, and A. L. Ahmad, "Equilibrium modeling and kinetic studies on the adsorption of basic dye by a low-cost adsorbent: coconut (*Cocos nucifera*) bunch

- waste," *Journal of Hazardous Materials*, vol. 158, no. 1, pp. 65–72, 2008.
- [7] A. S. Franca, L. S. Oliveira, and M. E. Ferreira, "Kinetics and equilibrium studies of methylene blue adsorption by spent coffee grounds," *Desalination*, vol. 249, no. 1, pp. 267–272, 2009.
- [8] S. Patil, S. Renukdas, and N. Patel, "Removal of methylene blue, a basic dye from aqueous solutions by adsorption using teak tree (*Tectona grandis*) bark powder," *International Journal of Environmental Sciences*, vol. 1, no. 5, pp. 711–726, 2011.
- [9] V. K. Gupta and Suhas, "Application of low-cost adsorbents for dye removal—a review," *Journal of Environmental Management*, vol. 90, no. 8, pp. 2313–2342, 2009.
- [10] G. Y. S. Mtui, "Recent advances in pretreatment of lignocellulosic wastes and production of value added products," *African Journal of Biotechnology*, vol. 8, no. 8, pp. 1398–1415, 2009.
- [11] S. I. Mussatto, G. Dragone, and I. C. Roberto, "Brewers' spent grain: generation, characteristics and potential applications," *Journal of Cereal Science*, vol. 43, no. 1, pp. 1–14, 2006.
- [12] S. Aliyu and M. Bala, "Brewer's spent grain: a review of its potentials and applications," *African Journal of Biotechnology*, vol. 10, no. 3, pp. 324–331, 2011.
- [13] V. Jaikumar, "Biosorption of acid yellow by spent brewery grains in a batch system: equilibrium and kinetic modelling," *International Journal of Biology*, vol. 1, no. 1, pp. 21–29, 2009.
- [14] J. P. Silva, S. Sousa, I. Gonçalves, J. J. Porter, and S. Ferreira-Dias, "Modelling adsorption of acid orange 7 dye in aqueous solutions to spent brewery grains," *Separation and Purification Technology*, vol. 40, no. 2, pp. 163–170, 2004.
- [15] G. Annadurai, R. S. Juang, and D. J. Lee, "Use of cellulose-based wastes for adsorption of dyes from aqueous solutions," *Journal of Hazardous Materials*, vol. 92, no. 3, pp. 263–274, 2002.
- [16] C. Palma, E. Contreras, J. Urra, and M. J. Martínez, "Eco-friendly technologies based on banana peel use for the decolorization of the dyeing process wastewater," *Waste and Biomass Valorization*, vol. 2, no. 1, pp. 77–86, 2010.
- [17] R. Sivaraj, C. Namasivayam, and K. Kadirvelu, "Orange peel as an adsorbent in the removal of Acid violet 17 (acid dye) from aqueous solutions," *Waste Management*, vol. 21, no. 1, pp. 105–110, 2001.
- [18] F. A. Pavan, Y. Gushikem, A. C. Mazzocato, S. L. P. Dias, and E. C. Lima, "Statistical design of experiments as a tool for optimizing the batch conditions to methylene blue biosorption on yellow passion fruit and mandarin peels," *Dyes and Pigments*, vol. 72, no. 2, pp. 256–266, 2007.
- [19] B. H. Hameed, D. K. Mahmoud, and A. L. Ahmad, "Sorption of basic dye from aqueous solution by pomelo (*Citrus grandis*) peel in a batch system," *Colloids and Surfaces A*, vol. 316, no. 1–3, pp. 78–84, 2008.
- [20] S. Hamid, Z. Mahmood, M. Imran, A. Saeed, and S. R. Gillani, "Potentiality of lemon peel as low cost adsorbent for the removal of trypan blue dye from aqueous solution," *Journal of the Chemical Society of Pakistan*, vol. 33, no. 3, pp. 364–369, 2011.
- [21] H. P. Boehm, "Some aspects of the surface chemistry of carbon blacks and other carbons," *Carbon*, vol. 32, no. 5, pp. 759–769, 1994.
- [22] P. B. Navas and A. Carrasquero, "Cargas eléctricas superficiales y propiedades adsorbentes del salvado de arroz," *Revista Facultad Agronomía (Maracay)*, vol. 26, no. 2, pp. 149–161, 2000.
- [23] M. A. Tshabalala, "Determination of the acid-base characteristics of lignocellulosic surfaces by inverse gas chromatography," *Journal of Applied Polymer Science*, vol. 65, no. 5, pp. 1013–1020, 1997.
- [24] D. Mamma, E. Kourtoglou, and P. Christakopoulos, "Fungal multienzyme production on industrial by-products of the citrus-processing industry," *Bioresource Technology*, vol. 99, no. 7, pp. 2373–2383, 2008.
- [25] X. Li, Y. Tang, X. Cao, D. Lu, F. Luo, and W. Shao, "Preparation and evaluation of orange peel cellulose adsorbents for effective removal of cadmium, zinc, cobalt and nickel," *Colloids and Surfaces A*, vol. 317, no. 1–3, pp. 512–521, 2008.
- [26] R. K. Schofield and A. W. Taylor, "The measurement of soil pH," *Soil Science Society American Proceedings*, vol. 19, pp. 164–167, 1955.
- [27] E. N. El Qada, S. J. Allen, and G. M. Walker, "Adsorption of basic dyes from aqueous solution onto activated carbons," *Chemical Engineering Journal*, vol. 135, no. 3, pp. 174–184, 2008.
- [28] E. F. Jaguaribe, L. L. Medeiros, M. C. S. Barreto, and L. P. Araujo, "The performance of activated carbons from sugarcane bagasse, babassu, and coconut shells in removing residual chlorine," *Brazilian Journal of Chemical Engineering*, vol. 22, no. 1, pp. 41–47, 2005.
- [29] C. Kaeprasit, E. Hequet, N. Abidi, and J. Gourlot, "Quality measurements: applications of methylene blue adsorption to cotton fiber specific surface area measurement: part I. methodology," *The Journal of Cotton Science*, vol. 2, no. 4, pp. 164–173, 1998.
- [30] H. El Bakouri, J. Morillo, J. Usero, and A. Ouassini, "Potential use of organic waste substances as an ecological technique to reduce pesticide ground water contamination," *Journal of Hydrology*, vol. 353, no. 3–4, pp. 335–342, 2008.
- [31] I. Langmuir, "The adsorption of gases on plane surfaces of glass, mica and platinum," *The Journal of the American Chemical Society*, vol. 40, no. 9, pp. 1361–1403, 1918.
- [32] H. Freundlich, "Of the adsorption of gases. Section II. Kinetics and energetics of gas adsorption," *Transactions of the Faraday Society*, vol. 28, pp. 195–201, 1932.
- [33] H. Benaïssa, "Removal of acid dyes from aqueous solutions using orange peel as a sorbent material," in *Proceedings of the 9th International Water Technology Conference (IWTC'05)*, p. 1175, Sharm El-sheikh, Egypt, 2005.
- [34] K. V. Kumar and K. Porkodi, "Batch adsorber design for different solution volume/adsorbent mass ratios using the experimental equilibrium data with fixed solution volume/adsorbent mass ratio of malachite green onto orange peel," *Dyes and Pigments*, vol. 74, no. 3, pp. 590–594, 2007.
- [35] V. Jaikumar, K. S. Kumar, and D. G. Prakash, "Biosorption of acid dyes using spent brewery grains: characterization and modeling," *International Journal of Applied Science and Engineering*, vol. 7, no. 2, pp. 115–125, 2009.
- [36] A. Rodríguez, J. García, G. Ovejero, and M. Mestanza, "Adsorption of anionic and cationic dyes on activated carbon from aqueous solutions: equilibrium and kinetics," *Journal of Hazardous Materials*, vol. 172, no. 2–3, pp. 1311–1320, 2009.
- [37] A. W. M. Ip, J. P. Barford, and G. McKay, "Reactive black dye adsorption/desorption onto different adsorbents: effect of salt, surface chemistry, pore size and surface area," *Journal of Colloid and Interface Science*, vol. 337, no. 1, pp. 32–38, 2009.
- [38] Y. S. Ho and G. McKay, "A Comparison of chemisorption kinetic models applied to pollutant removal on various sorbents," *Process Safety and Environmental Protection*, vol. 76, no. 4, pp. 332–340, 1998.

Research Article

Utilization of Agrowaste Polymers in PVC/NBR Alloys: Tensile, Thermal, and Morphological Properties

Ahmad Mousa,¹ Gert Heinrich,² Bernd Kretzschmar,² Udo Wagenknecht,² and Amit Das²

¹ Department of Materials Engineering, Faculty of Engineering, Al Balqa Applied University, Salt 19117, Jordan

² Leibniz-Institut für Polymerforschung Dresden e.V., Hohe Straße 6, 01069 Dresden, Germany

Correspondence should be addressed to Ahmad Mousa, mousa@rocketmail.com

Received 11 October 2011; Revised 25 January 2012; Accepted 2 February 2012

Academic Editor: Licínio M. Gando-Ferreira

Copyright © 2012 Ahmad Mousa et al. This is an open access article distributed under the Creative Commons Attribution License, which permits unrestricted use, distribution, and reproduction in any medium, provided the original work is properly cited.

Poly(vinyl chloride)/nitrile butadiene rubber (PVC/NBR) alloys were melt-mixed using a Brabender Plasticorder at 180°C and 50 rpm rotor speed. Alloys obtained by melt mixing from PVC and NBR were formulated with wood-flour- (WF-) based olive residue, a natural byproduct from olive oil extraction industry. WF was progressively increased from 0 to 30 phr. The effects of WF loadings on the tensile properties of the fabricated samples were inspected. The torque rheometry, which is an indirect indication of the melt strength, is reported. The pattern of water uptake for the composites was checked as a function WF loading. The fracture mode and the quality of bonding of the alloy with and without filler are studied using electron scanning microscope (SEM).

1. Introduction

Polymer alloys continue to represent a field of intensive research. One of the most common blends in the modern sense is PVC with NBR [1, 2]. Due to the miscible nature of PVC/NBR blend as evidenced from single glass transition (T_g) the soft blend of PVC/NBR can be categorized as a thermoplastic elastomer (TPE) and more specifically as a melt processable rubber (MPR) [3–5]. Fillers are incorporated mainly to improve service properties or to reduce material cost depending on the source of filler, type of filler, method of preparation, and treatment. Very large quantities of the natural lignocelluloses polymers are produced annually as agrowastes. A very small amount is used as antioxidants or fillers in polymers. The rest is used almost as fuel to generate energy. The field of wood-based agrowastes polymer composites is extensively reviewed in the open literature [5–8]. Recently, we report the effect of virgin olive pomace on the flexural and thermal performance of toughened PVC composites [9]. We found that the virgin olive pomace enhanced the flexural properties to a certain extent, which was due to the hydrogen bond formation, while the thermal stability was improved due to the phenolic hydroxyl group within the lignocellulosic powder. In this work, the effect of

wood-flour-based olive residue on the tensile properties, water absorption and morphology of PVC/NBR alloys are reported in the current investigation.

2. Experimental

2.1. Materials and Formulation. Acrylonitrile nitrile rubber with 34% acrylo content was supplied by Bayer AG, Germany. Suspension PVC grade in powder form with a k -value of 67 was supplied by SABIC of Saudi Arabia and stabilized with lead salt. Wood-flour-based agrowastes with particle size equal or less than 45 μm were used as received. The WF-based olive mill residue has been fully characterized and reported earlier; the major reactive functional group with its structure was the hydroxyl group from the cellulose and hemicellulose [10, 11]. The samples were formulated according to the following recipe: NBR: 20% PVC: 80%, WF: various in part per hundred-part polymer (phr), that is, the filler loading was based on the total amount of resin (PVC) and elastomer (NBR), which is 100 parts.

2.2. Sample Preparation. Mixing was carried out at 180°C and 50 $\text{rev} \cdot \text{min}^{-1}$ rotor speed using a computerized

brabender plasticorder Model PLE 331 for 8 minutes. The NBR was initially loaded into the mixing chamber of Brabender for one minute, followed by PVC and the wood flour.

2.3. Torque Rheometry. Melt rheological properties of the prepared blends were evaluated using a Brabender Plasticorder at the predetermined mixing variables. Mixing was continued until torque and temperature were stabilized to constant values of 8–10 min at 50 rev/min as the optimum mixing shear. The effect of WF loading on the shear heating (ΔT) in a Brabender Plasticorder results in temperature rise given as: $\Delta T = \text{melt temperature} - \text{set temperature}$. Mixing was performed until constant stabilization torque and temperatures values were recorded.

2.4. Tensile Properties. Tensile properties were carried out according to ASTM D638. The dumbbells specimens were cut from 2 mm thick molded sheets of wood-flour-filled PVC/NBR alloys. Five specimens were tested, and the median value was taken for each formulation.

2.5. Water Absorption. 2 mm thick rectangular samples were weighed in air. The samples were immersed in distilled water for seven days at room temperature. The samples were removed from water, wiped with tissue paper, and reweighed. The % water uptake was calculated according to the following equation:

$$\% \text{ Water uptake} = \frac{W_2 - W_1}{W_1} \times 100, \quad (1)$$

where W_1 is the sample weight in air and W_2 is the weight after immersion. The average of three samples was calculated.

2.6. Thermal Analysis. The composites were scanned by a Perkin-Elmer DSC-6 differential scanning calorimeter (DSC) in the range of -40 to 100°C at heating rate of $5^\circ\text{C}/\text{min}$.

2.7. Failure Mode. To check the failure mode and the quality of bonding the surfaces of the tensile fractured samples were viewed under scanning electron microscope (SEM) model (geol Tokyo, Japan). The specimens were sputtered with Au-Pd alloy prior to scanning to avoid electrostatic charges.

3. Results and Discussions

Figure 1 shows the effect of WF loading on tensile modulus of PVC/NBR alloy. It can be seen that tensile modulus increased steadily with filler loading. This trend is in line with earlier work on rigid and toughened PVC [9, 10]. The observed trend recorded in Figure 1 could be attributed to the reduction in free volume between the chains of the PVC/NBR alloy. Reduction in the free volume with filler loading leads to the observed trend shown in Figure 1. Figure 2 shows the influence of WF on the yield tensile strength of the PVC/NBR alloy as a function of filler loading. It is clear that the yield tensile strength decreased with WF loading.

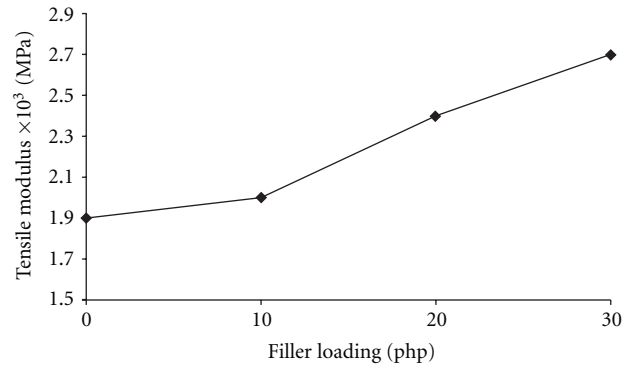


FIGURE 1: The influence of filler loading on tensile modulus of PVC/NBR alloy.

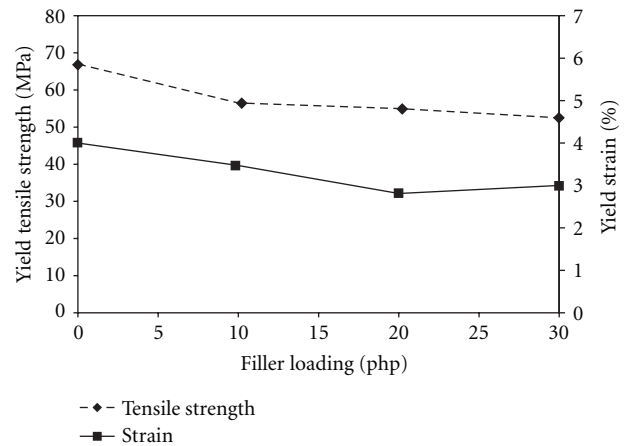


FIGURE 2: The influence of filler loading on the yield tensile strength of PV/NBR alloy.

Such observation might be due to the inability of WF to transfer the stress, possibly due to improper filler dispersion in the matrix and moisture pick-up which lead to insufficient interfacial bonding between the alloy and the filler.

Similar trends were recorded in the case of percentage strain at yield shown in Figure 2. Again this might be due to the rigidity of the PVC/NBR filled with WF due to the rigidity of the filler itself. The progress of the stock temperature as a function of WF loading is represented in Figure 3 for the PVC/NBR alloy. One can see that the stock temperature increased with WF loading over the set processing conditions. However, the extensive shearing causes the stock temperature to rise steeply above the mixing temperature even at the end of the 8th min of the mixing time, until the stock temperature undergoes a steady value. Interestingly, the equilibrium torque displayed in Figure 3, which is an indirect indication of the melt strength, showed a higher value with addition of WF as compared to the control sample. This suggested that the addition of WF has slightly restricted the mobility of the alloy due to the interaction between the matrix and the filler and hence increased the

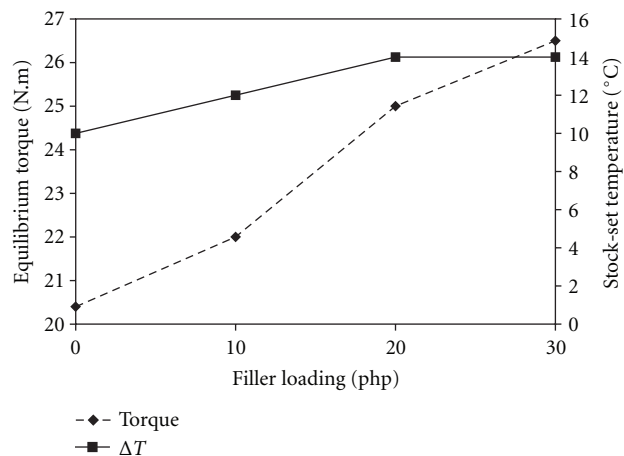


FIGURE 3: The influence of WF loading on the equilibrium torque and stock temperature of PV/NBR alloy.

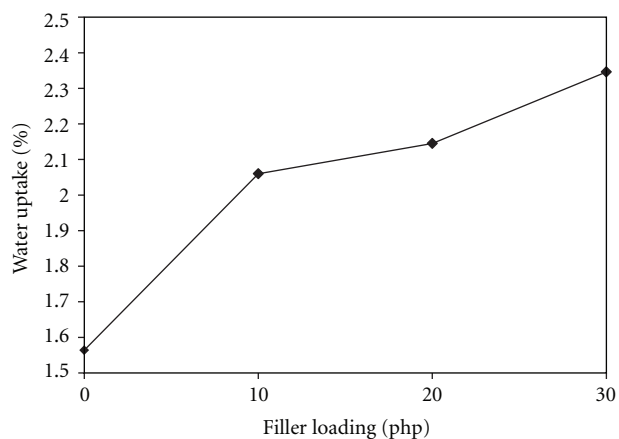


FIGURE 4: The influence of WF loading on % water uptake of PV/NBR alloy.

melt strength. Such finding suggests that certain types of interactions between the filler and the matrix have occurred, such interactions are expected to slightly restrict the mobility of the alloy chains and increased the torque. Figure 4 shows the water absorption behavior of the PVC/NBR alloy as a function of filler loading. It can be seen that water absorption has increased with WF content. This is mainly due to hydroxyl content of the WF. The low uptake in case of the unfilled composite could be due to the hydrophobic nature of the polymer.

3.1. Thermal Analysis. Figure 5 illustrates DSC curves (first run) for PVC/NBR control and for the composite with WF at 20 php loading of filler loading. Looking at the DSC curves presented in Figure 5 at the -40 – 90°C temperature interval, one can see that the endotherm peak was detected. Such peak was shifted to the right by the incorporation of the WF loading. One may conclude that this peak is caused by

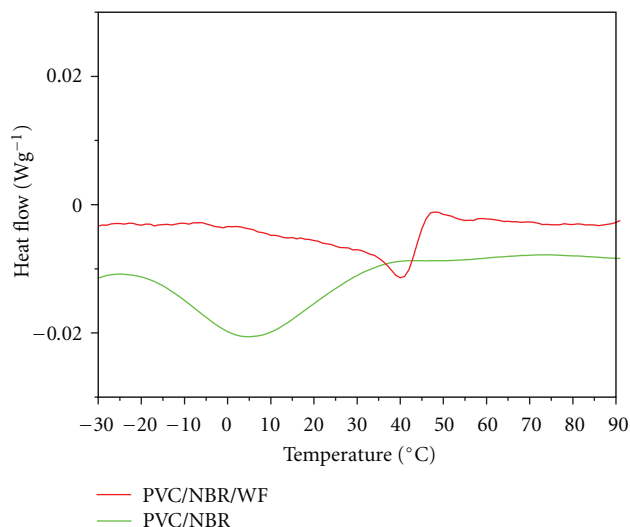


FIGURE 5: DSC traces of PVC/NBR alloy with and without WF.

molecular relaxation of the PVC/NBR alloy. Note that the addition of WF has delayed the molecular relaxation of the alloy. This should be related to the interaction between the WF and the PVC/NBR alloy via polar-polar interaction as reported earlier [9, 10].

3.2. SEM. Interfacial interactions and the strength of adhesion determine micromechanical deformation processes and the failure mode of the composites [11, 12]. The SEM micrographs that were taken from the surfaces of broken specimens offer indirect information about the failure mode and bonding quality. Figure 6(a) presents the fracture surface of the plain blend. It can be seen that the system is one phase with some particles that come from ingredients added to the PVC compound such as stabilizers and so forth. Figure 6(b) shows the fracture surface of sample with 10 php filler. It can be seen that the wood is covered with the polymer and the relatively small number of holes related to debonding or fiber pull-out indicates good adhesion. On the other hand, the opposite is observed in composites prepared with the higher amounts of filler doses, namely, 20 and 30 php loading, respectively, as shown in Figures 6(c) and 6(d). The number of debonded particles is quite large, the contours of particles remaining on the surface of the matrix are sharp, and adhesion seems to be poor, at least compared to Figure 6(b).

4. Conclusions

Based on this paper it can be concluded that pristine WF has improved the tensile modulus of the blend whereas the tensile strength remained more or less the same. It also can be concluded that the filler has good degree of interactions as indicated by the torque data obtained from the Brabender plasticorder. The DSC traces showed that the molecular relaxation of the blend was hindered with the presence of the WF. SEM micrographs showed that the failure mode was due

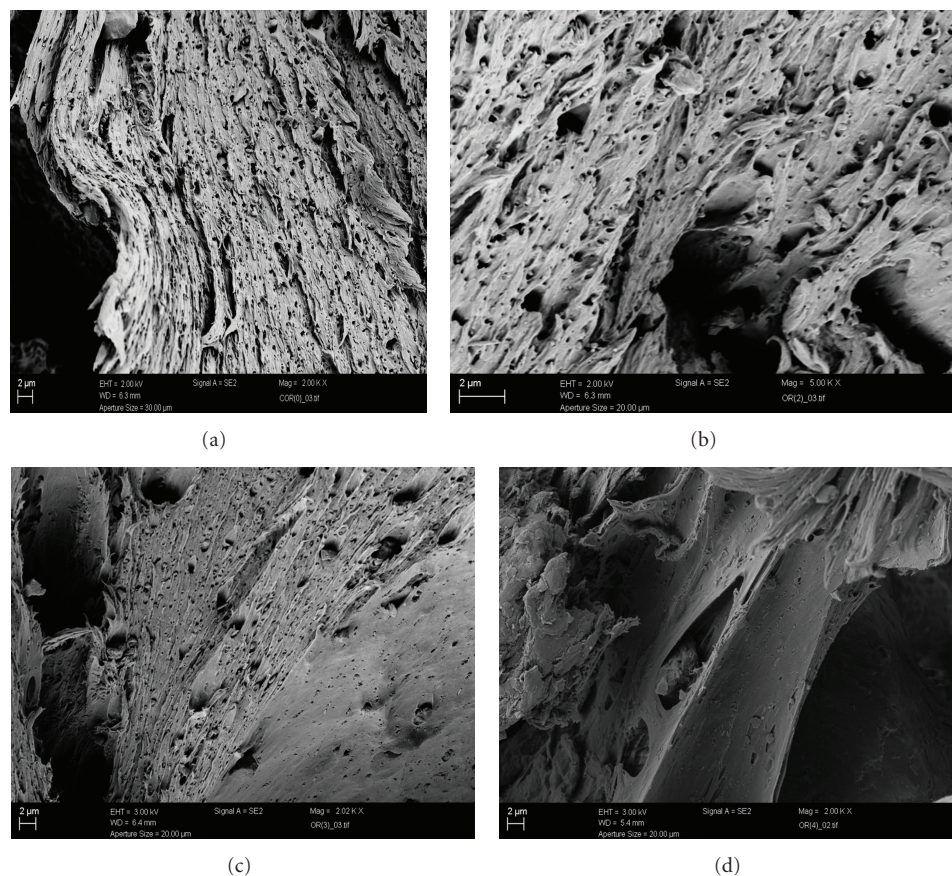


FIGURE 6: Scanning electron microscope images of (a) plain PVC/NBR alloy (b) PVC/NBR at 10 php filler loading, (c) 20 php filler, and (d) 30 php filler.

to the pull-out of the filler; furthermore, higher loading of the WF has led to agglomeration.

References

- [1] L. A. Utracki, D. J. Walsh, and R. A. Weiss, "Polymer alloys, blends, and Ionomers: an overview," in *Multiphase Polymers: Blends and Ionomers*, L. A. Utracki and R. A. Weiss, Eds., vol. 395 of *ACS symposium Series*, pp. 1–35, American Chemical Society, Washington, DC, USA, 1989.
- [2] K. T. Varughese, P. P. De, S. K. Sanyal, and S. K. De, "Miscible blends from plasticized poly(vinyl chloride) and epoxidized natural rubber," *Journal of Applied Polymer Science*, vol. 37, no. 9, pp. 2537–2548, 1989.
- [3] Y. Song, Q. Zheng, and C. Liu, "Green biocomposites from wheat gluten and hydroxyethyl cellulose: processing and properties," *Industrial Crops and Products*, vol. 28, no. 1, pp. 56–62, 2008.
- [4] G. Siracusa, A. D. la Rosa, V. Siracusa, and M. Trovato, "Eco-compatible use of olive husk as filler in thermoplastic composites," *Journal of Polymers and the Environment*, vol. 9, no. 4, pp. 157–161, 2001.
- [5] A. Abu Bakar, A. Hassan, and A. F. M. Yusof, "Effect of oil palm empty fruit bunch and acrylic impact modifier on mechanical properties and processability of unplasticized poly (vinyl chloride) composites," *Polymer-Plastics Technology and Engineering*, vol. 44, pp. 1125–1137, 2005.
- [6] H. D. Rozman, G. S. Tay, R. N. Kumar, A. Abusamah, H. Ismail, and Z. A. Mohd, "The effect of oil extraction of the oil palm empty fruit bunch on the mechanical properties of polypropylene-oil palm empty fruit bunch-glass fibre hybrid composites," *Polymer-Plastics Technology and Engineering*, vol. 40, no. 2, pp. 103–115, 2001.
- [7] Z. A. M. Ishak, A. Aminullah, H. Ismail, and H. D. Rozman, "Effect of silane-based coupling agents and acrylic acid based compatibilizers on mechanical properties of oil palm empty fruit bunch filled high-density polyethylene composites," *Journal of Applied Polymer Science*, vol. 68, no. 13, pp. 2189–2203, 1998.
- [8] L. Avérous and F. le Digabel, "Properties of biocomposites based on lignocellulosic fillers," *Carbohydrate Polymers*, vol. 66, no. 4, pp. 480–493, 2006.
- [9] A. Mousa, G. Heinrich, U. Gohs, R. Hässler, and U. Wagenknecht, "Application of renewable agro-waste-based olive pomace on the mechanical and thermal performance of toughened PVC," *Polymer-Plastics Technology and Engineering*, vol. 48, no. 10, pp. 1030–1040, 2009.
- [10] A. Mousa, G. Heinrich, and U. Wagenknecht, "Thermoplastic composites based on renewable natural resources: unplasticized PVC/olive husk," *International Journal of Polymeric Materials*, vol. 59, no. 11, pp. 843–853, 2010.

- [11] T. G. Vladkova, P. D. Dineff, and D. N. Gospodinova, "Wood flour: a new filler for the rubber processing industry. II. Cure characteristics and mechanical properties of NBR compounds filled with corona-treated wood flour," *Journal of Applied Polymer Science*, vol. 91, no. 2, pp. 883–889, 2004.
- [12] L. Fama, A. Mônica, B. Q. Bittante, P. J. A. Sobral, S. Goyanes, and L. N. Gerschenson, "Garlic powder and wheat bran as fillers: their effect on the physicochemical properties of edible biocomposites," *Materials Science and Engineering C*, vol. 30, no. 6, pp. 853–859, 2010.

Research Article

Application of Chemically Modified and Unmodified Waste Biological Sorbents in Treatment of Wastewater

John Kanayochukwu Nduka

Environmental Chemistry and Toxicology Research Unit, Pure & Industrial Chemistry Department, Nnamdi Azikiwe University, PMB 5025, Anambra State, Awka 420001, Nigeria

Correspondence should be addressed to John Kanayochukwu Nduka, johnnduka2000@yahoo.co.uk

Received 12 October 2011; Revised 10 February 2012; Accepted 13 February 2012

Academic Editor: Licínio M. Gando-Ferreira

Copyright © 2012 John Kanayochukwu Nduka. This is an open access article distributed under the Creative Commons Attribution License, which permits unrestricted use, distribution, and reproduction in any medium, provided the original work is properly cited.

Protein wastes (feathers, goat hair) and cellulosic wastes (corn cob, coconut husks) were collected and washed with detergent solution, thoroughly rinsed and sun dried for 2 days before drying in an oven, and then ground. One-half of ground material was carbonized at a maximum temperature of 500°C after mixing with H₂SO₄. The carbonized parts were pulverized; both carbonized and uncarbonized sorbents were sieved into two particle sizes of 325 and 625 µm using mechanical sieve. Sorbents of a given particle size were packed into glass column. Then, textile wastewater that had its physicochemical parameters previously determined was eluted into each glass column and a contact time of 60 and 120 mins was allowed before analysis. Results showed 48.15–99.98 percentage reduction of NO₃⁻, EC, Cl⁻, BOD, COD, DO, TSS, and TDS, 34.67–99.93 percentage reduction of NO₃⁻, EC, Cl⁻, BOD, COD, DO, TSS, and TDS, 52.83–97.95 percentage reduction of Pb²⁺, Ni²⁺, Cr³⁺ and Mn²⁺ and 34.59–94.87 percentage reduction of Pb²⁺, Ni²⁺, Cr³⁺ and Mn²⁺. Carbonization, small particle, size and longer contact time enhanced the sorption capabilities of the sorbents. These show that protein and cellulosic wastes can be used to detoxify wastewater.

1. Introduction

Wastewater may be purely domestic or may contain some industrial wastewater as well [1]. Residential wastewater is a combination of excreta, flush water, and all types of wastewater generated from household. It is more commonly known as sewage and much diluted. There are two types of domestic sewage: black water or wastewater from toilets and gray water, which is wastewater from all sources except toilets [2]. Industrial wastewater comes from commercial activities (shops, restaurants, fast food shops, hospitals, etc.), industries (e.g., chemical industries, pharmaceutical companies, textile manufacturing, etc.), agriculture (e.g., Slurry), and so forth. Wastewaters from dyeing operations are characterized by color caused by both organic and inorganic compounds [3].

The organic compounds are more problematic in industrial effluent than inorganic materials [4, 5] because, apart from the color, it imparts on the wastewater, biodegradation of organic material in the dye depleting the dissolved

oxygen of the water thereby stressing aquatic microbes [6]. Traditional wastewater treatment technologies have shown to be ineffective for handling synthetic dyes because of the chemical stability of these pollutants [7].

There is no single or economically attractive method of treatment of textile wastewater [8], although notable achievements were made in the use of biotechnological approaches to solving the problem recently as reviewed by dos Santos et al. [9]. In addition to biological treatment, many physical and chemical treatment methods have been employed for dye removal from wastewaters such as coagulation, flocculation, filtration, oxidation or reduction, complex formation, or neutralization [10]. New adsorption/oxidation, adsorption/reduction, and many combined processes were reviewed by Qu [11], while radiation-induced degradation process for treatment of wastewater was reviewed by Wojnarovites and Takacs [12]. Solid sorbents have been employed in adsorption techniques to remove certain classes of chemical pollutants from waters; activated carbon is the most successfully used, but the high operating

costs and problems with regeneration of the spent activated carbon discourage its large-scale application. Therefore, a number of nonconventional sorbents have been tried for the treatment of wastewaters, in this class are various industrial wastes, agrowaste, or natural materials available in large quantity at low cost and are classified as alternative sorbents for the removal of inorganic and organic pollutants from wastewaters [13–16]. In this present study, the aim is to determine the efficacy of chemically modified and unmodified biological (proteinous and cellulosic) waste sorbents in treatment of textile wastewater; also the effect of particle sizes, carbonization (activation), and contact time will be established.

2. Materials and Methods

2.1. Collection of Sorbents and Preparation. Cellulosic waste sorbents (corn cob and coconut-husk (coir)) were procured from a local market around Awka, while protein waste sorbents (goat hair and chicken feathers) were sourced from Awka main abattoir. They were thoroughly washed with soap solution, sun dried for two days before drying in an oven at 105°C for 2 hours, and then ground. One-half of each ground material was carbonized at a temperature of 300°C for 30 mins, cooled and activated with H₂SO₄, and further heated at a temperature of 500°C for complete carbonization. The carbonized materials were again pulverized. Both materials were sieved into two particle sizes of 325 μ m and 625 μ m using mechanical sieve.

2.2. Wastewater Collection and Analysis. Textile wastewater was collected from general cotton mills Onitsha. Physico-chemical parameters of the wastewater were analyzed before and after contacting with the adsorbents for each contact time and particle size.

Nitrate was determined according to American Public Health method [17], and chemical oxygen demand (COD) was determined by the dichromate method [18]. Biological oxygen demand (BOD) and dissolved oxygen (DO) were determined electrochemically [19].

The chloride content was determined by colorimetric method, while total suspended solid (TSS) and total dissolved solid (TDS) were determined by their respective standard methods [19]. A standard pH meter was used to determine the pH, and a digital conductometer (consort K120, Belgium) was used to determine electrical conductivity (EC). Heavy metals (Pb, Mn, Ni, and Cr) were determined at their respective wavelengths (281.5, 278, 231, and 358) nm after digestion using clean filtrates of the samples by means of atomic absorption spectrophotometry 205 A.

2.5 g of each sorbent (both carbonized and uncarbonized and each particle size) were separately packed in glass adsorption column with inner diameter 11 m, bed height 270 mm; the wastewater was eluted into it and allowed a contact time of 60 and 120 minutes. The wastewater was collected after 60 and 120 mins, respectively, and all the previous parameters were again determined to ascertain the

percentage absorption after each batch. Results are shown in Tables 1–4.

3. Results

From Table 1, nitrate, chemical oxygen demand (COD), biological oxygen demand (BOD), dissolved oxygen (DO), chloride (Cl⁻), total suspended solids (TSS), total dissolved solid (TDS), and electrical conductivity were drastically reduced, while the pH was increased to near neutrality. The reduction of the parameters increased at increased contact time. Feather, either carbonized (activated) or uncarbonized was more promising at both contact time and particle size than goat hair. Smaller particle size (large surface) absorbed/adsorbed more than large particle size (smaller surface area). More reduction in concentration of pollutants also occurred at longer contact time (120 mins); the trend of absorption is for carbonized sorbent at 60 mins: 325 μ m feather > 325 μ m goat hair > 625 μ m feather > 625 μ m goat hair. For uncarbonized: 325 μ m feather > 325 μ m goat hair > 625 μ m feather > 625 μ m goat hair. At 120 mins contact time, for carbonized, order of absorption is 325 μ m feather > 325 μ m goat hair > 625 μ m feather > 625 μ m goat hair. For uncarbonized, the same trend is observed, although variations exist. The percentage range in absorption of parameters at 60 mins contact time is nitrate (96.02–99.89), COD (49.11–96.43), BOD (48.15–97.84), DO (52.00–96.67), Cl⁻ (56.62–88.35), TSS (99.90–99.95), TDS (99.31–99.92), and EC (93.67–95.61), while the percentage range of absorption of the same parameters at 120 mins contact time were nitrate (99.69–99.92), COD (56.96–98.21), BOD (62.96–99.07), DO (71.33–98.00), Cl⁻ (63.49–89.13), TSS (99.95–99.98), TDS (99.29–99.93), and EC (95.00–95.92).

From Table 2, there is near equal reduction in concentration of parameters by corn cob and coconut husk; but in terms of number of parameters reduced (absorbed/adsorbed) more, the sorption order is for carbonized at 60 mins contact time: 325 μ m corn cob > 325 μ m coconut husk > 625 μ m coconut husk > 625 μ m corn cob. For uncarbonized, 325 μ m corn cob > 325 μ m coconut husk > 625 μ m coconut husk > 625 μ m corn cob. At 120 mins contact time, the high sorption capability of the adsorbents for the pollutants is in the order; for carbonized, 325 μ m corn cob > 325 μ m coconut husk > 625 μ m coconut husk > 625 μ m corn cob. For uncarbonized, 325 μ m corn cob > 325 μ m coconut husk > 625 μ m coconut husk > 625 μ m corn cob. The percentage ranges in absorption of the parameters at 60 mins contact time for both particle sizes are as follows; nitrate (67.35–99.29), COD (38.21–78.93), BOD (41.05–81.48), DO (36.67–81.33), Cl⁻ (50.20–83.61), TSS (94.76–97.57), TDS (97.61–99.91), and EC (87.50–89.58), while the range of percentage absorption of the parameters at 120 mins contact time for both particle size is thus; Nitrate (79.49–89.69), COD (42.86–80.36), BOD (51.85–96.30), DO (34.67–74.67), Cl⁻ (58.61–88.84), TSS (95.14–97.60), TDS (98.34–99.93), and EC (87.92–91.46).

From Table 3, at 60 mins contact time, carbonized 325 μ m feather showed higher percentage absorption of

TABLE 1: Use of carbonized/uncarbonized waste protein sorbents in removal of pollutants from wastewater.

S/no.	Sorbents	Particle size	Contact time (mins)	% absorption of physicochemical parameters								
				NO ₃ ⁻	COD	BOD	DO	Chloride	TSS	TDS	EC. (U.S/CM)	pH
(1)	Carbonized goat hair	325 μ m	60	99.89	90.54	93.21	88.00	88.35	99.95	99.88	95.00	8.00 (5.00)
(2)	Carbonized feather	325 μ m		99.89	96.43	97.84	96.67	86.82	99.95	99.90	95.61	8.00 (5.00)
(3)	Carbonized goat hair	625 μ m		99.69	81.07	71.30	62.00	73.29	99.81	99.84	94.38	7.00 (5.00)
(4)	Carbonized feather	625 μ m		99.39	71.43	62.96	78.67	77.86	99.95	99.78	94.67	8.00 (5.00)
(5)	Uncarbonized goat hair	325 μ m	120	99.49	75.71	71.60	81.33	83.79	99.95	99.31	93.75	7.00 (5.00)
(6)	Uncarbonized feather	325 μ m		99.59	85.71	70.99	91.33	85.32	99.95	99.85	93.83	7.50 (5.00)
(7)	Uncarbonized goat hair	625 μ m		96.02	49.11	56.79	52.00	56.62	99.90	99.92	93.75	7.50 (5.00)
(8)	Uncarbonized feather	625 μ m		99.79	54.64	48.15	52.67	71.04	99.95	99.88	93.67	8.00 (5.00)
(9)	Carbonized goat hair	325 μ m		99.89	92.68	96.91	92.00	89.13	99.95	99.29	95.50	8.00 (5.00)
(10)	Carbonized feather	325 μ m		99.92	98.21	99.07	98.00	88.38	99.98	99.93	95.42	8.50 (5.00)
(11)	Carbonized goat hair	625 μ m		99.79	80.54	68.52	72.00	76.60	99.88	99.88	95.21	7.80 (5.00)
(12)	Carbonized feather	625 μ m		99.79	80.36	72.84	92.00	80.35	99.98	99.85	95.75	7.80 (5.00)
(13)	Uncarbonized goat hair	325 μ m		99.69	78.57	67.28	90.67	87.69	99.95	99.48	92.50	7.50 (5.00)
(14)	Uncarbonized feather	325 μ m		99.80	88.93	80.86	94.67	87.11	99.98	99.88	95.92	8.00 (5.00)
(15)	Uncarbonized goat hair	625 μ m		96.91	56.96	62.96	78.67	63.49	99.95	99.94	95.00	8.00 (5.00)
(16)	Uncarbonized feather	625 μ m		99.90	58.57	62.96	71.33	75.55	99.95	99.93	95.08	8.00 (5.00)

Value in parenthesis is pH result before treatment.

Mn²⁺ and Cr³⁺, while carbonized 325 μ m goat hair showed higher percentage absorption of Ni²⁺. Carbonized 625 μ m feather had higher percentage absorption of Pb²⁺, Mn²⁺, and Cr³⁺ than carbonized 625 μ m goat hair which had higher percentage absorption of Ni²⁺. For uncarbonized, 325 μ m feather showed highest percentage absorption of Pb²⁺ and Cr³⁺, while 325 μ m goat hair absorbed highest percentage of Mn²⁺ and Ni²⁺, using 625 μ m, feather absorbed highest percentage of Mn²⁺ and Ni²⁺, while goat hair absorbed highest percentage of Pb²⁺ and Cr³⁺.

At 120 mins contact time, carbonized 325 μ m feather absorbed highest percentage of Pb²⁺, Mn²⁺, and Cr³⁺, while 325 μ m goat hair showed highest percentage absorption of Ni²⁺. Using 625 μ m, carbonized feather showed highest percentage absorption of Pb²⁺, Mn²⁺, and Cr³⁺, while goat hair showed highest percentage of Ni²⁺. Using uncarbonized sorbents, 325 μ m feather showed highest percentage absorption of Pb²⁺, Cr³⁺ from the solution, while 325 μ m goat hair removed highest percentage of Mn²⁺ and Ni²⁺. Using

625 μ m, goat hair had highest percentage absorption of Mn²⁺, Ni²⁺, and Cr³⁺, while feather had highest percentage absorption of Pb²⁺.

From Table 4, using carbonized sorbents at 60 mins contact time, 325 μ m corn cob showed highest percentage absorption of Pb²⁺ and Ni²⁺, while 325 μ m coconut husk showed highest percentage absorption of Mn²⁺ and Cr³⁺ from the wastewater. Using 625 μ m, coconut husk absorbed highest percentage Pb²⁺ and Cr³⁺, while 625 μ m corn cob showed highest percentage absorption of Mn²⁺ and Ni²⁺. Using the uncarbonized at the same contact time, 325 μ m coconut husk had more percentage affinity for Pb²⁺ and Cr³⁺ while 325 μ m corn cob did so for Mn²⁺ and Ni²⁺. Using 625 μ m, corn cob sorbed more percentage of Pb²⁺, Ni²⁺, and Cr³⁺, while 625 μ m coconut husk sorbed highest percentage of Mn²⁺.

At 120 mins contact time, carbonized 325 μ m corn cob sorbed highest percentage of Ni²⁺, while 325 μ m coconut husk sorbed highest percentage of Pb²⁺, Mn²⁺, and Cr³⁺.

TABLE 2: Use of carbonized/uncarbonized waste cellulosic sorbents in removal of pollutants from wastewater.

S/no.	Sorbents	Particle size	Contact time (mins)	% absorption of physicochemical parameters								
				NO ₃ ⁻	COD	BOD	DO	Chloride	TSS	TDS	EC (U.S./CM)	pH
(1)	Carbonized corn cob	325 μ m	60	85.61	78.93	81.48	81.33	80.26	95.14	99.66	89.58	8.0 (5.0)
(2)	Carbonized coconut husk	325 μ m		84.59	63.21	68.52	36.67	82.50	97.57	99.91	88.33	7.50 (5.00)
(3)	Carbonized corn cob	625 μ m		83.57	52.14	41.05	70.67	64.65	97.48	99.64	87.50	7.50 (5.00)
(4)	Carbonized coconut husk	625 μ m		82.14	52.14	49.38	58.00	70.09	97.48	99.80	88.13	7.50 (5.00)
(5)	Uncarbonized corn cob	325 μ m	120	81.02	78.57	75.31	54.00	63.01	97.38	99.37	88.75	8.00 (5.00)
(6)	Uncarbonized coconut husk	325 μ m		79.29	62.50	60.49	48.67	83.61	95.19	99.82	88.96	7.50 (5.00)
(7)	Uncarbonized corn cob	625 μ m		67.35	38.21	53.70	54.67	50.20	97.33	98.64	87.50	8.00 (5.00)
(8)	Uncarbonized coconut husk	625 μ m		99.29	47.14	69.75	44.00	68.01	94.76	97.61	88.13	7.50 (5.00)
(9)	Carbonized corncob	325 μ m		89.69	79.64	96.30	52.00	84.22	97.57	99.68	90.83	7.80 (5.00)
(10)	Carbonized coconut husk	325 μ m		79.49	63.93	69.75	73.33	88.84	95.19	99.93	91.04	8.00 (5.00)
(11)	Carbonized corncob	625 μ m		89.50	58.21	51.85	74.67	69.77	97.45	99.68	90.83	7.50 (5.00)
(12)	Carbonized coconut husk	625 μ m		89.59	78.57	70.37	60.00	73.18	95.14	99.86	91.25	7.50 (5.00)
(13)	Uncarbonized corn cob	325 μ m		80.61	80.36	69.75	34.67	88.76	95.83	99.45	91.46	8.50 (5.00)
(14)	Uncarbonized coconut husk	325 μ m		89.39	64.11	56.79	39.33	84.39	97.60	99.88	90.83	8.00 (5.00)
(15)	Uncarbonized corn cob	625 μ m		81.02	42.86	66.05	46.67	58.61	97.43	98.98	87.92	7.50 (5.00)
(16)	Uncarbonized coconut husk	625 μ m		87.14	56.07	54.94	58.67	73.18	97.38	98.33	88.13	8.00 (5.00)

Value in parenthesis is pH result before treatment.

When using larger particle size (625 μ m), coconut husk sorbed highest percentage of all the metal ions examined than corn cob; using the unactivated, 325 μ m corn cob sorbed highest percentage of Mn²⁺ and Ni²⁺, while 325 μ m coconut husk sorbed highest percentage of Pb²⁺ and Cr³⁺. Using unactivated sorbent, 625 μ m corn cob absorbed highest percentage of Ni²⁺ and Cr³⁺, while 625 μ m coconut husk absorbed highest percentage of Pb²⁺ and Mn²⁺.

4. Discussion

Solid wastes can be advantageously used as alternative sorbents because of their low cost and local availability. Adsorption of a basic dye-methylene blue and an acidic dye-eosin on wood dust of different particle size at varying speed has been studied by monitoring color reduction [20]. Sawdust and related waste materials from timber industry that are readily available and are inexpensive sorbents have

been used to remove unwanted chemical substances from waters including dyes, oils, toxic salt, and heavy metals [9, 21]. Several cellulose-based waste materials which originate from agroindustry can be used as sorbents for synthetic dyes, such include banana and orange peels [22], olive pomace [23], palm kernel fibre [24], cotton fibre [25], several others have also been used to sequester metals from aqueous solution [26, 27]. Since most applied materials are cellulosic, adequate attention has not been given to studies on sorption capacity of protein waste. This study has proved that protein-based waste sorbent are more efficacious in removal of pollutants from wastewater (Tables 1 and 3). This assertion is in comparison with cellulosic sorbents when placed side by side at the same particle size, activation (carbonization), and contact time, although cellulosic sorbents under study are highly efficient pollutant absorbent/adsorbent (Tables 2 and 4). A critical analysis of the results (Tables 1–4) shows high percentage reduction in the concentrations of parameters analyzed. The differences

TABLE 3: Use of carbonized/uncarbonized waste protein sorbents in removal of heavy metals from wastewater.

S/no.	Sorbents	Particle size	Contact time (mins)	% absorption of heavy metals			
				Pb	Mn	Ni	Cr
(1)	Carbonized goat hair	325 μm	60	87.05	80.84	94.62	81.89
(2)	Carbonized feather	325 μm		87.05	83.58	90.51	92.83
(3)	Carbonized goat hair	625 μm		65.88	78.53	77.18	58.87
(4)	Carbonized feather	625 μm		78.82	79.79	73.33	73.58
(5)	Uncarbonized goat hair	325 μm		76.00	76.21	90.51	78.11
(6)	Uncarbonized feather	325 μm		81.18	74.32	78.97	83.77
(7)	Uncarbonized goat hair	625 μm		77.65	63.16	70.77	61.51
(8)	Uncarbonized feather	625 μm		75.29	68.21	73.85	52.83
(9)	Carbonized goat hair	325 μm	120	85.41	77.26	97.95	84.15
(10)	Carbonized feather	325 μm		91.53	82.74	94.36	89.06
(11)	Carbonized goat hair	625 μm		71.76	80.21	76.64	66.79
(12)	Carbonized feather	625 μm		89.18	80.84	74.87	76.60
(13)	Uncarbonized goat hair	325 μm		75.53	83.58	90.26	85.66
(14)	Uncarbonized feather	325 μm		90.12	81.26	77.69	92.08
(15)	Uncarbonized goat hair	625 μm		65.18	68.84	74.87	63.77
(16)	Uncarbonized feather	625 μm		79.76	68.63	74.62	63.02

TABLE 4: Use of carbonized/uncarbonized waste cellulosic sorbents in removal of heavy metals from wastewater.

S/no.	Sorbents	Particle size	Contact time (mins)	% absorption of heavy metals			
				Pb	Mn	Ni	Cr
(1)	Carbonized corncob	325 μm	60	76.00	63.79	92.31	64.15
(2)	Carbonized coconut husk	325 μm		61.18	73.47	74.87	74.34
(3)	Carbonized corncob	625 μm		37.65	64.63	66.15	44.15
(4)	Carbonized coconut husk	625 μm		70.59	47.16	52.56	58.87
(5)	Uncarbonized corn cob	325 μm		66.35	65.68	76.15	63.02
(6)	Uncarbonized coconut husk	325 μm		75.29	57.47	63.08	70.19
(7)	Uncarbonized corn cob	625 μm		71.76	47.16	52.31	42.26
(8)	Uncarbonized coconut husk	625 μm		61.65	57.68	49.74	36.60
(9)	Carbonized corncob	325 μm	120	71.76	70.11	94.87	63.40
(10)	Carbonized coconut husk	325 μm		91.06	77.26	82.56	83.40
(11)	Carbonized corncob	625 μm		48.24	78.11	65.13	52.45
(12)	Carbonized coconut husk	625 μm		74.12	78.11	68.21	65.28
(13)	Uncarbonized corn cob	325 μm		69.41	74.74	89.23	79.62
(14)	Uncarbonized coconut husk	325 μm		79.76	57.89	73.85	81.51
(15)	Uncarbonized corn cob	625 μm		34.59	47.79	66.15	50.19
(16)	Uncarbonized coconut husk	625 μm		69.41	57.89	62.05	50.19

in the percentage absorption profiles of the sorbents for each pair of particle size at any given contact time for the parameters assessed were insignificant. The bottom line therefore is that the sorbent powders absorbed appreciable percentage concentrations of the pollutants. A number of natural features inherent in the adsorbents enable them to show high sorption capacity for the pollutants. Coconut husk and corn cob are both fibrous and granular and are with hollow internal conduits; xylem for transporting water and phloem for transporting dissolved nutrients. The pollutants are absorbed into the pits, voids, lacunae, or lumina. Activation of cellulosic adsorbents-coconut husk (coir) and corn cob causes the production of oleophilic resins

which enhances high percentage absorption of the pollutants [28]. Carbonization leads to the destruction of cellulose structure in the plant materials and the size of macro-, micro-, and mesopores increases. Developed structure with larger specific surface area and porosity are obtained than in uncarbonized adsorbent, hence high percentage absorption or removal of the pollutants by carbonized sorbents than in the uncarbonized. Uncarbonized protein (feathers and goat hair) and cellulose (coir and corn cob) adsorbents have a natural waxy water proof coating with large external surface which enables them to have high percentage absorption for the pollutants. High adsorption capability is determined by large specific surface and porous structure

of sorbents as well as by chemical interaction with the surface functional groups present in carbonized sorbents, hence high percentage removal of the pollutants by both carbonized cellulose and protein sorbents. The variations observed in the study may be as a result of adsorption-desorption phenomenon occurring at dynamic equilibrium as adsorption may be governed by physical interaction [29]. It may also be due to agitation from wind (atmospheric phenomenon) or structural vibration. It can also be due to the fact that absorption/adsorption is nonstoichiometry and there may be inhomogeneity in the shapes, particle sizes, surface area, pore size, morphology of the sorbents, and specific retention volume for each target compounds by the sorbents. Although only textile wastewater was used in this work [30], the method can be applied to all types of waters as present result compared well with previous work in which activated and unactivated powders of rice and groundnut husk were used to remediate brewery and beverage wastewater [31]. NO_3^- , BOD, COD and DO were analyzed to establish the presence of chromophores (group of atoms responsible for dye color as well as electron withdrawing or donating substituents that modify or intensify the color of chromophores called auxochromes). The most important chromophores are azo ($-\text{N}=\text{N}-$), carbonyl ($-\text{C}=\text{O}$), methine ($-\text{CH}$), nitro ($-\text{NO}_2$), and quinoid while auxochromes are amine ($-\text{NH}_2$), sulfonate ($-\text{SO}_3\text{H}$), carboxyl ($-\text{COOH}$), and hydroxyl ($-\text{OH}$) [9]. Electrical conductivities were drastically reduced by all the sorbents at all particle size, contact time, and activation following the normal trends already observed. There was also noticeable color reduction though not of interest in the present study. The decrease in the pH comparing with the base wastewater values shows that the active sites on the sorbents were protonated and the sorbents become positively charged; this may cause steric hinderance which may be responsible for the less percentage absorption of Cr^{3+} than other metal ions. This is despite the fact that Cr^{3+} is of lower density than other metal ions in the study, the densities are Cr^{3+} (7.19), Ni^{2+} (8.90), Mn^{2+} (7.42), and Pb^{2+} (11.34) [32]. It also depends on the lone pair of electrons available on the sorbents active sites and pore size, as pore size is inversely proportional to surface area [33]. Since absorption/adsorption of pollutants by sorbents in this study cannot be attributed to any chemical interaction between the sorbents and chemical pollutants, it can be merely be attributed to weak physical adhesive forces such as van der waal, London forces as well as by mere physical entanglement/occlusion. From this work, excluding minor variation, it is established that protein sorbents have high percentage absorption capacity than cellulose but the later tend to be more abundant and therefore cost effective. In both, carbonization (activation), small particle size (large surface area), and longer contact time have overriding effect on the efficiency of biological waste sorbent in remediating wastewater; this observation is supported by other works [25, 27]. It is suggested that if three (3) adsorption glass columns are to be connected in series and the sorbents in each column is allowed a contact time of 120 mins with the wastewater before the same water is allowed entering into the next (2nd) column, and allowed another 120 mins contact time before

passing into the third (3rd) column for another contact time of 120 mins, analysis of the wastewater after 360 mins (6 hrs) contact time may reveal that the wastewater is totally free of pollutants. It is therefore concluded that protein wastes (feather and goat hair) and cellulosic wastes (corn cob and coconut husk) are highly efficient in detoxification of wastewater.

References

- [1] M. F. Gordon, J. C. Geten, and A. D. Okun, *Water and Wastewater Engineering*, John Wiley and Son, New York, NY, USA, 1986.
- [2] A. Ofoefule, E. Uzodimma, and C. Ibeto, "Wastewater: treatment options and its associated benefits," in *Wastewater Evaluation and Management*, Fernando Sebastian Garcia Einschlag, Ed., Intech-Publishers Croatia, 2011.
- [3] R. Crites and G. Techobanoglous, *Small Decentralized Wastewaters Management Systems*, McGraw-Hill, Singapore, 1998.
- [4] J. W. Moore and E. A. Moore, *Environmental Small Decentralized Wastewater Management Systems*, McGraw-Hill, Academic Press, London, UK, 1976.
- [5] J. Passivirta, *Chemical Ecotoxicology*, Lewis Publishers, Chelsea, Mich, USA, 1991.
- [6] M. Calf and C. Eddy, *Wastewater Engineering*, Tata McGraw-Hill, New Delhi, India, 3rd edition, 1991.
- [7] E. Forgacs, T. Cserháti, and G. Oros, "Removal of synthetic dyes from wastewaters: a review," *Environment International*, vol. 30, no. 7, pp. 953–971, 2004.
- [8] Y. M. Slokar and A. M. Marechal, "Methods of decoloration of textile wastewaters," *Dyes and Pigments*, vol. 37, no. 4, pp. 335–356, 1998.
- [9] A. B. dos Santos, F. J. Cervantes, and J. B. Vanlier, "Review paper on current technologies for decoloration of textile wastewaters: perspective for anaerobic biotechnology," *Biore-source Technology*, vol. 918, pp. 2169–2385, 2007.
- [10] P. Janos, "Non-conventional sorbents for the Dye Removal from waters: mechanisms and selected applications," in *Sorbents Properties, Materials and Applications*, T. P. Wills, Ed., pp. 357–381, Nova Science, New York, NY, USA, 2009.
- [11] J. QU, "Research progress of novel adsorption processes in water purification: a review," *Journal of Environmental Sciences*, vol. 20, no. 1, pp. 1–13, 2008.
- [12] L. Wojnarovites and E. Takacs, "Irradiation treatment of azodye containing wastewater. An overview," *Radiation Physics and Chemistry*, vol. 77, no. 3, pp. 225–244, 2008.
- [13] T. A. Kurniawan, G. Y. S. Chan, W. H. Lo, and S. Babel, "Comparisons of low-cost adsorbents for treating wastewaters laden with heavy metals," *Science of the Total Environment*, vol. 366, no. 2–3, pp. 409–426, 2006.
- [14] G. Crini, "Non-conventional low-cost adsorbents for dye removal: a review," *Biore-source Technology*, vol. 97, no. 9, pp. 1061–1085, 2006.
- [15] S. Babel and T. A. Kurniawan, "Low-cost adsorbents for heavy metals uptake from contaminated water: a review," *Journal of Hazardous Materials*, vol. 97, no. 1–3, pp. 219–243, 2003.
- [16] S. E. Bailey, T. J. Olin, R. M. Bricka, and D. D. Adrian, "A review of potentially low-cost sorbents for heavy metals," *Water Research*, vol. 33, no. 11, pp. 2469–2479, 1999.
- [17] American Public Health Association, *Standard Methods for the Examination of Water and Wastewater*, APHA, AWWA, WEF, Washington, DC, USA, 20th edition, 1998.

- [18] F. R. Theroux, *Laboratory Manual for Chemical and Bacterial Analysis of Water and Sewage*, McGraw-Hill, New York, NY, USA, 3rd edition, 1943.
- [19] J. Bertram and R. Balance, *A Practical Guide to the Design and Implementation of Fresh Water Quality and Monitoring Programmes*, United Nations Environmental Programme (UNEP) and World Health Organization (WHO). E & FN Spon, 1996.
- [20] F. N. Emengo, J. K. Nduka, C. N. Anodebe, and P. A. C. Okoye, "Dye wastewaters, alternative physiochemical treatment reagent," in *Sorbents: Properties, Materials and Applications*, T. P. Willis, Ed., Nova Science, New York, NY, USA, 2009.
- [21] A. Shukla, Y. H. Zhang, P. Dubey, J. L. Margrave, and S. S. Shukla, "The role of sawdust in the removal of unwanted materials from water," *Journal of Hazardous Materials*, vol. 95, no. 1-2, pp. 137–152, 2002.
- [22] G. Annadurai, S. Juang, and D. J. Lee, "Use of cellulose-based wastes for adsorption of dyes from aqueous solutions," *Journal of Hazardous Materials*, vol. 92, no. 3, pp. 263–274, 2002.
- [23] F. Banat, S. Al-Asheh, R. Al-Ahmad, and F. Bni-Khalid, "Bench-scale and packed bed sorption of methylene blue using treated olive pomace and charcoal," *Bioresource Technology*, vol. 98, no. 16, pp. 3017–3025, 2007.
- [24] A. E. Ofomaja, "Kinetics and mechanism of methylene blue sorption onto palm kernel fibre," *Process Biochemistry*, vol. 42, no. 1, pp. 16–24, 2007.
- [25] M. Saleem, T. Pirzada, and R. Qadeer, "Sorption of acid violet 17 and direct red 80 dyes on cotton fiber from aqueous solutions," *Colloids and Surfaces A*, vol. 292, no. 2-3, pp. 246–250, 2007.
- [26] J. C. Igwe and A. A. Abia, "Studies on the effects of pH and modification of adsorbent on AS (V) removal from aqueous solution using sawdust and coconut fibre," *Chemical Society of Nigeria*, vol. 32, no. 2, pp. 24–28, 2007.
- [27] M. Musah, U. A. Birnin-Yauri, and A. U. Itodo, "Detoxification of Pb^{2+} and Cr^{3+} ions using derived palm kernel shell adsorbent," in *Proceedings of the 34th International Conference Chemical Society of Nigeria*, September 2011.
- [28] Y. Kato, K. Umehara, and M. Aoyama, "An oil sorbent from wood fiber by mild pyrolysis," *Holz als Roh- und Werkstoff*, vol. 55, no. 6, pp. 399–401, 1997.
- [29] S. Karaca, A. Gürses, and R. Bayrak, "Investigation of applicability of the various adsorption models of methylene blue adsorption onto lignite/water interface," *Energy Conversion and Management*, vol. 46, no. 1, pp. 33–46, 2005.
- [30] E. Gallego, F. J. Roca, J. F. Perales, and X. Guardino, "Use of Sorbents in air quality control systems," in *Sorbents; Properties, Materials and Applications*, T. P. Willis, Ed., Nova Science, New York, NY, USA, 2009.
- [31] J. K. C. Nduka, O. J. Ezeakor, and A. C. Okoye, "Characterization of wastewater and use of cellulosic waste as treatment option," *Journal of Engineering Science and Technology*, vol. 14, no. 11, pp. 7226–7234, 2007.
- [32] G. F. Liptrot, *Modern Inorganic Chemistry*, Unwin Hyman, London, UK, 4th edition, 1986.
- [33] E. Matisova and S. Skrabakova, "Cabon sorbents and their utilization for preconcentration of organic pollutant in environmental samples," *Journal of Chromatography A*, vol. 707, pp. 145–179, 1995.

Review Article

Biofuels Production from Biomass by Thermochemical Conversion Technologies

M. Verma,^{1,2} S. Godbout,¹ S. K. Brar,³ O. Solomatnikova,² S. P. Lemay,¹ and J. P. Larouche¹

¹ *Institut de Recherche et de Développement en Agroenvironnement Inc. (IRDA), 2700 Rue Einstein, QC, Canada G1P 3W8*

² *Centre de Recherche Industrielle du Québec (CRIQ), 333 Rue Franquet, QC, Canada G1C 4C7*

³ *Le Centre Eau Terre Environnement, Institut National de la Recherche Scientifique (INRS-ETE), 490 de la Couronne, QC, Canada G1K 9A9*

Correspondence should be addressed to M. Verma, mausam.verma@irda.qc.ca

Received 29 September 2011; Accepted 12 December 2011

Academic Editor: Santiago Esplugas

Copyright © 2012 M. Verma et al. This is an open access article distributed under the Creative Commons Attribution License, which permits unrestricted use, distribution, and reproduction in any medium, provided the original work is properly cited.

Agricultural biomass as an energy resource has several environmental and economical advantages and has potential to substantially contribute to present days' fuel demands. Currently, thermochemical processes for agricultural biomass to energy transformation seem promising and feasible. The relative advantage of thermochemical conversion over others is due to higher productivity and compatibility with existing infrastructure facilities. However, the majority of these processes are still under development phase and trying to secure a market share due to various challenges, right from suitable infrastructure, raw material, technical limitations, government policies, and social acceptance. The knowledge at hand suggests that biomass can become a sustainable and major contributor to the current energy demands, if research and development are encouraged in the field of thermochemical conversion for various agricultural biomass types. This paper intends to explore the physical and chemical characteristics of biofuel substitutes of fossil fuels, potential biomass sources, and process parameters for thermochemical conversion.

1. Introduction

Current energy crisis is a product of tremendous amount of pressure on world fossil fuel supply and reserve, which is also implicated with the recent strides of economic developments of countries such as China and India, among others, which are net importers of fossil fuels [1]. The surge in fossil fuel cost (\approx US\$150 per barrel) in the recent past clearly indicated that biomass-based fuel options could be more competitive during peak demand periods and a viable mode at other times. The increasing concern over climate change is another important factor that has highlighted the environmental benefits (minimal net greenhouse gas emissions) of the biomass utilization. Most recently, the deep sea crude oil spewing disaster in April 2010 (BP PLC.-Deepwater Horizon oil spill; about 207 million gallons within 3 months period) has undoubtedly confirmed the risks of over exploitation fossil fuel. This incident strengthen the notion of gradual implementation of safe renewable sources to fuel existing fleet of fossil fuel powered domestic, commercial, transportation, and industrial sector. Over the last several decades various

researchers have investigated biomethanation, fermentation, and thermochemical pathways for the conversion of biomass to biofuels as energy sources, which is currently getting the attention that was deserved. In general, the biomass could be a complex mixture of organic materials such as carbohydrates (hemicellulose, cellulose, and starch), lignin, fats, and proteins; however, the physiochemical characteristics of biomass vary in discrete fashion with their source. For example, the primary components of the biomass from plant/crop origins are carbohydrates and lignin which can vary with plant type. The source of some biomass includes plant/crop roots, seeds, and seed residue which are rich in starch and fats. On the other hand, many of the biomass types are by products/waste of crops, forest residue, construction and demolition waste, municipal waste, cattle, and human waste. As it was mentioned above, the utilization of biomass as liquid biofuels is a necessary alternative to avoid harmful effects of direct combustion of biomass (as unprocessed/raw solid fuels) which can led to poor air quality, secondary pollution, and undesired health impacts [2].

At present, several biomass thermochemical conversion equipments exist which can transform agricultural biomass into biofuels/bioenergy [3–6]. Nevertheless, there is a great challenge for a farm producer to select the best option due to the infancy of these technologies, intended application (mainly, wood biomass at large scale) as well as a lack of a standard protocol/strategy for agricultural biomass management into bioenergy/biofuels. In brief, a methane digester could be a very attractive solution for handling cattle manure; however, in cold climatic conditions, sensitivity of anaerobic fermentation and secondary waste from digestion process can be huge setbacks [7, 8]. Similarly, land spreading of cattle manure as fertilizer is often limited due to excess nutrient and heavy metals in addition to the agricultural soil [9]. Fermentation of cellulosic biomass for second generation ethanol production itself is a great technical hurdle which requires consistent biomass source, advanced equipments, distribution/collection network, and highly skilled labor. Direct combustion has excellent efficiency for heat utilization but requires advanced technology for the treatment of exhaust gases and secondary waste (e.g., ash) [10–12]. Thermochemical transformation of agricultural biomass is in principle, a highly established technology developed for petroleum and other chemical products. However, the complexity of agricultural biomass and factors (such as moisture, oxygen, sulfur, nitrogen, and metal contents) makes it a challenging task [10, 13–17].

Biofuels are derived from biomass; however, the conversion pathways: biological, physical, chemical, or a combination of processes are pivotal to their type and characteristics. For example, biogas, ethanol, and biodiesel can be produced via microbial/enzymatic fermentations with or without using physical and chemical pretreatment steps [18, 19]. On the other hand, conversion of biomass into bio-oil, biochar, syn-gas, and others requires entirely thermochemical processes, such as torrefaction, carbonization, thermal liquefaction, pyrolysis, and gasification [20–22]). In view of present energy crisis, research and developments in thermochemical processes hold key to a major part of the practical and sustainable energy solution. Therefore, this paper shed light on the recent advancements in the thermochemical production pathways (mainly pyrolysis) for fossil fuel alternative biofuels such as bio-oil, biochar, and combustible gaseous mixtures from forest, agriculture, and municipal residues/wastes. A sustainable farm-practice concept for residue/waste management has also been proposed to generate biofuels from farm manure waste, thereby, serving multiple purposes: reducing the net greenhouse gas emissions, solid waste reduction, carbon sequestration, soil enrichment, and economic benefits among others.

2. Thermochemical Biofuels

Biofuels have distinct physicochemical characteristics depending upon their source/raw material as well as the applied transformation process. Some of the commercially available biofuels are ethanol from corn/cellulosic biomass [23, 24], biodiesel from soybean, canola, *Jatropha*, animal fat, waste

cooking oil, and algae [25], biogas from anaerobic digestion of animal manure [8], and thermochemical transformation of various biomass into solid, liquid, and gaseous fuels [20]. With respect to other renewable energy sources, thermochemical biofuels are relatively newer from commercial point of view; however, they are getting much more attention lately as these biofuels offer several technical and strategic advantages [26]. For example, the industrial infrastructure to supply thermochemical transformation equipments for innovative technologies is highly developed. Moreover, the biofuels can be produced from virtually all sorts of available biomass in reasonable timeframe without significant modification in the overall process. On the other hand, despite having certain benefits, bioconversion using microbes and enzymes lacks robustness at industrial scale due to complexity and variable nature of biomass as feedstock both in terms of availability of quality and quantity. In addition, thermochemical transformation is virtually independent of environmental conditions for production purposes. Therefore, it would be imperative to understand the properties of thermochemical biofuels to assess their future market potential.

2.1. Bio-Oil. Bio-oil is a term used for liquid fuel product of biomass pyrolysis. The color varies from light brownish yellow to dark brown for various fractions during condensation phases with pungent-smoky odor and acidic pH. Bio-oils are complex mixtures of chemical compounds that are obtained from the decomposition of cellulose, hemicelluloses, lignin along with other organic entities [35]. The single most abundant compound in any bio-oil would be water (up to 40% w/w) which is crucial in determining the energetic value as well as physicochemical properties such as pH, viscosity, and phase separation. Bio-oils can also contain some fine solid particles (aerosols). The fuel characteristics of bio-oils are in principle due to hundreds of organic compounds that belong to sugars, organic acids, alcohols, aldehydes, ketones, phenols, esters, ethers, furans, nitrogen and sulfur compounds, and multifunctional compounds [44]. Evidently, the molecular weights of bio-oil compounds vary from 18 (water) to 5000 or even more for partially degraded pyrolytic lignins. The average molecular weight for different fractions of bio-oils can vary in the range of 370–1000 g/mol. For now, more than 300 organic compounds have been reported in various bio-oils from different source. Table 2 represents physicochemical characteristics of bio-oils obtained from different pyrolysis processes/conditions studied by various researchers. These properties can vary substantially with respect to biomass source. In order to facilitate analysis and quantification of compounds, fractionation chromatography of bio-oils is used to separate bio-oils into different groups of chemical compounds [45, 46]. However, complete chemical characterization of bio-oils is practically not feasible due to the formation of pyrolytic lignins, which are randomly broken at different lengths of the polymeric chain [17]. The structural and compositional complexity of lignin could be assessed by its pyrolysis products such as guaiacol from coniferous wood and guaiacol and pyrogallol dimethyl ether from deciduous woods [47]. Despite having a much higher methoxyl content than wood, lignin results in higher yields

of charcoal and tar. [21, 29, 33, 48, 49]. It is postulated that pyrolysis reaction produces the most substituted phenols on a selective basis. In fact, the syringyl-propan units are linked to the lignin skeleton to a lesser extend with respect to the less substituted: guaiacyl-propane and phenyl-propane [50]. Thus, lignin derivatives are major constituents of any bio-oil and contribute to its complexity and distinct characteristics for different biomass source.

Bio-oils are the most preferred pyrolysis fuel types for transportation and storage purposes for obvious reasons such as compatibility with many existing equipments, pumping, and safety. However, in most cases it may not be suitable to use it directly and would require refining and further processing steps similar to fossil crude oil in petroleum refineries. The aging or stability of bio-oils is also of great concern as once pyrolysis is over, bio-oils start degrading or undergo further reactions among different chemical species albeit at much slower pace [6]. Furthermore, bio-oils from specific wood biomass are used as starting raw materials for the production of high value food flavoring agents, likewise, bio-oils from waste/renewable biomass could be refined by modified processes by the existing petroleum refineries for the production of commercial grade fuels and some high-value chemicals [44].

2.2. Biochar. Biochar is a pyrolysis byproduct along with bio-oil and flue gases. In recent times, biochar is less preferred over bio-oil as fuel source due to handling, incompatibility with transportation sector (automobile engines), storage, and secondary pollutants issues (higher ash content) [37–39]. This was also reflected in the literature citation for the present review, where much more research studies were aimed at the production of bio-oil than biochar (Tables 1 and 2). Nevertheless, except for incompatibility as biofuels for transportation sector, biochar has several merits, which make it an important byproduct of pyrolysis from the economic feasibility point of view. The usefulness of biochar in agricultural sector as well as in general has been the focus of several recent studies [20, 26, 34, 51–54]. Therefore, it is quite essential to explore the optimal and sustainable utilization of biochar in order to achieve environmental and economic goals of pyrolysis process. Gaunt and Lehmann [54], have reported energy balance and emission reduction potential of biochar in soil amendment application. The authors carried out the study based on their previous findings about net reduction in methane (CH_4) and nitrous oxide (N_2O) of soil amended with biochar [55]. The potential applications of biochar include soil enhancer, bulking agent for composting, activated carbon, remediation of water and soil, energy, and carbon sequestration [26, 51, 52, 54]. It is an established fact that biochar is very stable compared to raw biomass and has positive effects on overall plant growth. The very basic physical and chemical characteristics of biochar such as pH, porosity, affinity for metal adsorption, slow release of nutrients such as phosphorous and nitrogen, among others help in improvement of soil quality (Table 3). This can potentially reduce the requirements of conventional dosage of fertilizers, thereby, improving the economic output as well as abate the chances of nutrient runoff, erosion, and

TABLE 1: Advantages of thermochemical conversion of biomass over biological/biochemical process.

Thermochemical	Biological/biochemical
(1) Effectively applied to almost any biomass feedstock	Involves the use of microbes, enzymes, and/or chemicals to utilize the limited range of biomass
(2) Relatively higher productivity (production per unit time) due to completely chemical nature of reaction	Productivity is limited due to biological conversion. Increase would require higher capital investment such as bigger reactor
(3) Multiple high-value products possible using fractional separation of products	Normally, limited to one or few products and would require additional microbial culture, enzymes for more products
(4) Independent of climate conditions, operates at much higher temperature range, therefore, effect of ambient temperature will be minimal	Mostly susceptible to ambient temperature, and so forth such as anaerobic digester, sunlight for algal ponds
(5) Mostly complete utilization of the waste/biomass	Production of secondary wastes such as biomass sludge

greenhouse gas release. The above views and facts are based on the results of several authors [54, 55] which reported a reduction of 50–100% of CH_4 and N_2O as well as increase in efficiency of fertilizer utilization in soil amended with biochar. The use of biochar as reducer in metallurgical industry, particularly in Brazil, has also expanded the potential market of biochar [33]. Another important advantage about the biochar application as soil amendment product is the amount of carbon sequestered. Research studies have shown the stability of biochar obtained from different biomass to be between 100–10000 years or even more [56]. Therefore, the potential of generation of revenue from carbon emissions trading for biochar production can further reduce the overall operational costs of a pyrolysis plant [54]. Our own experience with an experimental pyrolysis reactor under development has proved that it is relatively easier to produce biochar at desired yield with respect to bio-oil. Therefore, the production technology for biochar is no hurdle, but dissemination of knowledge about practical utilization of biochar in agriculture and formulation of regulatory standards of its use and C emissions trading values remains to be established.

2.3. Noncondensable Pyrolysis Gas. The gaseous fraction of pyrolysis vapor is, in general, referred to as pyrolysis gas, flue gas, and noncondensable pyrolysis gas. It is composed of various gases such as CO_2 , CO, NO_x , SO_x , H_2S , H_2 , aldehydes, ketones, volatile carboxylic acids, and gaseous hydrocarbons. However, pyrolysis gases can also be composed of volatile compounds in the absence of efficient condensation system. The major gas components of pyrolysis are CO_2 and CO, which have been reported by several researchers for different

TABLE 2: Physicochemical characteristics of bio-oils obtained by different processes/biomass types.

Study	Biomass source	Pyrolysis temperature (°C)	Bio-oil yield (wt%)	Moisture content (wt%)	pH	Specific gravity @°C	C	H	N	O	Ash (wt%)	Calorific value (MJ/kg)	Viscosity (cP) @ temperature (°C)	Solids (wt%)	Distillation residue (wt%)
Salahi et al., [6]	Sawdust of mixture of woods	500	33–45	39	1.85	1.05@15	30.72	6.67	1.07	61.54	—	10.93	9.84@25	—	—
Czernik and Bridgwater, [27]	Wood	—	—	15–30	2.5	1.20@15	54–58	5.5–7.0	0–0.2	35–40	0–0.2	16–19*	40–100@50	0.2–1.0	up to 50
Ates and Isikdag, [28]	Oat straw	600	20.3	—	—	—	65.0	6.9	1.3	26.9	—	32.74*	—	—	—
	Wheat straw		19.1	—	—	—	71.1	8.5	0.5	19.8	—	27.09*	—	—	—
	Beech		62.7	22.2	2.5	—	41.4	7.1	0.2	51.2	—	16.9	15.2**@40	0.2	15 [#]
	Spruce		62.7	22	2.8	—	42.3	7.2	0.2	50.3	—	17.2	14.8**@40	0.1	15.4 [#]
Azeez et al., [29]	Iroko	470	50.6	32.3	2.9	—	38.2	7.5	0.3	54	—	15.9	—	0.2	14.1 [#]
	Albizia		54.7	25.1	2.9	—	41.9	7.4	0.6	50.1	—	17.4	57.1**@40	0.2	12.2 [#]
	Corn cob		56.7	32.2	3	—	38.1	8	0.7	53.2	—	15.8	6.7**@40	0.1	8.5 [#]
	Pine: polystyrene (50:50 w/w)	525	64.9	9.47	2.82	0.98@15	66.27	6.72	<0.5	7.02	—	28.42*	28.94**@—	—	—
	Pine: high-density polyethylene (50:50 w/w)	450	38.9	10.65	3.21	1.24@15	74.38	9.11	<0.5	6.33	—	27.68*	—	—	—
Bhattacharya et al., [30]	Pine: polypropylene (50:50 w/w)	450	46	5.44	3.02	1.09@15	79.7	10.64	<0.5	9.5	—	36.94*	23.6**@—	—	—
	Pine wood	450	50.10	13	3.1	1.19@15	57.2	7	<0.09	32.2	—	—	80.7**@—	—	—
Boateng et al., [31]	Switchgrass	480	60.71	23.02	—	1.25@15	40.78	6.98	0.33	47.25	0.011	16.02	22.14**@40	—	—
Fonts et al., [32]	Wastewater sludge	550	~50	27.2–46.6	—	0.972–0.975@15	—	—	—	—	—	30.60–32.09*	—	0.07–0.12	—
García-Pérez et al., [33]	Softwood	500	45.0–53.9	—	3.0	1.188@20	62.59	7.02	1.05	29.02	0.25	27.9*	62**@50	—	—
He et al., [34]	Swine manure	350	76.2	—	—	—	77.9	9.4	4.6	7.0	1.0	38.63*	—	—	—
Hiltten et al., [35]	Pine wood pellets	450	57.7	10.0	2.48	1.18@15	64.9	7.1	0.2	27.8	—	27.6*	300**@40	—	—
Miao and Wu, [36]	Microalgae	450	57.2	—	—	0.92	76.22	11.61	0.93	11.24	—	41*	20@40	—	—
Mullen et al., [37]	Corn cob	500	61.0	—	—	—	55.14	7.56	0.56	36.9	0.08	19.5*	—	—	—
	Corn stover		61.6	—	—	—	53.97	6.92	1.18	37.94	0.09	22.1*	—	—	—

TABLE 2: Continued.

Study	Biomass source	Pyrolysis temperature (°C)	Bio-oil yield (wt%)	Moisture content (wt%)	pH	Specific gravity @°C	C	H	N	O	Ash (wt%)	Calorific value (MJ/kg)	Viscosity (cP) @ temperature (°C)	Solids (wt%)	Distillation residue (wt%)
Mullen et al., [38]	Whole barley straw	~500	42–50	26.7	2.4	—	50.78	3.2	1.37	44.42	—	24.2*	23.5**@40	—	—
	Whole barley hulls			13.8	2.4	—	54.73	5.32	1.79	38.49	—	24.1*	102**@40	—	—
	Distiller's dried grains with solubles			18.7	6.5	—	74.02	8.92	5.05	6.24	—	32.9*	277**@40	—	—
Oasmaa et al., [3]	<i>Pinus sylvestris</i>	480–520	72.7	23.9	2.7	1.206	40.6	7.6	<0.1	51.7	0.03	20.1	17	0.01	—
	Forest residue (brown)		57.9	26.7	3.2	1.194	41.4	7.4	0.3	50.9	0.3	20.9	17	0.17	—
	Forest residue (green)		63.7	25.5	—	1.21	41.2	8	0.3	50.5	0.1	20.4	24	0.09	—
	<i>Eucalyptus grandis</i>		70.8	20.6	2.2	1.229	42.3	7.5	0.1	50.1	0.03	19.7	23	0.09	—
	Barley straw		52.0	51.1	3.7	—	26.5	9	0.9	62.7	—	18.6	—	0.43	—
	Timothy hay		52.5	39.3	3.4	1.15	32.1	8.5	0.6	58.7	0.004	18.4	5	0.01	—
Uzun et al., [39]	Reed canary grass	550	75.0	27.4	3.6	—	39.3	7.7	0.6	51.8	—	19.7	—	0.15	—
	Olive-oil residue		—	—	—	—	69.52	8.62	1.76	21.24	—	32.13	—	—	—
	Swine manure		24.2	2.37	—	—	72.58	9.76	4.47	13.19	0.13	36.05*	843@50	—	—
Yin et al., [42]	Cattle manure	310	48.76	—	—	—	73.72	8.13	1.39	16.76	—	35.53*	—	—	—
Zhang et al., [43]	Corn cob	550 (without catalyst)	56.9	—	2.8	1.18	51.94	6.96	0.82	40.28	—	18.8*	—	0.30	—
		550 (with catalyst)	~51.0	—	5.2	0.95	74.1	9.33	1.88	14.69	—	34.6*	—	0.20	—

— Not available.

* High heating value (HHV).

** Kinematic viscosity, cSt.

Lignin content.

TABLE 3: Characteristics of biochar produced by different processes/biomass types.

Study	Biomass source	Moisture (wt%)	C	H	N	O	Ash (wt%)	Calorific value (MJ/kg)	Temperature (°C)	Yield (wt%)
Boateng et al., [31]	Switchgrass	3.78	60.71	3.99	0.75	8.7	25.85	19.37	500	12.9
Mullen et al., [38]	Wheat straw	—	71.10	2.99	0.29	25.62	—	28.05*	500	~35–40
Abdullah and Wu, [57]	Mallee wood	4.6	60.3	5.3	0.18	34.14	0.70	22*	300	~56
Acikgoz et al., [58]	Linseed	—	61.63	2.57	4.08	31.73	—	24.12*	550	~15–20
Cao and Harris, [51]	Dairy manure	—	25.2	—	2.22	—	~55	—	350	~20–35
Mohan et al., [59]	Oak wood	3.17	82.83	2.70	0.31	8.05	2.92	31.03*	400	17–27
	Pine wood	2.69	83.47	2.99	0.27	8.25	2.30	31.68*		
	Oak bark	1.56	71.25	2.63	0.46	12.99	11.09	25.75*	450	
	Pine bark	2.31	68.25	2.51	0.34	10.80	15.75	25.25*		
Mullen et al., [37, 38]	Corn cobs	—	77.60	3.05	0.85	5.11	13.34	30.0*	500	18.9
	Corn stover	—	57.26	2.86	1.47	5.45	32.78	21.0*		17.0
Mulligan et al., [60]	Wheat straw	4.6	73.6	2.34	2.58	8.0	13.3	28.1*	500	32
	Mallee wood	4.6	78.7	2.48	1.18	8.7	8.9	29.9*		36
Salehi et al., [6]	Mixed sawdust	—	83.11	3.69	0.18	13.02	—	30.77*	500	20–27
Uzun et al., [39]	Olive oil residue	—	54.98	2.76	0.53	41.73	13.81	15.06*	400	—
		—	56.21	2.16	0.32	41.31	16.77	14.27*	500	—
		—	59.01	1.61	—	39.38	20.17	15.18*	550	—
		—	61.16	1.03	—	37.81	21.60	15.36*	700	—
Yang et al., [61]	Palm oil waste	—	76.81	1.46	2.32	11.47	—	—	600	28.57

* High heating value (HHV).

biomass types [62–64]. Pyrolysis gases have relatively lower average calorific value (an approximate estimation based on gas composition and concentration data from few studies in this paper is around 1.3 MJ/kg, [65]), therefore, almost all pyrolysis processes involve utilization of pyrolysis gases to contribute to heat the pyrolysis reaction [12, 44]. The presence of H₂O in pyrolysis gas is governed by the cleavage of aliphatic hydroxyl groups, which is not easily possible to avoid during pyrolysis, and it also affects the overall fuel quality of the pyrolysis products [62]. Tihay and Gilard [62], also detected the possibilities of formation of CO₂ via cleavage and reforming of functional groups of carboxyl (C=O). The production of CO was proposed from the cleavage of carbonyl groups (C=O) and of the bonds C–O, C–O–C, and C–C, and the production of CH₄ was mainly caused by the cleavage of methoxyl groups (–O–CH₃) and the break of methylene [62]. In general, pyrolysis gas is not a desired product; nevertheless, it is inevitable during pyrolysis process. The pyrolysis gas can be used to directly or indirectly preheat the biomass followed by burning via burner to generate heat requirements for pyrolysis process. The burning of pyrolysis gases poses a burden of treatment of combustion products which cannot be directly introduced into the environment. The presence of potential pollutant

gases NO_x, SO_x, H₂S, and aerosols in pyrolysis gases depends upon the biomass source such as animal waste, agricultural waste, and municipal waste. Nevertheless, there are many options for the treatment and purification of the pyrolysis gases such as electrostatic precipitator, NO_x scrubbers, adsorption systems based on activated carbon for volatile organic compounds, flares, flue gas desulfurization systems for SO_x, and biofilters [66].

3. Feedstock

In Canada only, there are about 6 004 944, and 8 700 000 dry tonnes/year production of municipal biosolids (organics), and forest residue (wood) [67]. Canada is also a global figure in biomass pellets production and exports about 10% of the 10 million tonnes per year of world demand for green energy market. In addition, cereal straw, corn stover, and flax straw are significant contributor to agricultural biomass residue as they occupy more than 85% of 36.4 million hectares of cropland in Canada [67]. Multiple options for natural resources for energy such as hydroelectricity, biomass, fossil fuels, tidal, wind, and solar enable Canada as a net exporter of energy and energy sources. However, in order to mitigate greenhouse gases and climate change effects and enhance

economic output, innovative biomass/waste utilization skills for energy and valuable products should be universally applied.

3.1. Agricultural Biomass. The greenhouse gas emissions coming from the agricultural sector accounted for 8.6%, which is based upon the use of either fossil fuels or their products (e.g., fertilizers) in agriculture. The estimated potential of agricultural residues for energy production is overwhelming, which is 1 and 9 billion barrels, respectively, for USA and world; nevertheless, a pragmatic utilization of agricultural residue for bioenergy should be carried out [68, 69]. In the literature, there are many studies on agricultural residues such as olive seed residue, hazelnut bagasse, corncobs, tea waste, sugar cane bagasse, and cotton [11, 65, 70]. It is essential to understand that most of the agricultural residues (such as crop residues) can be transformed to other valuable products. Even without any transformation, simple tillage practice of crop practice is very important to conserve soil physiochemical and microbial characteristics. Intense animal farming puts substantial load on animal feed supply, which is dependent on crop/crop residue production. Therefore, if a required fraction of the animal waste is not returned to the cropland, the overall approach could not be sustainable even in case of biofuels or added value products. In this regard, production of bio-oil and biochar from pyrolysis of animal waste or agricultural residue could be an interesting approach since application of biochar (as soil enhancer/conditioner) to the cropland has great potential [51, 52, 54, 56, 57]. Therefore, agricultural biomass has a good potential for the sustainable production of biofuels and valuable products via pyrolysis.

3.2. Municipal Waste. Municipal waste can consist of organic solids of up to 65% or more depending upon urban waste management practices (e.g., source separation) and socioeconomic status. Utilization of the bioorganic part of the municipal waste as biomass feedstock for pyrolysis can be a rational approach, if it is integrated to the electricity generation using heavy oil-based generators. In this case, the biochar and pyrolysis gas can be entirely utilized to provide heat requirements for pyrolysis process and the ash generated could be diverted to manufacture construction materials. In the literature, there are several reported studies on municipal solids at different stages (without and after biological treatments) [32, 71–75]. However, municipal solids have many conventional and newer treatment methods (biological, incineration, anaerobic digestion, and landfill) and are regarded as priority pollutants by municipalities. Therefore, economic aspects of the disposal and management of municipal solids have not been a major concern until lately. Nowadays, most municipalities are looking forward for biomass-to-energy conversion technologies in order to improve their treatment efficiency, reduce greenhouse gases emission and economic viability. In the present scenario, pyrolysis technologies of municipal solids to energy products could be a feasible option. However, the mass scale initiatives are taken based on local conditions of quality and quantity of

municipal solids, existing electricity cost, conventional methods of disposal of secondary wastes (landfill or composting).

3.3. Forest Residue. The initiatives of application of pyrolysis technologies to biomass were mainly taken for forestry residue and sawdust from timber industry. Therefore, nearly all existing demo- or commercial scale biomass pyrolysis plants are designed for wood residues (Dynamotive Corp., Ensyn Inc., BTG-BTL Inc., RTI Inc., and many others). The most appealing features of forest residue for pyrolysis process are the sustainable supply network on large scale basis, and suitability of the feedstock (lower moisture, ash, metals, nitrogen, and sulfur contents). Forest residue could be a reliable and sustainable biomass feedstock for pyrolysis plants in forest biomass countries like Canada, USA, and others with developed forest industry sector. However, in order to compete with fossil fuels the forest residue based on pyrolysis plants should be strategically placed to minimize cost of forest residue transportation. Analogous to fossil fuels, many mid to small scale pyrolysis units can be placed near to forest region as in the case of land-based or offshore oil rigs. The bio-oils produced by these multiple units can then be converged to a commercial scale bio-oil refinery for value addition or electricity generation plant depending upon the economics, similar to transportation of fossil fuels to petroleum refineries. In fact, some of the large scale pyrolysis plants in Europe are under experimental or demonstration phase for the evaluation of this apparently promising approach [12].

4. Thermochemical Processes

4.1. Fast/Flash Pyrolysis. In recent times, pyrolysis process is getting unprecedented attention from forestry, municipalities, and agricultural sector due to its potential for conversion of virtually all types of biomass into commercially viable biofuels and valuable chemical feedstocks for industrial sector. The concept of pyrolysis is not a novel approach as such, which is already in use for the production of several valuable chemical feedstocks. Nevertheless, it is a relatively recent process for the production of liquid fuels and electricity. However, in principle, any type of high temperature heating of organic matter in the absence or substantial deficiency of oxygen can be defined as some type of pyrolysis process. The term “biomass pyrolysis” is normally associated with the processes involving bio-oils and chemical feedstock production. The terms, torrefaction/carbonization, thermal liquefaction, and gasification can be separately used based upon operational parameters and intended applications. These processes are also mentioned briefly to provide an overview (Figure 1).

The term fast/flash pyrolysis is used for pyrolysis processes with very short residence time of intense thermal treatment, usually, it lasts from 0.5–3 s at 400–600°C [17]. The shorter time of heat exposure of the organic matter (e.g., biomass) in fast/flash pyrolysis process results in increased significance of heat and mass transfer, and phase transition along with chemical reaction kinetics [12]. Long residence

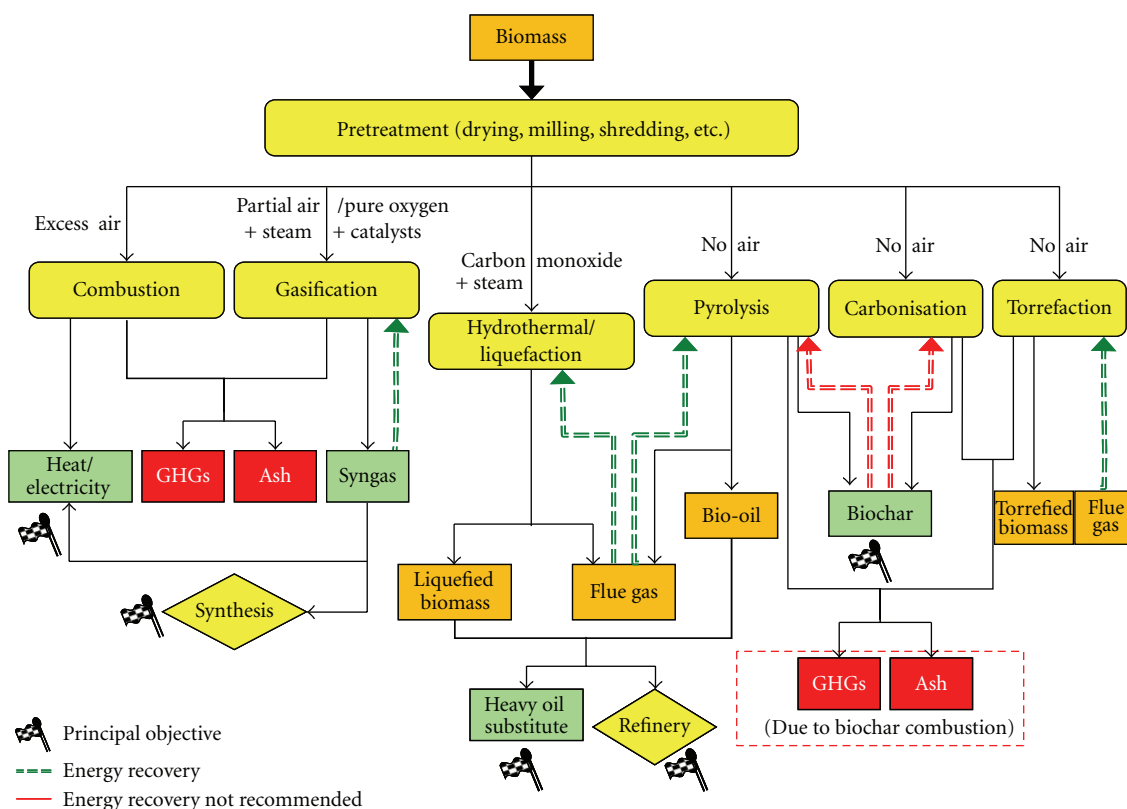


FIGURE 1: Biomass thermochemical conversion pathways.

times (few minutes to hours) and lower temperature range (200–350°C) favor charcoal formation. In principle, fluidized bed reactors use smaller particle size and high temperature to achieve very fast heat transfer, thereby, minimizing char formation. Interestingly, the low thermal conductivity of biomass particles is very well exploited in ablative reactors where biomass pellets are pressed against heated surface, forming pyrolysis vapor as well as exposing unaffected inner surface. Some of the prerequisites for fast pyrolysis are dry biomass ($\leq 10\%$ moisture), small particle size (≤ 3 mm), short residence times, moderate-to-high temperatures, and rapid quenching of pyrolyzed vapor. The lack of predictive kinetic constants for fast pyrolysis is due to its unsteady state nature as the biomass complexity requires multistage thermal decomposition with production of substantial quantities of highly unstable compounds (at process temperatures). All these factors have great impact on the design of a fast pyrolysis system which should rapidly heat biomass to desired temperature as well as quickly quench down the products.

4.2. Thermal Liquefaction. Thermal liquefaction can often be confused with pyrolysis in simplified comparisons [47]. The two processes differ in operating parameters, requirement of catalyst, and final products. Liquefaction produces mainly liquid and some amounts of gaseous components at temperature and pressure ranges of 250–350°C and 700–3000 psi, respectively, in the presence of alkali metal salts

as catalyst. The liquefaction may also require supplemental CO and H₂ as reactants to facilitate the overall process. The mechanisms of liquefaction reactions lack sufficient description about role of catalysts. In the past, some researchers have proposed possible mechanisms for Na₂CO₃ and K₂CO₃ for biomass liquefaction [76–78]. The catalysts hydrolyse the cellulose, hemicelluloses, and lignin macromolecules into smaller micellar-like fragments, which are further degraded to smaller compounds via dehydration, dehydrogenation, deoxygenation, and decarboxylation reactions. In comparison to torrefaction/carbonization, thermal liquefaction can provide liquid fuels in line with petroleum products along with several high value chemicals; however, recent trends in biomass thermochemical conversion, liquefaction, could not be successful at commercial scale. The possible factors that limit the liquefaction commercialization could be the lower overall yield of oil (between 20–55% w/w) compared to contemporary options like pyrolysis (discussed later), inferior oil quality (heavy tar like liquid), stricter operational parameters (higher reaction temperature and pressure), and requirements of catalysts and/or other reactants (CO, propanol, butanol, and glycerine).

4.3. Carbonization and Torrefaction. Carbonization and torrefaction are closely related processes (Figure 2). The former is mainly intended for biochar production, whereas, the latter is a thermal treatment to convert biomass into more efficient

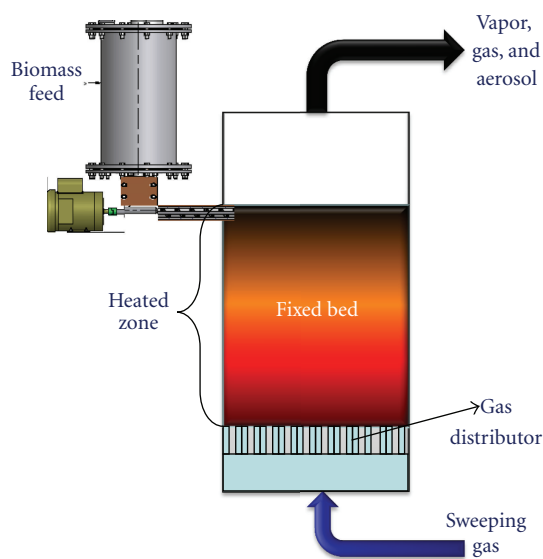


FIGURE 2: Fixed bed reactor concept for biomass pyrolysis.

form of energy source with less moisture and high fixed carbon, production of chemical feedstocks and to reduce the associated transportation costs.

For carbonization, the biomass is thermochemically treated in the temperature range between 200 to 315°C in the absence of oxygen [79]. Carbonization is accomplished by complete conversion of biomass into biochar. Thus, the product gains much higher energy density than the raw biomass, which lowers the transportation cost of the carbonized biomass.

In the case of torrefaction, there is partial decomposition of the biomass (especially the hemicellulose), giving off various types of volatiles resulting in brittle, dried and more volatile free solid product.

Moreover, carbonized/torrefied biomass has favorable characteristics such as, hydrophobic nature, similar or closely related properties as coal, easy to crush, grind or pulverize. The end-products comprise condensable gases such as water vapor, formic acid, acetic acid, furfural, methanol, lactic acid, phenol, and other oxygenates. Noncondensable gases such as carbon dioxide, carbon monoxide and small amounts of hydrogen and methane are also obtained. Thus, carbonization and torrefaction processes are used for the conversion of biomass into more efficient forms of energy source and to reduce the associated transportation costs. Nevertheless, it is not in competition with petroleum fuels in transport sector.

4.4. Gasification. Biomass gasification has also received much attention in recent times [2, 7, 10, 12, 20, 24, 71, 80–83]. The biomass is converted to simplified products, CO and H₂, in the optimized concentrations of oxygen and H₂O (steam reforming) at temperatures $\geq 800^\circ\text{C}$ which is completely distinct from gasification via anaerobic digestion. The final products are syngas (CO and H₂ mixture), CO₂, NO_x, SO_x, and ash/metal slag (quantity will depend upon

the type of the waste: municipal, agricultural, or wood biomass). Syngas has multiple applications such as fuel cells, synthetic fuel, and chemical feedstocks. Thus, technically gasification is an excellent method of extracting bioenergy free from N, P, S, Cl and metals contamination from diverse biomass types without further treatment/upgrading. Many biomass gasification processes are under development or at trial stage for biofuels and electricity generation, and waste disposal such as Enerkem, Thermoselect, GE Energy-Nexterra, Choren, among many others. However, positive electricity efficiency, biomass drying and grinding, oxygen input, reactor cleaning and maintenance, and economic feasibility are some major challenges for biomass gasification which are at research, pilot and demo scales.

5. Fast/Flash Pyrolysis Reactors

There are several types of fast/flash pyrolysis reactors both at developmental and commercial scale [12, 17, 44, 84, 85]. Different reactor configurations were inspired by the requirements such as the high heat transfer rates, separation of solids and gas phase, rapid condensation, and energy autonomy (Table 4). In the past, there are some excellent reviews about various pyrolysis reactors [12, 44]. Nevertheless, the highly dynamic research environment of biomass fast pyrolysis required timely update about developments in fast pyrolysis reactors. In this paper, major fast pyrolysis reactors are discussed in the following with their most recent information.

5.1. Fixed Bed. Fixed bed fast pyrolysis of biomass has been mentioned by many researchers [5, 6, 28, 57, 58, 80, 86–88]. However, in most of the cases the quantity of biomass taken for pyrolysis was in the range of few grams (g) and were aimed at analytical and laboratory scale investigation. A schematic diagram of a fixed bed reactor is shown in Figure 2. Schröder [88], used 2 kg of biomass of ~ 10 mm particle size and examined the validity of the fixed bed model. The author explained the importance of studying the chemical kinetics using larger particle size in comparison to common TGA analysis, where small sample of fine particles is used, therefore, the effect of transport phenomena becomes insignificant. Acikgoz et al. [58], investigated the pyrolysis of linseed seed samples in a well-swept resistively heated fixed bed tubular reactor (0.8 cm i.d., and 90 cm long), consisting of steel wool as fixed bed and constructed from 310 stainless steel. The pyrolysis operation was conducted by putting 2 g of air-dried sample of average particle size between 0.6–1.8 mm onto the fixed bed. A sweep gas velocity of 100 mL min^{-1} was maintained with heating rate that was kept as high as $300^\circ\text{C min}^{-1}$. Although the bio-oil yields were comparable to prior literature, no possible future scale-up of the reactor was mentioned. Likewise, fixed bed pyrolysis reactors have been used for evaluation of operating parameters such as temperature, heating rate, particle size, and cooling methods for different types of biomass, but no practical or commercial applications have been developed to the best of our knowledge. The possible reasons for lack of commercial scale fixed bed pyrolysis reactors could

TABLE 4: Comparison of various biomass pyrolysis reactors based on overall performance and efficiency.

Pyrolyzer	Status (units)	Bio-oil yield (wt%)	Operational complexity	Particle size	Biomass variability	Scale-up	Inert gas flow rate
Fixed bed	Pilot (single), lab (multiple)	75	Medium	Large	High	Hard	Low
Fluidized bed	Demo (multiple), lab (multiple)	75	Medium	Small	Low	Easy	High
Recirculating bed	Pilot (multiple), lab (multiple)	75	High	Medium	Low	Hard	High
Rotating Cone	Demo (single)	70	Medium	Medium	High	Medium	Low
Ablative	Pilot (single), lab (multiple)	75	High	Large	High	Hard	Low
Screw/auger reactor	Pilot (multiple), lab (multiple)	70	Low	Medium	High	Easy	Low
Vacuum	Pilot (single), lab (few)	60	High	Large	Medium	Hard	Low

be maintenance problems such as clogging of reactor bed with char and tar compounds, and increased resistance for sweeping gas flow, which could be easily resolved in the other reactor types mentioned in the following.

5.2. Fluidized Bed. Fluidized bed pyrolysis reactors are the most documented and commercially available reactor types amongst all pyrolyzers [29, 31, 32, 37, 38, 43, 89, 90]. More precisely, these are also known as bubbling fluidized bed reactors, where a hydrodynamically stable bed of smaller size biomass particles (0.5–2 mm) is maintained using an inert fluidizing gas such as nitrogen (Figure 3). In order to provide better heat transfer, entrapment of char particles, and temperature control, sand/carrier material is also entrained along with fluidizing gas to increase attrition/abrasion of biomass particles. The lack of mechanical parts allows easy scale up and maintenance, but fluidizing high volumes of biomass and carriers (e.g., sand) requires relatively higher energy and considerable part of capital investment in gas blowers. Fluidized bed reactor concept is well understood; therefore, it was possible to design and develop pyrolyzers at pilot and commercial scale as many crucial heat and mass transfer models during particle fluidization from prior studies were available. The fluidized bed reactor design enables minimizing catalytic cracking of pyrolysis vapor by char via quick separation of char particles using cyclones. Several fluidized bed pyrolyzers are operating at high quality bio-oil yields around 70–75% w/w with trouble-free operation and minimal maintenance [44] while, many other types of pyrolyzers have many operational as well as product quality challenges (discussed later). Therefore, the relatively higher energy requirements and considerable part of capital investment in gas blowers are easily disregarded by the investors. Furthermore, fluidized bed pyrolyzers have some established technologies in the market, such as RTP (Ensyn Inc.), and RTI (Dynamotive Corp.) along with many small scale reactors. However, increasing competition from other biofuels, and fossil crude oil, other potential concepts for fast

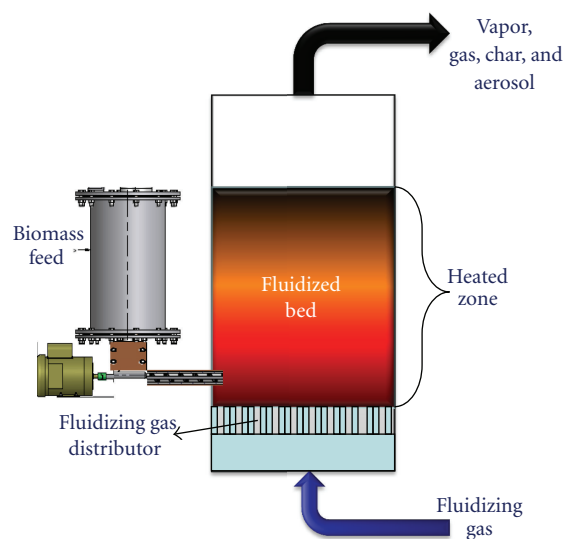


FIGURE 3: Generalized diagram for fluidized bed reactors for biomass pyrolysis.

pyrolysis involving lesser energy requirement and ability to use waste biomass are also getting increased attention.

5.3. Recirculating Fluidized Bed. Recirculating fluidized bed reactors are also referred as circulating fluidized bed or transport bed reactors which are more complex version of bubbling fluidized bed reactors (Figure 4). Similar to bubbling fluidized bed, this pyrolyzer type is also well understood and substantial literature data is available on its operation including biomass pyrolysis [31, 32, 37, 89]. In contrast to bubbling fluidized bed reactors, these pyrolyzers have lower heat transfer but better char attrition due to higher gas velocities via recirculation/reflux. The bio-oil yield of recirculating bed reactors is also similar to fluidized bed reactors but reheating of sand/carrier particles requires

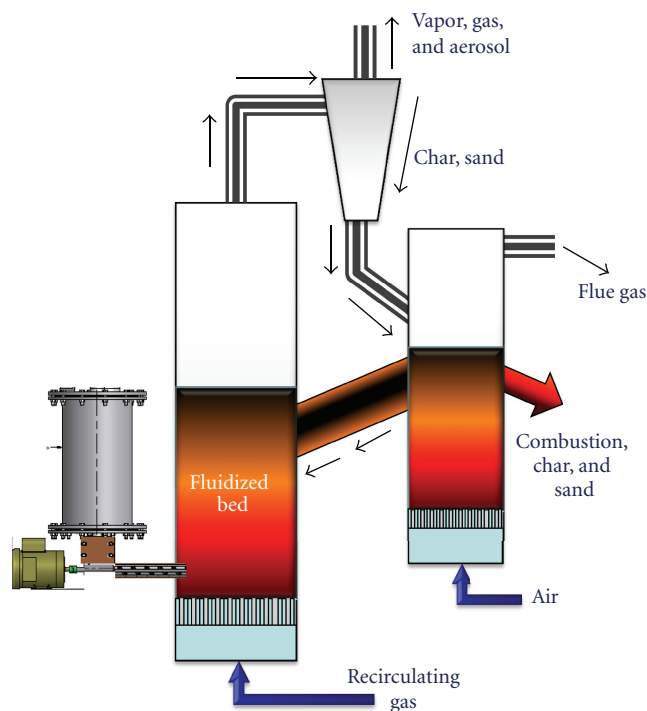


FIGURE 4: Schematic of recirculating fluidized bed pyrolyzer.

combustion of entrapped char which may lead to ash build up in the circulating bed. The major advantages of this reactor type are energetically self-sustainable pyrolysis which is easy, and high throughput volumes of biomass are possible due to high gas velocities. On the other hand, ash buildup can cause catalytic cracking of pyrolysis vapor and lead to some decrease in volatile matter in bio-oil, and very high gas velocities require even higher energy requirements for gas blowers. The operation and maintenance of this pyrolyzer type is robust, hence, process energy input concerns are overlooked in most of the cases as it is quite rare to find literature on energy input on such reactors.

5.4. Rotating Cone. Rotating cone pyrolyzer was developed at University of Twente, The Netherlands. This technology was the basis for the BTG-BTL process for the pyrolysis of various biomass types. The advantage of this technology is the absence of inert/carrier gas, thereby, relatively smaller energy requirement. In a rotating cone pyrolyzer, biomass is poured on a high-speed rotating cone along with hot sand in the absence of oxygen (Figure 5). The high speed rotation causes vigorous mixing of biomass and sand particles which in turn lead to fast heat transfer and biomass surface abrasion due to high speed heated sand particles [17, 91]. Thus, fast pyrolysis conditions are achieved with combined efforts of mechanical and fluid mixing. The energy requirements are met by char combustion and the process can be autonomous in terms of energy input for heating the pyrolyzer. Depending upon the biomass source, up to 75% w/w of bio-oil yield has been achieved with an estimated cost of 5 €/GJ which was comparable to diesel

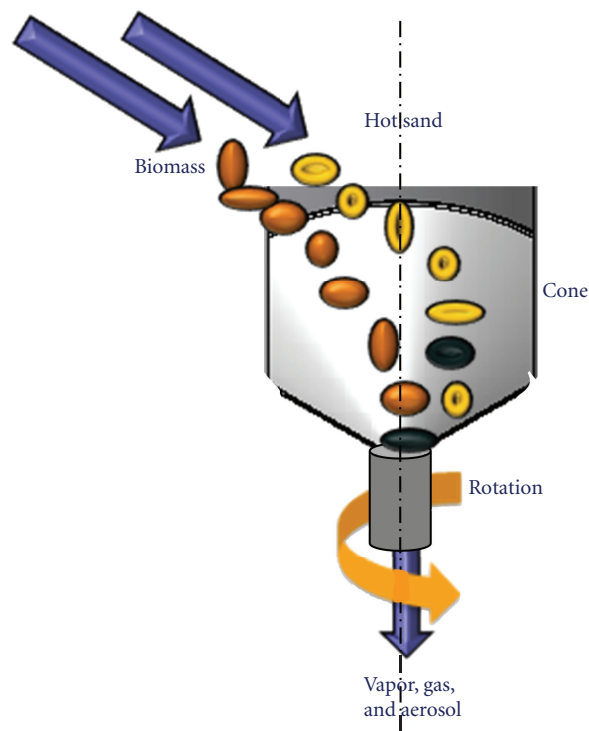


FIGURE 5: Rotating cone reactor.

fuel cost of up to 6.64 €/GJ (<http://www.btgworld.com/en>). This process has many upbeat features as mentioned by the company website. However, due to complete utilization of char for process heating, it may not be suitable for agricultural applications, where char (for CO₂ sequestration and soil enhancement) could have much higher added-value compared to bio-oil only orientation. Furthermore, high speed rotating cone (~600 rpm) may require considerable attention for operation and mechanical wear.

5.5. Ablative. Ablative pyrolysis reactors are being researched since 1980s; however, ablative pyrolysis is still under pilot scale studies due to its operational and scale up complexities [85, 92–96]. The ablative pyrolyzer requires simultaneous heating and surface renewal of the biomass feedstock via mechanical (rotating hot disc) or fluid dynamics (inert gas flow in wire mesh) (Figure 6). Mohan et al. [44] have correlated ablative pyrolysis to enhanced melting of a butter cube while pressing against a hot surface. It is said that the pyrolysis vapor and liquid produced during ablative pyrolysis can provide lubrication to the moving surface against which biomass is pressed; however, if the pyrolysis liquid stays longer on the rotating hot surface, it may undergo further undesired reactions. In order to avoid such reactions, fast removal of the pyrolysis vapor and liquids from the pyrolysis zone could nullify such lubrication effects. Ablative pyrolyzers could be based on direct contact [85, 94, 96, 97] or radiation ablation [92, 95]. The experimental reactors like wire-mesh reactor are more close to ablative reactor; nevertheless, the practical applicability seems to be

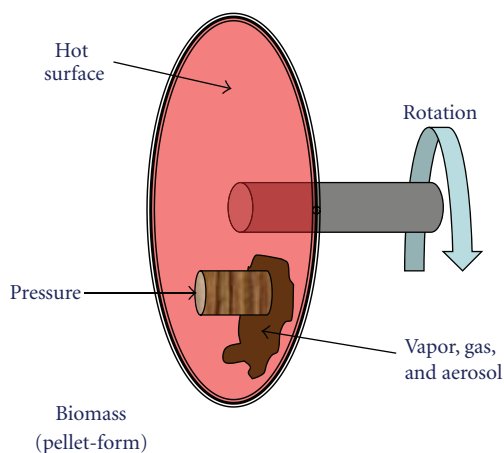


FIGURE 6: Ablative biomass pyrolysis reactor concept.

far from viable [92, 95]. On the other hand, direct contact ablative reactors appear to be practical but experiences with recent designs have been different from intuition. For example, in order to achieve flexibility in biomass types, extra biomass pretreatments are needed such as pelletization for fibrous biomass. High speed rotation of heated surface and sliding friction due to the intense pressure applied to the biomass pose great challenges to the scale up and operational simplicity.

5.6. Auger. Auger or screw pyrolyzer variants is getting increasing attention from many small and mid-size industries (Biogreen, [98] <http://www.biogreen-energy.com/biogreen.html>; EnerSysNet LLC, personal communication). The concept of solids handling using auger is integrated to almost all industries due to energy, space requirements, and related efficiencies. Interestingly, all other types of pyrolysis systems require auger unit to transport biomass at some point of process (feeding to the reaction chamber, char removal). However, application of auger concept to biomass pyrolysis is relatively recent. In fact, no pilot scale auger pyrolyzer was mentioned in the literature until early 2000s [12]. In this type of pyrolyzer, auger is used to transport the biomass through a heated (pyrolysis) zone (Figure 7). The biomass temperature is raised to the desired pyrolysis temperature during the transport through the heated zone by manipulating the auger rotation speed, diameter, flight-pitch, biomass particle size, and heating modes. The auger design provides a good control of biomass residence time inside the heated zone with minimal energy requirement. An apparent disadvantage could be moving parts and mechanical wear and tear; however, careful design (slow rotation) and developments in material science and machining (precision for tolerance and minimal contact between moving parts) can easily overcome this challenge. Auger pyrolyzers have major strengths in design compactness and simplicity, little or no carrier gas requirement, easy separation of bio-oil and char, and lower energy requirements. The simple operation of auger pyrolyzer is also an advantage from a farm scale utilization/application point of view. The recent surge in interest of small and mid-size industries

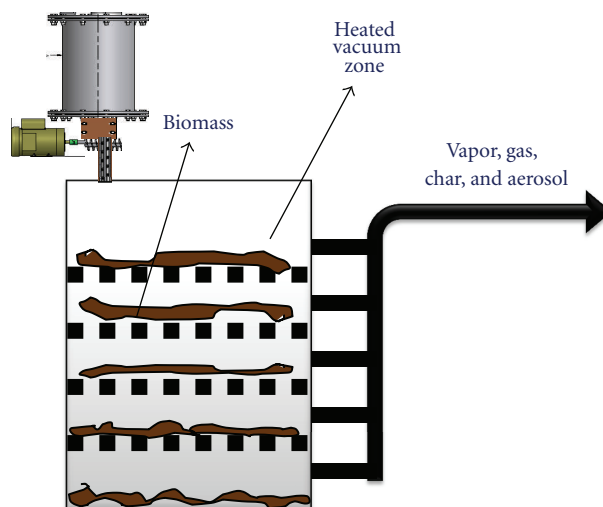


FIGURE 7: Vacuum pyrolysis reactor.

(including spinoffs from university research) is driven by the above-mentioned facts (BIOGREEN, EnerSysNet LLC, ROI LLC, Mississippi State University, Iowa State University). There are also several patents on auger reactor concept for the treatment of tire waste, municipal waste, and coal processing which justify the importance of auger design in the pyrolysis of biomass solids [99–107]. All of these pyrolysis systems work on the same principle, that is, pyrolysis reaction during transportation via auger/screw mechanism inside a heated zone, nevertheless, operating parameters (temperature, feedstock type, feedstock flow rates, particle size, use of sweeping gas, carrier material (sand/steel shots), direct or indirect heating among others), and pyrolysis system configurations vary greatly from one another. This also holds true for biomass pyrolysis systems.

5.7. Vacuum. The potential of vacuum pyrolysis for biomass as well as carbonaceous wastes has also shown some fruitful results after the pilot scale experiments [33, 108]. Vacuum pyrolysis does pose challenges such as lower heat- and mass-transfer, larger equipment size, and high capital investments which were required [109]. Also, maintaining fast pyrolysis conditions inside a vacuum pyrolyzer requires special inlet and outlet design for feed material and pyrolysis products (Figure 8). Furthermore, continuous operation of vacuum pyrolyzer requires special feedstock input mechanism. These are huge discouragement to the potential investors and eventual commercialization. On the other hand, vacuum pyrolysis offers very good control over vapor residence time; therefore, it minimizes the secondary decomposition reactions of bio-oil. The rapid volatilization due to reduced pressure also enables in decreasing the pyrolysis temperature and a possible decrease in heat input. In the literature, vacuum pyrolysis has been depicted as able to utilize larger size biomass. It may be advisable to add up the advantage of vacuum or low intensity vacuum conditions inside other possible reactor configurations such as auger or ablative reactors

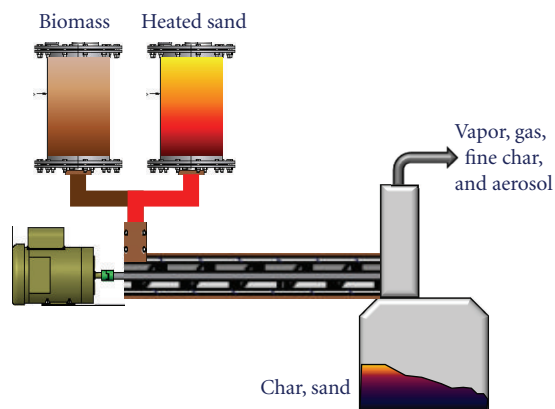


FIGURE 8: Auger/screw pyrolysis reactor concept using heat carrier.

to manipulate vapor residence time, pyrolysis temperature while also having better heat- and mass-transfer conditions.

6. Farm-Practice Concept for Residue/Waste Management via Pyrolysis

Farm residues/wastes can consist of up to 90% or more of organics/biomass [3]. This creates various opportunities to recover useful products via innovative management skills but also poses technical and economic challenges. Biological treatment of farm wastes is becoming increasingly challenging due to stricter regulations (limit to land spreading of biosolids due to metals and other nutrients) [9] as well as economic feasibility (increasing energy and utility cost). Anaerobic digestion provides energetic benefits to the agricultural producer; however, it is susceptible to various factors such as climate (low temperature), limited types and variations in waste composition, availability of land, among many. Most of the conventional farm waste disposal or transformation strategies falter either at technical or economic front. For example, composting of farm waste has many challenges such as control of odor, nutrient leaching, maturity, and net energy input [110, 111]. Pyrolysis of organic materials can have a potential of technical and can contribute to economic transformation of farm wastes into energy and valuable products, and sequestration of carbon. An overview of farm-scale application of pyrolysis for residue biomass management, transformation, and minerals and nutrient recycle is shown in Figure 9. Plants use CO_2 and sunlight to grow via photosynthesis as a natural process. The plant harvest could be diverted to food, valuable commodity, and animal feed. The animal farming requires animal feed (e.g., about 6 to 7 times plant biomass per unit mass of animal meat) and generates significant amounts of manure as farm wastes [112]. The animal manure could be separated via chemical or mechanical process into $\geq 60\%$ w/w solids and a liquid stream. The liquid stream could be further treated via biological process for removal of pathogens and toxic compounds and returned back to the soil, thereby, preserving water and soil minerals and nutrients (N and P). The biomass generated by the liquid treatment process and the

solids from the manure separation unit could be transferred to a drying unit. The drying unit should utilize energy from the combustion of the pyrolysis gases and should be able to reduce moisture to $\leq 10\%$ w/w. The pyrolysis unit could be operated by external energy source or could also utilize a portion of pyrolysis products (e.g., biochar and flue gases) to meet energy requirements. The bio-oil thus produced could either be used for heating and electricity generation for farm, or be sold to a bio-oil refinery network for purification and value addition. The biochar can be returned back to the soil to replenish minerals and nutrients as well as enhance physicochemical characteristics of soil such as pH, porosity, and density. Biochar has also been found to adsorb heavy metals and slow release of N, P, and other nutrients. This will help in enhancing the efficiency of fertilizers [56, 57, 113]. In addition, biochar has high self-life (100 to 1000 years), thus a significant portion of CO_2 from the atmosphere will be sequestered in soil with every crop cycle. This solution should be able to contain a significant part of the present GHGs emissions (agriculture sector contribute to about 8%) for a long term until a more comprehensive strategy is in place. In order to validate this scheme, life cycle analysis and technoeconomic study are currently being performed on the application of pyrolytic transformation of farm wastes (e.g., animal manure, plant residues) in our researches facility. In the past, there are only a few researches on pyrolytic conversion of farm wastes to bio-oil, biochar, and combustible gases [7]. However, the incumbent combined adverse effects of global warming/climate change, fossil fuel crisis, and risks to the environment have propelled the interests of governments and commercial sectors across the world towards the transformation of biomass residues and wastes into energy, carbon sequestration, and other valuable products. Many countries and conglomerates of countries have either initiated or at least planned subsidies and aid for biomass to energy concept. In most cases, the large scale commercial ventures are based on forest biomass/residue which may be suitable for long-term or sustainable development if they are well managed. At present, disposal and management of farm residue/wastes are major problems and should be actively considered as another important biomass source. As farm waste generation is related to the population consumption of farm goods which is growing rapidly, the transformation of farm wastes to energy, carbon sequestration, and valuable products could help in minimizing the net GHGs by decreasing the net use of fossil fuels.

7. Conclusions

The present study briefly reviewed various available technologies for thermochemical conversion of biomass to biofuels alternatives to fossil fuels and focused on biomass pyrolysis. Thermochemical processes have advantage over “biological only” processes where lignocellulosic biomass needs various pretreatment steps, time, and investments. At present, thermochemical processes such as gasification and combustion have a foothold at commercial scale for heat and electricity, mainly due apparent simple working principle and lack of research about their effect on sustainable

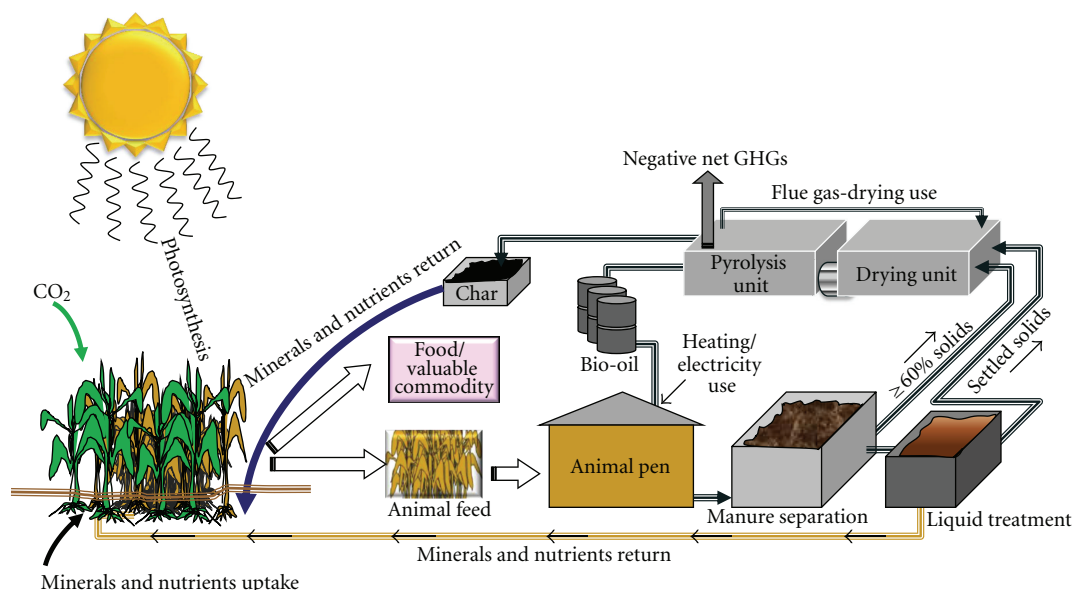


FIGURE 9: Possible farm practice of biomass residue.

development. However, in the recent years many studies have suggested biomass pyrolysis to be more favorable to the sustainable development in comparison to combustion and gasification. Biomass pyrolysis generates bio-oil, and biochar, which can have miscellaneous utilization such as energy, chemical feedstocks for industries, liquid fuels, carbon sequestration, bioremediation, and soil enhancement. On the other hand, gasification and combustion have limited uses to heating and energy. The established pyrolysis technologies at demonstration and commercial scale are fluidized bed variants and rotating cone types. Auger reactors for biomass pyrolysis are currently under laboratory, pilot, and demonstration stages and show good potential for mobile and farm scale uses due to simplicity of design and operation features. Ablative reactors need more research at laboratory scale and probably developments in material science to be successful at higher scale. The initial attempts with vacuum pyrolysis were successful despite challenges of lower heat and mass transfer, vacuum sealing requirements, and other operating and investment factors. Currently, vacuum pyrolysis can be considered to be a potential technology for commercialization. The physicochemical characteristics of bio-oil and biochar produced from pyrolysis are dependent on the biomass; however, the yields are related to pyrolysis reactor types and process used. A simplified farm-practice concept for waste management is depicted using biomass pyrolysis. This approach will produce bio-oil and biochar where bio-oil can be used for heating and electricity generation purposes and biochar can be applied for soil enhancement. Thus, a substantial portion of minerals and nutrients can be recycled back to the soil. Moreover, bio-oil will add to farm economy, and the overall process will be free of net energy requirement. However, these initiatives of biomass pyrolysis for sustainable development

will require subsidies and technology transfer for a successful venture.

Acknowledgments

The authors would like to extend their gratitude to Conseil pour le développement de l'Agriculture du Québec (CDAQ), NSERC, CRIQ, and IRDA for providing financial support in terms of Industrial Postdoctoral Fellowship to one of the authors, Dr. M. Verma.

References

- [1] A. Steve, 2008 Oil Recap. and What is Next, 2009, <http://www.oil-price.net/>.
- [2] M. Baratieri, P. Baggio, L. Fiori, and M. Grigante, "Biomass as an energy source: thermodynamic constraints on the performance of the conversion process," *Bioresource Technology*, vol. 99, no. 15, pp. 7063–7073, 2008.
- [3] A. Oasmaa, Y. Solantausta, V. Arpiainen, E. Kuoppala, and K. Sipilä, "Fast pyrolysis bio-oils from wood and agricultural residues," *Energy and Fuels*, vol. 24, no. 2, pp. 1380–1388, 2010.
- [4] <http://www.btg-btl.com/index.php?r=technology>.
- [5] W. T. Tsai, J. H. Chang, K. J. Hsien, and Y. M. Chang, "Production of pyrolytic liquids from industrial sewage sludges in an induction-heating reactor," *Bioresource Technology*, vol. 100, no. 1, pp. 406–412, 2009.
- [6] E. Salehi, J. Abedi, and T. Harding, "Bio-oil from sawdust: pyrolysis of sawdust in a fixed-bed system," *Energy and Fuels*, vol. 23, no. 7, pp. 3767–3772, 2009.
- [7] K. B. Cantrell, T. Ducey, K. S. Ro, and P. G. Hunt, "Livestock waste-to-bioenergy generation opportunities," *Bioresource Technology*, vol. 99, no. 17, pp. 7941–7953, 2008.

- [8] J. Martinez-Almela and J. M. Barrera, "SELCO-Ecopurin® pig slurry treatment system," *Bioresource Technology*, vol. 96, no. 2, pp. 223–228, 2005.
- [9] Québec. Ministère de développement durable, Environnement et Parcs, Québec. Guide sur la valorisation des matières résiduelles fertilisantes Critères de référence et normes réglementaires, 2008.
- [10] L. Zhang, C. Xu, and P. Champagne, "Overview of recent advances in thermo-chemical conversion of biomass," *Energy Conversion and Management*, vol. 51, no. 5, pp. 969–982, 2010.
- [11] J. A. Conesa, R. Font, A. Fullana et al., "Comparison between emissions from the pyrolysis and combustion of different wastes," *Journal of Analytical and Applied Pyrolysis*, vol. 84, no. 1, pp. 95–102, 2009.
- [12] A. V. Bridgwater, A. J. Toft, and J. G. Brammer, "A techno-economic comparison of power production by biomass fast pyrolysis with gasification and combustion," *Renewable and Sustainable Energy Reviews*, vol. 6, no. 3, pp. 181–246, 2002.
- [13] L. Deng, Z. Yan, Y. Fu, and Q. X. Guo, "Green solvent for flash pyrolysis oil separation," *Energy and Fuels*, vol. 23, no. 6, pp. 3337–3338, 2009.
- [14] H. Guoxin, H. Hao, and L. Yanhong, "Hydrogen-rich gas production from pyrolysis of biomass in an autogenerated steam atmosphere," *Energy and Fuels*, vol. 23, no. 3, pp. 1748–1753, 2009.
- [15] K. S. Ro, K. B. Cantrell, P. G. Hunt, T. F. Ducey, M. B. Vanotti, and A. A. Szogi, "Thermochemical conversion of livestock wastes: carbonization of swine solids," *Bioresource Technology*, vol. 100, no. 22, pp. 5466–5471, 2009.
- [16] X. Wang, H. Chen, K. Luo, J. Shao, and H. Yang, "The influence of microwave drying on biomass pyrolysis," *Energy and Fuels*, vol. 22, no. 1, pp. 67–74, 2008.
- [17] D. Meier and O. Faix, "State of the art of applied fast pyrolysis of lignocellulosic materials—a review," *Bioresource Technology*, vol. 68, no. 1, pp. 71–77, 1999.
- [18] G. Carucci, F. Carrasco, K. Trifoni, M. Majone, and M. Beccari, "Anaerobic digestion of food industry wastes: effect of codigestion on methane yield," *Journal of Environmental Engineering*, vol. 131, no. 7, pp. 1037–1045, 2005.
- [19] K. B. Cantrell, K. C. Stone, P. G. Hunt, K. S. Ro, M. B. Vanotti, and J. C. Burns, "Bioenergy from Coastal bermudagrass receiving subsurface drip irrigation with advance-treated swine wastewater," *Bioresource Technology*, vol. 100, no. 13, pp. 3285–3292, 2009.
- [20] L. Catoire, M. Yahyaoui, A. Osmont et al., "Thermochemistry of compounds formed during fast pyrolysis of lignocellulosic biomass," *Energy and Fuels*, vol. 22, no. 6, pp. 4265–4273, 2008.
- [21] M. Müller-Hagedorn and H. Bockhorn, "Pyrolytic behaviour of different biomasses (angiosperms) (maize plants, straws, and wood) in low temperature pyrolysis," *Journal of Analytical and Applied Pyrolysis*, vol. 79, no. 1–2, pp. 136–146, 2007.
- [22] A. Demirbas, "Effect of initial moisture content on the yields of oily products from pyrolysis of biomass," *Journal of Analytical and Applied Pyrolysis*, vol. 71, no. 2, pp. 803–815, 2004.
- [23] P. Kumar, D. M. Barrett, M. J. Delwiche, and P. Stroeve, "Methods for pretreatment of lignocellulosic biomass for efficient hydrolysis and biofuel production," *Industrial and Engineering Chemistry Research*, vol. 48, no. 8, pp. 3713–3729, 2009.
- [24] D. R. Keshwani and J. J. Cheng, "Switchgrass for bioethanol and other value-added applications: a review," *Bioresource Technology*, vol. 100, no. 4, pp. 1515–1523, 2009.
- [25] R. Manurung, D. A. Z. Wever, J. Wildschut et al., "Valorisation of *Jatropha curcas* L. plant parts: nut shell conversion to fast pyrolysis oil," *Food and Bioproducts Processing*, vol. 87, no. 3, pp. 187–196, 2009.
- [26] J. Yang and K. Q. Qiu, "Preparation of activated carbon by chemical activation under vacuum," *Environmental Science and Technology*, vol. 43, no. 9, pp. 3385–3390, 2009.
- [27] S. Czernik and A. V. Bridgwater, "Overview of applications of biomass fast pyrolysis oil," *Energy and Fuels*, vol. 18, no. 2, pp. 590–598, 2004.
- [28] F. Ateş and M. A. İşikdağ, "Evaluation of the role of the pyrolysis temperature in straw biomass samples and characterization of the oils by GC/MS," *Energy and Fuels*, vol. 22, no. 3, pp. 1936–1943, 2008.
- [29] A. M. Azeez, D. Meier, J. Odermatt, and T. Willner, "Fast pyrolysis of African and European lignocellulosic biomasses using Py-GC/MS and fluidized bed reactor," *Energy and Fuels*, vol. 24, no. 3, pp. 2078–2085, 2010.
- [30] P. Bhattacharya, P. H. Steele, E. B. M. Hassan, B. Mitchell, L. Ingram, and C. U. Pittman, "Wood/plastic copyrolysis in an auger reactor: chemical and physical analysis of the products," *Fuel*, vol. 88, no. 7, pp. 1251–1260, 2009.
- [31] A. A. Boateng, D. E. Daugaard, N. M. Goldberg, and K. B. Hicks, "Bench-scale fluidized-bed pyrolysis of switchgrass for bio-oil production," *Industrial and Engineering Chemistry Research*, vol. 46, no. 7, pp. 1891–1897, 2007.
- [32] I. Fonts, M. Azuara, G. Gea, and M. B. Murillo, "Study of the pyrolysis liquids obtained from different sewage sludge," *Journal of Analytical and Applied Pyrolysis*, vol. 85, no. 1–2, pp. 184–191, 2009.
- [33] M. García-Pérez, A. Chaala, H. Pakdel, D. Kretschmer, and C. Roy, "Vacuum pyrolysis of softwood and hardwood biomass. Comparison between product yields and bio-oil properties," *Journal of Analytical and Applied Pyrolysis*, vol. 78, no. 1, pp. 104–116, 2007.
- [34] B. J. He, Y. Zhang, T. L. Funk, G. L. Riskowski, and Y. Yin, "Thermochemical conversion of swine manure: an alternative process for waste treatment and renewable energy production," *Transactions of the American Society of Agricultural Engineers*, vol. 43, no. 6, pp. 1827–1833, 2000.
- [35] R. N. Hilten, B. P. Bibens, J. R. Kastner, and K. C. Das, "In-line esterification of pyrolysis vapor with ethanol improves Bio-oil quality," *Energy and Fuels*, vol. 24, no. 1, pp. 673–682, 2010.
- [36] X. Miao and Q. Wu, "High yield bio-oil production from fast pyrolysis by metabolic controlling of *Chlorella protothecoides*," *Journal of Biotechnology*, vol. 110, no. 1, pp. 85–93, 2004.
- [37] C. A. Mullen, A. A. Boateng, N. M. Goldberg, I. M. Lima, D. A. Laird, and K. B. Hicks, "Bio-oil and bio-char production from corn cobs and stover by fast pyrolysis," *Biomass and Bioenergy*, vol. 34, no. 1, pp. 67–74, 2010.
- [38] C. A. Mullen, A. A. Boateng, K. B. Hicks, N. M. Goldberg, and R. A. Moreau, "Analysis and comparison of bio-oil produced by fast pyrolysis from three barley biomass/byproduct streams," *Energy and Fuels*, vol. 24, no. 1, pp. 699–706, 2010.
- [39] B. B. Uzun, A. E. Pütün, and E. Pütün, "Composition of products obtained via fast pyrolysis of olive-oil residue: effect of pyrolysis temperature," *Journal of Analytical and Applied Pyrolysis*, vol. 79, no. 1–2, pp. 147–153, 2007.

- [40] S. Xiu, A. Shahbazi, V. Shirley, M. R. Mims, and C. W. Wallace, "Effectiveness and mechanisms of crude glycerol on the biofuel production from swine manure through hydrothermal pyrolysis," *Journal of Analytical and Applied Pyrolysis*, vol. 87, no. 2, pp. 194–198, 2010.
- [41] S. Xiu, A. Shahbazi, V. Shirley, and D. Cheng, "Hydrothermal pyrolysis of swine manure to bio-oil: effects of operating parameters on products yield and characterization of bio-oil," *Journal of Analytical and Applied Pyrolysis*, vol. 88, no. 1, pp. 73–79, 2010.
- [42] S. Yin, R. Dolan, M. Harris, and Z. Tan, "Subcritical hydrothermal liquefaction of cattle manure to bio-oil: effects of conversion parameters on bio-oil yield and characterization of bio-oil," *Bioresource Technology*, vol. 101, no. 10, pp. 3657–3664, 2010.
- [43] H. Zhang, R. Xiao, H. Huang, and G. Xiao, "Comparison of non-catalytic and catalytic fast pyrolysis of corn cob in a fluidized bed reactor," *Bioresource Technology*, vol. 100, no. 3, pp. 1428–1434, 2009.
- [44] D. Mohan, C. U. Pittman, and P. H. Steele, "Pyrolysis of wood/biomass for bio-oil: a critical review," *Energy and Fuels*, vol. 20, no. 3, pp. 848–889, 2006.
- [45] T. A. Milne, F. Agblevor, M. Davis, S. Deutch, and D. Johnson, "A review of chemical composition of fast pyrolysis oils," in *Developments in thermochemical biomass conversion*, A. V. Bridgwater, Ed., pp. 409–424, Blackie Academic and Professional, London, UK, 1997.
- [46] A. Oasmaa, E. Kuoppala, and Y. Solantausta, "Fast pyrolysis of forestry residue. 2. Physicochemical composition of product liquid," *Energy and Fuels*, vol. 17, no. 2, pp. 433–443, 2003.
- [47] A. Demirbaş, "Mechanisms of liquefaction and pyrolysis reactions of biomass," *Energy Conversion and Management*, vol. 41, no. 6, pp. 633–646, 2000.
- [48] A. Oasmaa, E. Kuoppala, J. F. Selin, S. Gust, and Y. Solantausta, "Fast pyrolysis of forestry residue and pine. 4. Improvement of the product quality by solvent addition," *Energy and Fuels*, vol. 18, no. 5, pp. 1578–1583, 2004.
- [49] K. I. Kuroda and D. R. Dimmel, "Effect of pyrofoil composition on pyrolysis of lignin," *Journal of Analytical and Applied Pyrolysis*, vol. 62, no. 2, pp. 259–271, 2002.
- [50] F. L. Brown, *Theories on the combustion of wood and its control*. US Forest Product Lab Rep, 1958.
- [51] X. Cao and W. Harris, "Properties of dairy-manure-derived biochar pertinent to its potential use in remediation," *Bioresource Technology*, vol. 101, no. 14, pp. 5222–5228, 2010.
- [52] B. O. Dias, C. A. Silva, F. S. Higashikawa, A. Roig, and M. A. Sánchez-Monedero, "Use of biochar as bulking agent for the composting of poultry manure: effect on organic matter degradation and humification," *Bioresource Technology*, vol. 101, no. 4, pp. 1239–1246, 2010.
- [53] D. Kalderis, S. Bethanis, P. Paraskeva, and E. Diamadopoulos, "Production of activated carbon from bagasse and rice husk by a single-stage chemical activation method at low retention times," *Bioresource Technology*, vol. 99, no. 15, pp. 6809–6816, 2008.
- [54] J. L. Gaunt and J. Lehmann, "Energy balance and emissions associated with biochar sequestration and pyrolysis bioenergy production," *Environmental Science and Technology*, vol. 42, no. 11, pp. 4152–4158, 2008.
- [55] M. Rondon, J. Ramirez, and J. Lehmann, "Charcoal additions reduce net emissions of greenhouse gases to the atmosphere," in *Proceedings of the 3rd USDA Symposium on Greenhouse Gases and Carbon Sequestration*, p. 208, Baltimore, Md, USA, March 2005.
- [56] D. D. Warnock, J. Lehmann, T. W. Kuyper, and M. C. Rillig, "Mycorrhizal responses to biochar in soil—concepts and mechanisms," *Plant and Soil*, vol. 300, no. 1–2, pp. 9–20, 2007.
- [57] H. Abdullah and H. Wu, "Biochar as a fuel: 1. Properties and grindability of biochars produced from the pyrolysis of mallee wood under slow-heating conditions," *Energy and Fuels*, vol. 23, no. 8, pp. 4174–4181, 2009.
- [58] C. Acikgoz, O. Onay, and O. M. Kockar, "Fast pyrolysis of linseed: product yields and compositions," *Journal of Analytical and Applied Pyrolysis*, vol. 71, no. 2, pp. 417–429, 2004.
- [59] D. Mohan, C. U. Pittman, M. Bricka et al., "Sorption of arsenic, cadmium, and lead by chars produced from fast pyrolysis of wood and bark during bio-oil production," *Journal of Colloid and Interface Science*, vol. 310, no. 1, pp. 57–73, 2007.
- [60] C. J. Mulligan, L. Strezov, and V. Strezov, "Thermal decomposition of wheat straw and mallee residue under pyrolysis conditions," *Energy and Fuels*, vol. 24, no. 1, pp. 46–52, 2010.
- [61] H. Yang, R. Yan, H. Chen, D. H. Lee, D. T. Liang, and C. Zheng, "Mechanism of palm oil waste pyrolysis in a packed bed," *Energy and Fuels*, vol. 20, no. 3, pp. 1321–1328, 2006.
- [62] V. Tihay and P. Gillard, "Pyrolysis gases released during the thermal decomposition of three Mediterranean species," *Journal of Analytical and Applied Pyrolysis*, vol. 88, no. 2, pp. 168–174, 2010.
- [63] R. L. Johnson, S. S. Liaw, M. Garcia-Perez et al., "Pyrolysis gas chromatography mass spectrometry studies to evaluate high-temperature aqueous pretreatment as a way to modify the composition of bio-oil from fast pyrolysis of wheat straw," *Energy and Fuels*, vol. 23, no. 12, pp. 6242–6252, 2009.
- [64] R. Zhang, H. M. El-Mashad, K. Hartman et al., "Characterization of food waste as feedstock for anaerobic digestion," *Bioresource Technology*, vol. 98, no. 4, pp. 929–935, 2007.
- [65] M. C. Blanco López, C. G. Blanco, A. Martínez-Alonso, and J. M. D. Tascón, "Composition of gases released during olive stones pyrolysis," *Journal of Analytical and Applied Pyrolysis*, vol. 65, no. 2, pp. 313–322, 2002.
- [66] S. Rappert and R. Müller, "Odor compounds in waste gas emissions from agricultural operations and food industries," *Waste Management*, vol. 25, no. 9, pp. 887–907, 2005.
- [67] Statistics Canada, *Computing in the Humanities and Social Sciences (CHASS)*, *Canadian Socio-Economic Information Management (CANSIM)*, University of Toronto Data Library Service, Toronto, Canada, 2007.
- [68] R. Lal, "Soil carbon sequestration impacts on global climate change and food security," *Science*, vol. 304, no. 5677, pp. 1623–1627, 2004.
- [69] P. B. Weisz, "Basic choices and constraints on long-term energy supplies," *Physics Today*, vol. 57, no. 7, pp. 47–52, 2004.
- [70] I. Demiral and S. Şensöz, "The effects of different catalysts on the pyrolysis of industrial wastes (olive and hazelnut bagasse)," *Bioresource Technology*, vol. 99, no. 17, pp. 8002–8007, 2008.
- [71] S. Werle and R. K. Wilk, "A review of methods for the thermal utilization of sewage sludge: the Polish perspective," *Renewable Energy*, vol. 35, no. 9, pp. 1914–1919, 2010.
- [72] M. H. Romdhana, A. Hamaïdi, B. Ladevie, and D. Lecomte, "Energy valorization of industrial biomass: using a batch frying process for sewage sludge," *Bioresource Technology*, vol. 100, no. 15, pp. 3740–3744, 2009.

- [73] S. Yaman, "Pyrolysis of biomass to produce fuels and chemical feedstocks," *Energy Conversion and Management*, vol. 45, no. 5, pp. 651–671, 2004.
- [74] H. P. Wenning, "The VEBA OEL technologie pyrolysis process," *Journal of Analytical and Applied Pyrolysis*, vol. 25, pp. 301–310, 1993.
- [75] A. N. García, R. Font, and A. Marcilla, "Kinetic studies of the primary pyrolysis of municipal solid waste in a Pyroprobe 1000," *Journal of Analytical and Applied Pyrolysis*, vol. 23, no. 1, pp. 99–119, 1992.
- [76] E. Chornet and R. P. Overend, *Fundamentals of Thermochemical Biomass Conversion*, Academic Press, Amsterdam, The Netherlands, 1985.
- [77] J. A. Russell, R. K. Miller, and P. M. Molton, "Formation of aromatic compounds from condensation reactions of cellulose degradation products," *Biomass*, vol. 3, no. 1, pp. 43–57, 1983.
- [78] H. R. Appell, "The production of oil from wood waste," in *Fuels from Waste*, L. Anderson and D. A. Tilman, Eds., Academic Press, New York, NY, USA, 1977.
- [79] S. Sadaka and S. Negi, "Improvements of biomass physical and thermochemical characteristics via torrefaction process," *Environmental Progress and Sustainable Energy*, vol. 28, no. 3, pp. 427–434, 2009.
- [80] T. Phuphuakrat, N. Nipattummakul, T. Namioka, S. Kerd-suwan, and K. Yoshikawa, "Characterization of tar content in the syngas produced in a downdraft type fixed bed gasification system from dried sewage sludge," *Fuel*, vol. 89, no. 9, pp. 2278–2284, 2010.
- [81] A. G. Barneto, J. A. Carmona, A. Gálvez, and J. A. Conesa, "Effects of the composting and the heating rate on biomass gasification," *Energy and Fuels*, vol. 23, no. 2, pp. 951–957, 2009.
- [82] X. J. Guo, B. Xiao, X. L. Zhang, S. Y. Luo, and M. Y. He, "Experimental study on air-stream gasification of biomass micron fuel (BMF) in a cyclone gasifier," *Bioresource Technology*, vol. 100, no. 2, pp. 1003–1006, 2009.
- [83] E. Chornet, D. Wang, S. Montane, S. Czernik, D. Johnson, and M. Mann, "Biomass to hydrogen via fast pyrolysis and catalytic steam reforming," in *Proceedings of the U.S. DOE Hydrogen Program Review*, pp. 707–730, Coral Gables, Fla, USA, 1995.
- [84] D. S. Scott, P. Majerski, J. Piskorz, and D. Radlein, "Second look at fast pyrolysis of biomass—the RTI process," *Journal of Analytical and Applied Pyrolysis*, vol. 51, no. 1, pp. 23–37, 1999.
- [85] G. V. C. Peacocke and A. V. Bridgwater, "Ablative plate pyrolysis of biomass for liquids," *Biomass and Bioenergy*, vol. 7, no. 1–6, pp. 147–154, 1994.
- [86] W. T. Tsai, M. K. Lee, and Y. M. Chang, "Fast pyrolysis of rice straw, sugarcane bagasse and coconut shell in an induction-heating reactor," *Journal of Analytical and Applied Pyrolysis*, vol. 76, no. 1–2, pp. 230–237, 2006.
- [87] W. T. Tsai, M. K. Lee, and Y. M. Chang, "Fast pyrolysis of rice husk: product yields and compositions," *Bioresource Technology*, vol. 98, no. 1, pp. 22–28, 2007.
- [88] E. Schröder, "Experiments on the pyrolysis of large beechwood particles in fixed beds," *Journal of Analytical and Applied Pyrolysis*, vol. 71, no. 2, pp. 669–694, 2004.
- [89] M. J. Lázaro, R. Moliner, I. Suelves, C. Domeo, and C. Nerin, "Co-pyrolysis of a mineral waste oil/coal slurry in a continuous-mode fluidized bed reactor," *Journal of Analytical and Applied Pyrolysis*, vol. 65, no. 2, pp. 239–252, 2002.
- [90] R. Font, A. Marcilla, J. Devesa, and E. Verdú, "Kinetic study of the flash pyrolysis of almond shells in a fluidized bed reactor at high temperatures," *Journal of Analytical and Applied Pyrolysis*, vol. 27, no. 2, pp. 245–273, 1993.
- [91] D. A. Johnson, D. Maclean, J. Feller, J. Diebold, and H. L. Chum, "Developments in the scale-up of the vortex-pyrolysis system," *Biomass and Bioenergy*, vol. 7, no. 1–6, pp. 259–266, 1994.
- [92] T. Damartzis, G. Ioannidis, and A. Zabaniotou, "Simulating the behavior of a wire mesh reactor for olive kernel fast pyrolysis," *Chemical Engineering Journal*, vol. 136, no. 2–3, pp. 320–330, 2008.
- [93] C. Di Blasi, "Heat transfer mechanisms and multi-step kinetics in the ablative pyrolysis of cellulose," *Chemical Engineering Science*, vol. 51, no. 10, pp. 2211–2220, 1996.
- [94] R. Helleur, N. Popovic, M. Ikura, M. Stanculescu, and D. Liu, "Characterization and potential applications of pyrolytic char from ablative pyrolysis of used tires," *Journal of Analytical and Applied Pyrolysis*, vol. 58–59, pp. 813–824, 2001.
- [95] J. Lédé, "Comparison of contact and radiant ablative pyrolysis of biomass," *Journal of Analytical and Applied Pyrolysis*, vol. 70, no. 2, pp. 601–618, 2003.
- [96] H. Martin, J. Lede, H. Z. Li, J. Villermaux, C. Moyne, and A. Degiovanni, "Ablative melting of a solid cylinder perpendicularly pressed against a heated wall," *International Journal of Heat and Mass Transfer*, vol. 29, no. 9, pp. 1407–1415, 1986.
- [97] C. Di Blasi, A. Galgano, and C. Branca, "Influences of the chemical state of alkaline compounds and the nature of alkali metal on wood pyrolysis," *Industrial and Engineering Chemistry Research*, vol. 48, no. 7, pp. 3359–3369, 2009.
- [98] EnerSysNet LLC, personal communication, <http://www.biogreen-energy.com/biogreen.html>.
- [99] B. Masemore and R. Zarrizski, Apparatus for pyrolyzing tire shreds and tire pyrolysis systems. United States Patent 7329329, 2008.
- [100] R. M. Satchwell and R. M. Facey, Thermal remediation process. United States Patent 6840712, 2005.
- [101] A. Boguslavsky and Y. Rabiner, Method and apparatus for treating refuse. United States Patent 6202577, 2001.
- [102] B. P. Faulkner, R. J. Unterweger, and R. W. Hansen, Pyrolysis process for reclaiming desirable materials from vehicle tires. United States Patent 6221329, 2001.
- [103] J. Moriarty, B. Moriarty, and N. Moriarty, Pyrolizer. United States Patent 5993751, 1999.
- [104] W. R. Meador, Method and apparatus for recovering constituents from discarded tires. United States Patent 5720232, 1998.
- [105] D. R. Kanis, Pyrolysis system and a method of pyrolyzing. United States Patent 5636580, 1997.
- [106] D. D. Thomas, Horizontal oil shale and tar sands retort. United States Patent 4347119, 1982.
- [107] P. R. Ryason, Continuous coal processing method. United States Patent 4206713, 1980.
- [108] C. Roy, A. Chaala, and H. Darmstadt, "Vacuum pyrolysis of used tires end-uses for oil and carbon black products," *Journal of Analytical and Applied Pyrolysis*, vol. 51, no. 1, pp. 201–221, 1999.
- [109] A. V. Bridgwater, "Principles and practice of biomass fast pyrolysis processes for liquids," *Journal of Analytical and Applied Pyrolysis*, vol. 51, no. 1, pp. 3–22, 1999.
- [110] M. P. Bernal, J. A. Albuquerque, and R. Moral, "Composting of animal manures and chemical criteria for compost maturity assessment. A review," *Bioresource Technology*, vol. 100, no. 22, pp. 5444–5453, 2009.

- [111] P. Wang, C. M. Changa, M. E. Watson, W. A. Dick, Y. Chen, and H. A. J. Hoitink, "Maturity indices for composted dairy and pig manures," *Soil Biology and Biochemistry*, vol. 36, no. 5, pp. 767–776, 2004.
- [112] P. C. Badger and P. Fransham, "Use of mobile fast pyrolysis plants to densify biomass and reduce biomass handling costs—a preliminary assessment," *Biomass and Bioenergy*, vol. 30, no. 4, pp. 321–325, 2006.
- [113] N. Mahinpey, P. Murugan, T. Mani, and R. Raina, "Analysis of bio-oil, biogas, and biochar from pressurized pyrolysis of wheat straw using a tubular reactor," *Energy and Fuels*, vol. 23, no. 5, pp. 2736–2742, 2009.

Research Article

Use of Iron (II) Salts and Complexes for the Production of Soil Amendments from Organic Solid Wastes

Amerigo Beneduci,^{1,2} Ilaria Costa,^{2,3} and Giuseppe Chidichimo^{1,2}

¹ Department of Chemistry, University of Calabria, Via P. Bucci, Cubo 17/D, 87036 Arcavacata di Rende, Italy

² Consorzio TEBAID, Department of Chemistry, University of Calabria, Via P. Bucci, Cubo 17/B, 87036 Arcavacata di Rende, Italy

³ Biochimica Control S.r.l., 88900 Crotone, Italy

Correspondence should be addressed to Giuseppe Chidichimo, chidichi@unical.it

Received 18 October 2011; Revised 24 January 2012; Accepted 31 January 2012

Academic Editor: Licínio M. Gando-Ferreira

Copyright © 2012 Amerigo Beneduci et al. This is an open access article distributed under the Creative Commons Attribution License, which permits unrestricted use, distribution, and reproduction in any medium, provided the original work is properly cited.

A method to obtain rapidly stabilized composts for crops from solid organic wastes is evaluated. Here we used a laboratory scale reaction chamber where solid waste treatment was performed under strictly controlled temperature and pressure conditions. The raw organic waste was mixed with acid solutions containing iron (II) ions either in the fully hydrated form or in the form of complexes with the diethylenetriaminopentaacetic acid. Data from elemental analysis distribution and GC/MS analysis of the polar and non polar dissolved organic matter, clearly showed that Fe(II) ions significantly enhance organic substrate oxidation of the initial solid waste, compared to a material obtained without the addition of the Fe(II) ions to the raw organic matrix. These results suggest that Fe(II) ions might be involved in a catalytic oxidation pathway that would be activated under the experimental conditions used. The extent of the oxidation process was evaluated by the value of the C/N ratio and, qualitatively, by the molecular composition of the dissolved organic matter. After about 6 hours of incubation, dark-brown and dry organic matrices were obtained with C/N ratio as low as 12 and a high degree of oxidative decomposition into low-molecular-weight compounds at high oxidation state.

1. Introduction

Solid organic waste managing, treatment, and disposal is one of the most important worldwide environmental problems. Among the various options (minimization, recycling, sanitary landfilling, incineration, and composting) composting is one of the most interesting and economically feasible. This is especially true because the produced compost can be used for soil amendment or fertilizer when the organic waste does not contain pollutants such as heavy metals. The composting process is defined as “the biological decomposition of biodegradable solid waste under controlled predominantly aerobic conditions to a state that is sufficiently stable for nuisance-free storage and handling and is satisfactorily matured for safe use in agriculture” [1]. In this process, the raw organic material is progressively broken down by a succession of populations of living organism at different stages of the decomposition process (mesophilic, thermophilic,

and maturation stages) [2]. Micro- and macroflora are key process factors controlling the composting process. Other key factors are temperature, pH, moisture content, and aeration as well as the chemical and physical availability of the nutrients in the organic waste, respectively, determined by the molecules vulnerability to microbes attack and by the particle size.

The most limiting problem affecting the full exploitation of this technology is its intrinsic slowness related to the natural biodegradation process that takes more than 3 months to go through. In addition, another disadvantage is due to the foul odor produced, particularly during the mesophilic stage of the process. Recently, several processes were advanced in order to overcome the above limits. Common feature of some of them is to dry the organic waste after a first sterilization stage made either by a boil-ripening treatment of the organic waste at high pressure (15–25 atm) and temperature (150–250°C) [3] or by addition of

lime so as to increase the pH to values under which aerobic fermentation is inhibited [4]. The drying process stabilizes the organic material but, in the absence of a fermentation stage, most of the organic material cannot be broken down to small molecules and, therefore, the compost cannot be stored for long periods of time under nonsterile conditions. This is partly overcome by a more complicated two-stage process: (1) fermentation and (2) drying [5, 6]. The fermentation stage was shown to be improved by addition of strong oxidizing agents such as metal alkali peroxides and chlorates whose reduced products are retained in the final compost [6].

The aim of the present work is to evaluate the catalytic performances of iron (II)-based catalysts in the composting process of solid organic wastes. Ferrous ions, when mixed with hydrogen peroxide, form a very effective oxidizing agent known as Fenton reagent [7–9]. It has been extensively used as a method for the oxidation of organic pollutants of different molecular origin in industrial wastewater [9–20]. Even though the mechanism of the Fenton reaction has not yet been fully clarified, two main mechanisms have been advanced [8, 21–23]: a radical one, involving the hydroxyl radical as reactive oxygen species, and a nonradical one, involving the formation of an intermediated iron (IV) complex. The hypothesis undergoing the present project is that an iron (II) overload into the organic material may activate Fenton chemistry or Fenton-like chemistry reactions in combination with endogenous hydrogen peroxide always produced in aerobic conditions by microorganisms [21] responsible for the early stages of the biodegradation process.

2. Materials and Methods

2.1. Organic Solid Waste and Treatment. Raw organic material (OM) was derived from restaurant refuses containing pasta, pizza, fruit (pineapple, apple, and melon), potatoes, vegetables, and eggs. OM was minced with a rotating blade mill provided with a 10 mm sieve and introduced into the reaction chamber where temperature and pressure were under control. The chamber was a 25-liter steel cylinder provided with an axial blade stirrer. A pressure gradient of about 0.01 bars was kept between the cylinder extremities in order to allow a constant air circulation. The temperature of the chamber could be regulated by an external strip resistor. The ferrous ion-based catalysts were added to the organic waste and the reaction mixture was continuously stirred. Experiments have been performed on 12 Kg of solid waste having the same initial composition. In some experiments, 1 kg of soil containing inert inorganic material (IM) made of oxides of Ca, Al, Fe, and Si and several other microelements present in traces (~1 ppb) such as Cu^{++} , Zn^{++} , Co^{++} , Mn^{++} , Pb^{++} , and Sr^{++} , was mixed with OM. In order to dry and stabilize the organic mass, the mixture was heated at 55°C under an air constant flow rate of 20 liters/s, ensuring its slow drying. The initial moisture content was about 72%, and, after 6 hours of treatment, a final moisture content of about 15% was obtained. The stability of the composts produced by the above procedure was evaluated by means of their odor and color properties and by their C/N ratio [24].

These properties were monitored for a period of up to six months on composts stored in a dry environment.

In addition, compost stability was qualitatively estimated by the degree of the oxidative decomposition process evaluated by GC/MS analysis of the polar and nonpolar dissolved organic matter (see below).

2.2. Catalyst. Two different solutions of iron (II) catalyst were studied: a 15% (w/w) solution of FeSO_4 acidified at pH 3.8 with sulfuric acid (solution A) and a 6% (w/w) solution of the Fe(II) -diethylenetriaminepentaacetic acid complexes (Fe(II) -DTPA) at pH 5 (solution B) [25].

2.3. Elemental Analysis: Determination of Total Organic Carbon (TOC) by the Official Method UNI EN 13137: 2002. TOC was determined by high temperature combustion of the sample ($T \geq 900^\circ\text{C}$), after a digestion process, in a SHIMADZU instrument model SM 5000 A. This equipment can analyze liquid sample too, but not water solutions.

Determination of S and Cl percentages was performed by the following procedure: the sample was oxidized by combustion into a bomb containing oxygen under pressure, according to the method EPA 5050 1994 (preparation) + EPA 9056A 2007 (analysis). After complete sample digestion, the % Cl and % S were estimated by analyzing water produced using the ion chromatography method. The instrument used was a LECO AC500 Mahler bomb calorimeter. It completely burns the sample in a total oxidative digestion process.

The remaining elements (O, H, N) were determined by combustion with the elemental analyzer THERMO ELECTRON NC Soil Flash EA1112, according to the method UNI EN 15407: 2006. This instrument is a two-furnace system: an oxidative and a reductive one. Analytes (in gaseous state) are determined by passing each one in a thermoconductivity detector (TCD) and by the conductivity difference between a reference carrier gas and the sample gas; it is possible to evaluate the concentration of C, H, and N in terms of their percentage.

2.4. GC/MS Analysis. From a representative amount of OM (~20 g) the polar and nonpolar soluble fractions were extracted, respectively, in methanol and n-hexane. Extraction was performed by an ASE 100 DIONEX automatic extractor at 100°C under nitrogen atmosphere at high pressure. 1 microliter of the dissolved organic matter was injected, without purification, into the GC/MS system for analysis. In order to increase the sensitivity of the analysis and to detect a larger number of degradation products, the dissolved organic matter was concentrated to 1/3 of the original volume and 1 microliter used for GC/MS characterization. All analyses were performed with a GC VARIAN model 3800 coupled with a triple quadrupole mass detector VARIAN model 320-MS TQ. The column used was a VARIAN model “Factor Four” VF-5 ms capillary column; 30 m; 0.25 mm; 0.25 μm .

Mass spectra were collected as raw data by EI mode (electron impact) with collision energy of 70 eV. All peaks were identified by comparison with a NIST certified library

TABLE 1: Elemental percentages (organic mass) of the composts under different biodegradation conditions.

Elemental %	Compost					Commercial compost
	OM	C1	C2	C3	C4	C5
C (TOC)	58.86	50.35	47.29	46.52	39.01	52.0
H	7.10	5.99	6.09	6.35	5.02	5.5
N	4.50	2.60	2.53	2.67	3.20	2.5
O	28.42	38.5	44.55	43.37	52.20	38.8
Cl	0.88	0.89	0.65	0.89	0.87	1.0
S	0.24	1.61	0.25	0.20	0.18	0.2
C/N	31	19	19	17	12	21
OM (Kg)		12	12	12	12	
Fe(II) solution type		/	A	A	B	/
Fe(II) solution (g)		/	250	250	250	
IM (Kg)		1	1	/	/	

* C1–5: compost 1–5.

of mass spectra (acquired at 70 eV) as the most probable component in the mixture.

2.4.1. Acquisition Method for Liquid Mode (Determination of Extractable Components, Polar and Apolar). Mass range: 50–2000 uma; EDR system: active; delay: 4 minutes; source temperature: 250°C; transfer line temperature: 300°C; dwell time: 0,5 sec; injection mode: splitless; injector temp.: 220°C; inj. volume: 1 μ L; carrier flow: 1 mL/min helium; oven program: init.: 40°C; hold 2 min.; 5°C/min 270°C; hold 20 minutes.

2.4.2. Acquisition Method for Head Space Mode (H. S.) (Determination of Volatile and Light Components). Mass range: 50–500 uma; EDR system: active; delay: 0 minutes; source temperature: 250°C; transfer line temperature: 300°C; dwell time: 0,5 sec; Injection mode: splitless; injector temp.: 100°C; inj. volume: 2500 μ L; carrier flow: 1 mL/min helium; oven program: init.: 45°C; hold 2 min.; 5°C/min 250°C; hold 5 minutes.

3. Results

3.1. Elemental Analysis. Table 1 shows the elemental distribution of the row organic mass (OM) and that of the organic mass of the various composts obtained from OM under different biodegradation conditions. They are compared with those of a typical compost used as fertilizer (C5) as well as with those of a compost obtained by drying the row organic waste when mixed with the IM (C1). It can be seen that in all of the composts C1–C4 the percentages of C, H, and N are lower than those found in the initial organic waste (OM). This reduction is mainly due to a significant increase of the percentage of oxygen in all of the composts examined. This increase becomes very large for the compost C4 that exhibited about a 45% increase of the % of oxygen atoms relative to the untreated waste. These data unequivocally suggest that during the organic waste treatment, extensive oxidative biodegradation

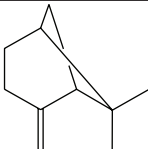
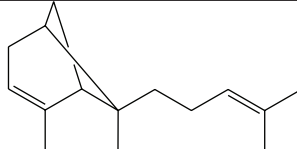
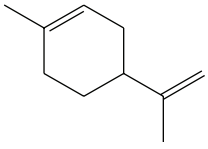
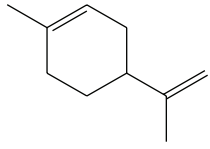
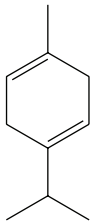
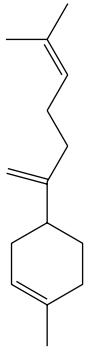
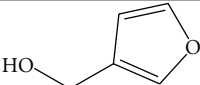
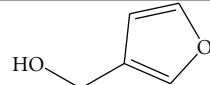
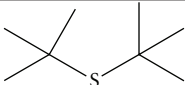
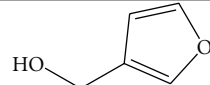
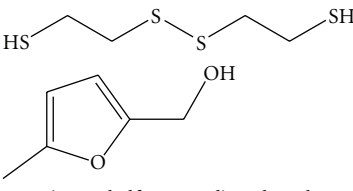
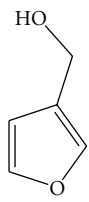
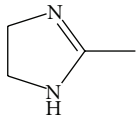
processes occur. Another interesting data is the significant reduction of the C/N ratio that gradually decreases from OM that has the largest value equal to 31 to C4 for which this ratio becomes 12.

Significant differences in the elemental distribution were also observed between the composts obtained with the Fe(II) containing solutions (C2–C4) and without them (C1). In particular, it is worth to note that, when the Fe(II) ions were present, the increase of the percentage of oxygen was higher than in their absence, when the ferrous ions were added to the waste either in the fully hydrated form (solution A) or in a complex with the diethylenetriaminepentaacetic acid (solution B). This suggests that Fe(II) ion plays a major role in the biodegradation process. However, it can be further noted, from Table 1, that the oxidative biodegradation process appears to be more efficient when the ferrous ion complex is used. Indeed, the compost C4 had the highest percentage of oxygen and the lowest C/N ratio.

The composts prepared in the presence of the iron (II) catalyst were dark-brown, dry, granulous (almost 1 mm grains), without smell. Odor and color properties of C4 as well as its C/N ratio and its molecular composition were monitored for up to 6 months. After this period we did not observe significant changes of the above parameters, indicating that this compost was stable. In contrast, C1 was not stable and after few days from the treatment it was covered by molds and gave a foul odor characteristic of volatile mercaptans.

3.2. GC/MS Results. Due to the very interesting elemental distribution differences between C1 and C4, we deeply studied the molecular composition of these two materials by means of the GC/MS analysis. Figures 1 and 2 show the chromatograms of the nonpolar and polar dissolved organic matter, respectively, for C1 (A) and C4 (B). All the peaks in the chromatograms were identified by the corresponding mass fragmentation spectra. Tables 2 to 4 summarize the classes of functional groups found in the above organic matters. Major differences in the chromatograms of the two composts can be seen at low retention times and on the

TABLE 2: Molecular composition of the low-molecular-weight fraction of the extracts from composts C1 and C4. Hydrocarbons, alcohols, thiols, ethers, thioethers, sulfones, and amines.

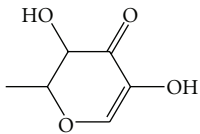
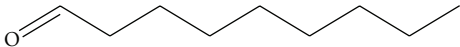
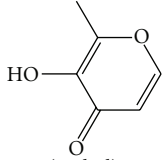
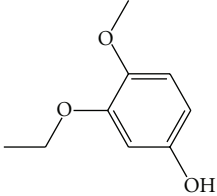
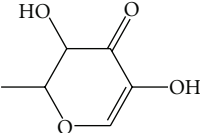
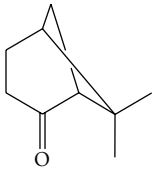
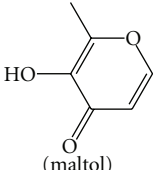
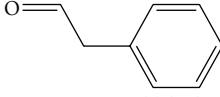
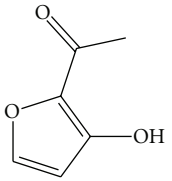
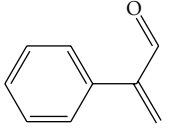
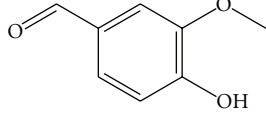
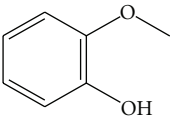
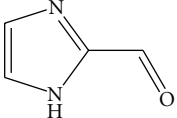
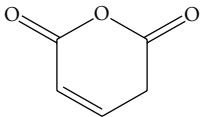
Functional group	C1	C4
Hydrocarbons	 6,6-Dimethyl-2-methylenebicyclo[3.1.1]heptane	 2,6-Dimethyl-6-(4-methylpent-3-enyl)bicyclo[3.1.1]hept-2-ene(caryophyllene)
	 1-Methyl-4-(prop-1-en-2-yl)cyclohex-1-ene(limonene)	 1-Methyl-4-(prop-1-en-2-yl)cyclohex-1-ene(limonene)
	 1-Isopropyl-4-methylcyclohexa-1,4-diene	
	 1-Methyl-4-(6-methylhepta-1,5-dien-2-yl)cyclohex-1-ene	
Alcohols		
Ethers	 3-(Hydroxymethyl)furan	 3-(Hydroxymethyl)furan
Thiols		
Thioethers		
Sulfones	 Di-tert-butylsulfone	 3-(Hydroxymethyl)furan
Amines		
		 (5-Methylfuran-2-yl)methanol
		 Furan-3-ylmethanol
		 2-Methyl-4,5-dihydro-1H-imidazole

extracts as such without concentration pretreatment. This is to be attributed to significant differences in the low-molecular-weight content of the two extracts. Actually, the identification of the light fraction of the extracts by MS revealed that C4 was reached in compounds at high oxidation state such as aldehydes, ketones, and cyclic esters (Tables 2, 3,

and 4). These were detected to a lower extent in the extracts of C1 too, but it was mainly composed by hydrocarbons, alcohols, ethers, and thioethers (Tables 2–4).

The high-molecular-weight fractions of the C1 and C4 extracts were very similar and contained long-chain (C10–C23) fatty acids and their corresponding methyl and ethyl

TABLE 3: Molecular composition of the low-molecular-weight fraction of the extracts from composts C1 and C4. Aldehydes and ketones.

Functional group	C1	C4
Aldehydes Ketones	 3,5-Dihydroxy-2-methyl-2H-pyran-4-one	 Nonanal
	 (maltol) 3-Hydroxy-2-methyl-4H-pyran-4-one	
	 3-Ethoxy-4-methoxyphenol	 3,5-Dihydroxy-2-methyl-2H-pyran-4-one
	 6,6-Dimethylbicyclo[3.1.1]heptan-2-one	 (maltol) 3-Hydroxy-2-methyl-4H-pyran-4-one
		 Benzeneacetaldehyde
		 1-(3-Hydroxyfuran-2-yl)ethanone
		 2-Phenylpropenal
		 4-Hydroxy-3-methoxybenzaldehyde
		 2-Methoxyphenol
		 1H-Imidazole-2-carbaldehyde
		 3H-Pyran-2,6-dione

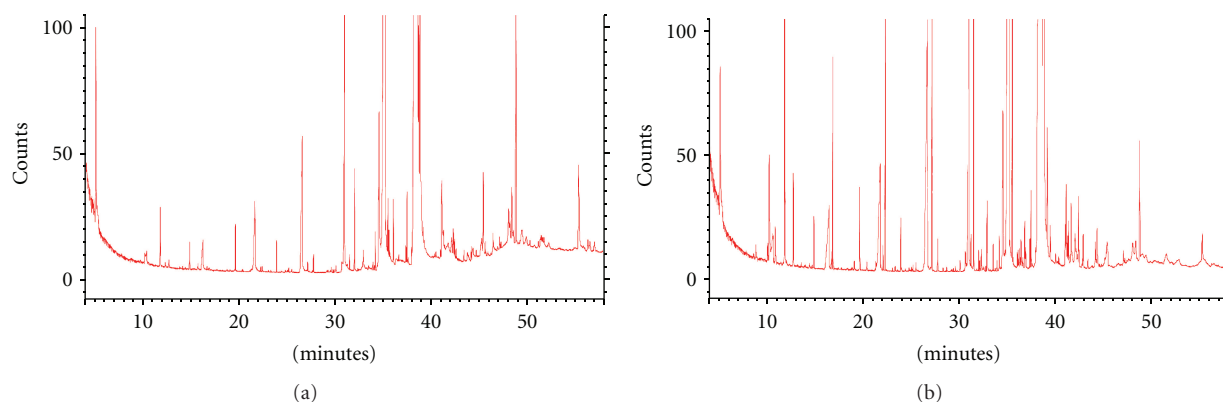


FIGURE 1: GC chromatograms of the non polar dissolved organic matter extracted in n-hexane from composts C1 (a) and C4 (b). Some of the classes of the functional groups are reported here as a function of the retention time (minutes): up to 32' we have terpene, decanoic, dodecanoic, and tetradecanoic acids, and tetradecenal. The remaining peaks were attributed to C16–C18 fatty acids and relative esters. At 50' squalene was found. It can be seen that the region at low retention times in chromatogram (b) is more crowded than in (a).

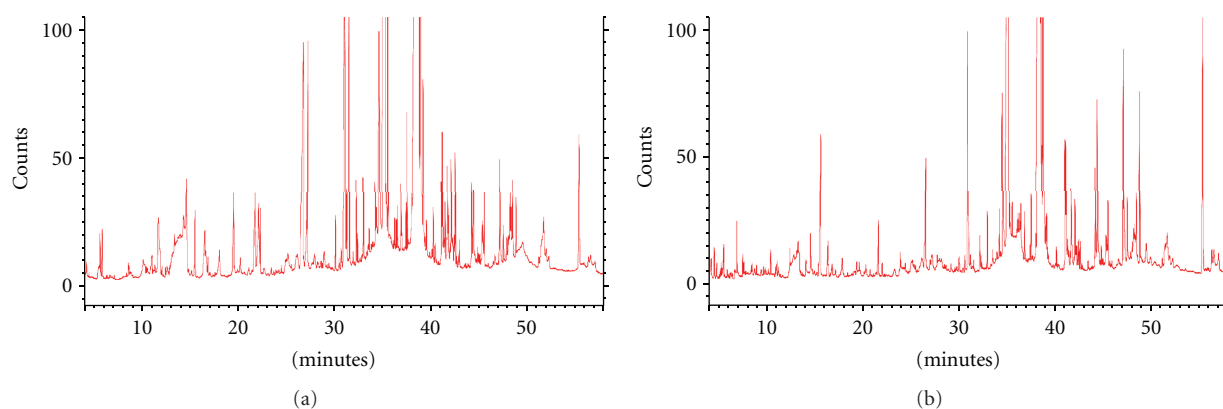


FIGURE 2: GC chromatograms of the extracts in methanol of the composts C1 (a) and C4 (b). Some of the classes of the functional groups are reported here as a function of the retention time (minutes): up to 20' we have low-molecular-weight ketones, aldehydes, and polyalcohols and at 20'–40' fatty acid and fatty acid esters. It can be seen that the region at low retention times in chromatogram (b) is more crowded than in (a).

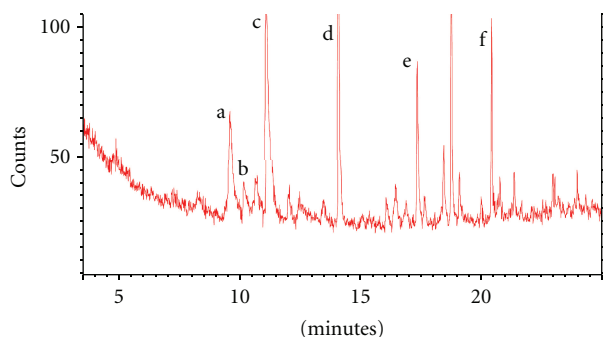


FIGURE 3: Headspace GC analysis of the volatile fraction obtained from compost C1. a: light terpene; b: butyrate; c: limonene; d: propanethiol; e: 2-decenale; f: 2-undecenale.

esters as well as cholesterol (3 beta-cholest-5-en-3-ol) and high-molecular-weight terpenes like squalene.

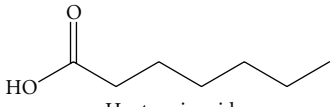
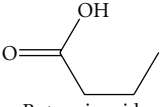
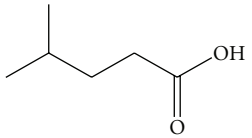
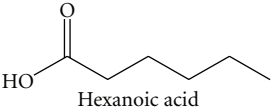
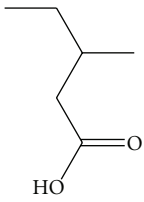
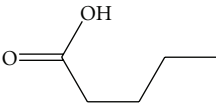
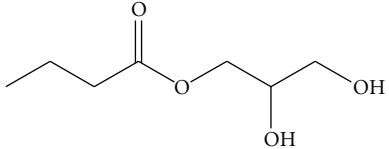
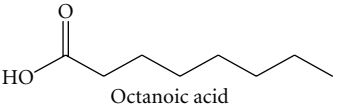
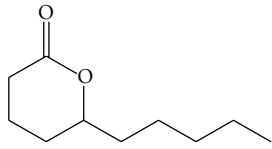
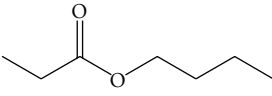
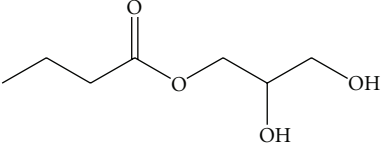
These data strongly support the quantitative results on the elemental distribution of the various composts (Table 1). Indeed, the high relative amount of oxygen-rich low-molecular-weight compounds at high oxidation state determined in C4 is in very good agreement with the high percentage of elemental oxygen found in this compost.

The analysis by headspace chromatography coupled to MS essentially confirmed the data reported in Table 2 for the compost C4 but revealed the presence of cyclic hydrocarbons, butyrate, and low-molecular-weight thiols responsible for the rancid smell of C1 (Figure 3).

4. Discussion

The data presented here clearly shows that if the organic waste is treated in a reactor under the temperature and pressure conditions here described (see “Section 2”), the addition of Fe(II) ions improves the oxidative degradation processes of the waste and leads, in a few hours, to organic matrices characterized by low-molecular-weight compounds

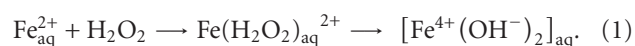
TABLE 4: Molecular composition of the low-molecular-weight fraction of the extracts from composts C1 and C4. Carboxylic acids, esters, and amides.

Functional group	C1	C4
Carboxylic acids Esters Amides	 Heptanoic acid	 Butanoic acid
	 4-Methylpentanoic acid	 Hexanoic acid
	 3-Methylpentanoic acid	 Pentanoic acid
	 2,3-Dihydroxypropyl butyrate	 Octanoic acid
		 6-Pentyl-tetrahydropyran-2-one
		 Butyl propionate
		 2,3-Dihydroxypropyl butyrate

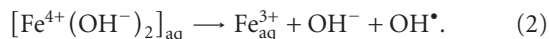
at high oxidation state, like acids and esters. In addition, composts obtained by this method exhibited low C/N ratios and were stable at least from the point of view of their odor and color properties and their molecular composition. Even if further studies are required to evaluate the usefulness of the obtained composts in agriculture practice, nonetheless, the treatment of organic solid waste here proposed seems to be very promising for many potential applications (soil amendment, fuels, etc.).

The results discussed above suggest that ferrous ion plays a significant role in the oxidative process of the raw organic material. It is therefore necessary to hypothesize that this ion

is involved in a reaction mechanism that may significantly contribute to enhance the oxidation process. One of the most probable mechanisms is a catalytic process known as Fenton reaction in which the highly reactive oxygen species hydroxyl radical HO^\bullet and/or ferryl ion $[\text{Fe}^{4+}(\text{OH}^-)_2]_{\text{aq}}$ are produced [9, 21–23]. Under the assumption that the Fenton reaction proceeds via an inner-sphere two-electron-transfer mechanism [22], the following simplified reaction scheme may be suggested for organic substrates oxidation by Fenton reaction:

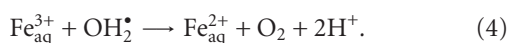
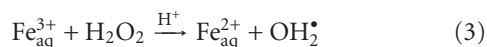


The intermediate iron (IV) complex may oxidize the organic substrates. Alternatively, it could react further, leading to the formation of a free hydroxyl radical and $\text{Fe}_{\text{aq}}^{3+}$:



The hydroxyl radical that takes place in step (2) could react with the organic substrate leading to its oxidation.

The Fe(III) formed in the oxidation steps is reduced, under acidic conditions, leading again to ferrous ion that can reenter in the oxidative Fenton cycle [22]:



Even though reaction (3) is slow, reaction (4) is irreversible and the sequence is therefore shifted to the right favoring the reduction of $\text{Fe}_{\text{aq}}^{3+}$ to $\text{Fe}_{\text{aq}}^{2+}$ and the oxidation of H_2O_2 to O_2 .

The hypothesis that Fenton chemistry is involved in the biodegradation of the organic waste appears to be reasonable if we take into account that the presence of a variety of aerobic microorganisms populates the organic material that might be the endogenous source of hydrogen peroxide through the mechanism of molecular oxygen reduction. In this process, which is ubiquitous in aerobic systems, the molecular oxygen can undergo an initial one-electron reduction by an electron donor to form the superoxide anion O_2^- that is subsequently converted to H_2O_2 .

5. Conclusions

Here we have treated solid organic wastes into a 25 L reaction chamber under strictly controlled temperature and pressure conditions and we have evaluated the effects of iron (II) ion on the oxidative decomposition process of the solid waste. We have found that Fe(II) ion enhances such a process especially when it is introduced into the raw organic matter in form of complexes of the ethylenetriaminepentaacetic acid. This observation is very interesting and deserves further studies. After 6 hours of waste treatment, we observed a high degree of oxidative decomposition revealed by GC/MS analysis of the polar and non polar dissolved organic matter that led to composts with C/N ratios as low as 12, compared to an initial value of 31. In addition, the composts obtained exhibited dark-brown color they did not emanate smell and have humidity of the order of 15%. The product obtained in the present work cannot be considered as a conventional compost. At the actual stage of investigation, we only claim to have transformed the original organic waste material into a stabilized organic matrix. We mean in this case that the material does not go, at least within 6 months, in further biochemical transformation when stored under dry conditions. The property of the material as a soil fertilizer needs to be inquired by determining the further biochemical and chemical transformations it will undergo when added to soil. In particular, its influence on the vegetable growth needs to be determined. Studies are in progress in these directions.

References

- [1] UNEP, "Composting," in *Solid Waste Management*, United Nation Environmental Program, Ed., vol. 1, part 2, chapter 8, pp. 198–235, 2005.
- [2] M. de Bertoldi, G. Vallini, and A. Pera, "The biology of composting: a review," *Waste Management and Research*, vol. 1, no. 2, pp. 157–176, 1983.
- [3] M. Kosaku, "Method of manufacturing full-ripe fertilizer using organic waste," *JP2003055078 (A)*, 2003.
- [4] Z. Xianjin, X. Weijian, and S. Jinghu, "Production of a natural catalyst by drying of natural organic waste," CN2003-01-08.
- [5] L. M. Hyoung, "Method for producing organic fertilizer using organic wastes and inorganic materials and devices used therefor," *KR20010091641 (A)*, 2001.
- [6] T. Hitoshi, "Chemical-physical process for fertilizer production from organic waste and production plant," JP5295376, 1993.
- [7] H. J. H. Fenton, "Oxidation of tartaric acid in presence of iron," *Journal of the Chemical Society, Transactions*, vol. 65, pp. 899–910, 1894.
- [8] H. B. Dunford, "Oxidations of iron(II)/(III) by hydrogen peroxide: from aquo to enzyme," *Coordination Chemistry Reviews*, vol. 233–234, pp. 311–318, 2002.
- [9] K. Barbusiński, "Fenton reaction. Controversy concerning the chemistry," *Ecological Chemistry and Engineering S*, vol. 16, no. 3, pp. 347–358, 2009.
- [10] C. P. Huang, C. Dong, and Z. Tang, "Advanced chemical oxidation: its present role and potential future in hazardous waste treatment," *Waste Management*, vol. 13, no. 5–7, pp. 361–377, 1993.
- [11] E. Neyens and J. Baeyens, "A review of classic Fenton's peroxidation as an advanced oxidation technique," *Journal of Hazardous Materials*, vol. 98, no. 1–3, pp. 33–50, 2003.
- [12] I. Casero, D. Sicilia, S. Rubio, and D. Pérez-Bendito, "Chemical degradation of aromatic amines by Fenton's reagent," *Water Research*, vol. 31, no. 8, pp. 1985–1995, 1997.
- [13] W. G. Kuo, "Decolorizing dye wastewater with Fenton's reagent," *Water Research*, vol. 26, no. 7, pp. 881–886, 1992.
- [14] S. Nam, V. Renganathan, and P. G. Tratnyek, "Substituent effects on azo dye oxidation by the Fe^{III} -EDTA- H_2O_2 system," *Chemosphere*, vol. 45, no. 1, pp. 59–65, 2001.
- [15] K. Barbusiński, "The modified Fenton process for decolorization of dye wastewater," *Polish Journal of Environmental Studies*, vol. 14, no. 3, pp. 281–285, 2005.
- [16] P. L. Huston and J. J. Pignatello, "Degradation of selected pesticide active ingredients and commercial formulations in water by the photo-assisted Fenton reaction," *Water Research*, vol. 33, no. 5, pp. 1238–1246, 1999.
- [17] K. Barbusiński and K. Filipek, "Use of Fenton's reagent for removal of pesticides from industrial wastewater," *Polish Journal of Environmental Studies*, vol. 10, no. 4, pp. 207–212, 2001.
- [18] K. Ikehata and M. G. El-Din, "Aqueous pesticide degradation by hydrogen peroxide/ultraviolet irradiation and Fenton-type advanced oxidation processes: a review," *Journal of Environmental Engineering and Science*, vol. 5, no. 2, pp. 81–135, 2006.
- [19] S. H. Lin, C. M. Lin, and H. G. Leu, "Operating characteristics and kinetic studies of surfactant wastewater treatment by Fenton oxidation," *Water Research*, vol. 33, no. 7, pp. 1735–1741, 1999.
- [20] M. Kitis, C. D. Adams, and G. T. Daigger, "The effects of Fenton's reagent pretreatment on the biodegradability of

- nonionic surfactants,” *Water Research*, vol. 33, no. 11, pp. 2561–2568, 1999.
- [21] J. Prousek, “Fenton chemistry in biology and medicine,” *Pure and Applied Chemistry*, vol. 79, no. 12, pp. 2325–2338, 2007.
- [22] S. H. Bossmann, E. Oliveros, S. Göb et al., “New evidence against hydroxyl radicals as reactive intermediates in the thermal and photochemically enhanced fenton reactions,” *Journal of Physical Chemistry A*, vol. 102, no. 28, pp. 5542–5550, 1998.
- [23] M. D. Paciolla, G. Davies, and S. A. Jansen, “Generation of hydroxyl radicals from metal-loaded humic acids,” *Environmental Science and Technology*, vol. 33, no. 11, pp. 1814–1818, 1999.
- [24] M. P. Bernal, C. Paredes, M. A. Sanchez-Monedero, and J. Cegarra, “Maturity and stability parameters of composts prepared with a wide range of organic wastes,” *Bioresource Technology*, vol. 63, no. 1, pp. 91–99, 1998.
- [25] J. Vandegaer, S. Chaberek, and A. E. Frost, “Iron chelates of diethylenetriaminepentaacetic acid,” *Journal of Inorganic and Nuclear Chemistry*, vol. 11, no. 3, pp. 210–221, 1959.

Research Article

Degradation of Abamectin Using the Photo-Fenton Process

Thiago Augusto de Freitas Matos, Alexandra Lemos Nunes Dias, Amanda Di Piazza Reis, Milady Renata Apolinário da Silva, and Márcia Matiko Kondo

ICE-DFQ, Universidade Federal de Itajubá, Avenida BPS 1303, 37500-903 Itajubá, MG, Brazil

Correspondence should be addressed to Márcia Matiko Kondo, marciamkondo@gmail.com

Received 15 October 2011; Revised 11 January 2012; Accepted 16 January 2012

Academic Editor: Licínio M. Gando-Ferreira

Copyright © 2012 Thiago Augusto de Freitas Matos et al. This is an open access article distributed under the Creative Commons Attribution License, which permits unrestricted use, distribution, and reproduction in any medium, provided the original work is properly cited.

The cultivation of strawberries generally requires substantial use of pesticides, and abamectin is the active principle of one of those most commonly employed. Conventional water treatment does not remove pesticides efficiently, so there is a need to investigate alternative procedures. The use of advanced oxidation processes (AOPs) can achieve good results in removal of toxic organic compounds present in aqueous solutions. The photo-Fenton process, one example of an AOP, was employed to study the degradation of abamectin. Results showed that when natural water samples contaminated with abamectin were treated using the photo-Fenton process, 70% of the initial amount of the compound was removed within 60 minutes of UV irradiation, and 60% mineralization was observed after 180 minutes of reaction.

1. Introduction

Biocides are one of the most important classes of compounds introduced into surface waters by human activities [1]. They are widely used in agriculture and can contaminate rivers and other water bodies due to transport from cultivated areas [2–5]. Although the pesticide industry has developed new compounds that are more effective, even at lower concentrations, and that present lower environmental impacts [6], the misuse of such pesticides can pose considerable toxicity risks to operators, consumers, and the wider environment [7].

The cultivation of strawberries uses large amounts of pesticides. One of the most commonly employed is Vertimec 18 EC, which contains 1.8% (w/v) of abamectin, the active principle. Abamectin belongs to the avermectin group and has the molecular formula $C_{48}H_{72}O_{14}$ (avermectin B1a) + $C_{47}H_{70}O_{14}$ (avermectin B1b). It is used primarily as a biocide. Abamectin is a toxic chemical and can be fatal if inhaled, ingested, or absorbed by the skin. It causes skin and eye irritation, and at high doses can cause damage to the central nervous system (CAS no., 71751-41-2). The substance is also highly toxic to fish and aquatic invertebrates. The maximum

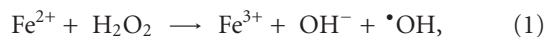
acceptable daily intake (ADI) is 0.01 mg kg^{-1} body weight, and the maximum residue limit is 0.02 mg kg^{-1} of the commercial product [8].

Effluents containing biocides cannot usually be treated efficiently using biological techniques, since the effluents are toxic to the microorganisms involved so that the biodegradation efficiency is reduced [9].

An alternative treatment that has been investigated is based on the use of advanced oxidation processes (AOPs), which are very efficient for the removal of potentially toxic organic compounds from water systems. In AOPs, hydroxyl radicals ($\cdot\text{OH}$) are formed as highly reactive intermediates, and can mineralize organic compounds to H_2O , CO_2 , and mineral acids [10–13].

The photo-Fenton process, an AOP, has attracted considerable interest due to its high efficiency in producing hydroxyl radicals during H_2O_2 decomposition catalysed by Fe^{2+} in acid solution under UV irradiation (1) and (2) [14]. Advantages of this process include the ability to use relatively low-cost reagents, and solar irradiation as the UV source. At the end of the process, the iron ions present can

be precipitated by increasing the pH, while the H_2O_2 is consumed during the reaction [15]:



The $\cdot\text{OH}$ generated can degrade organic pollutants present in aqueous solutions. Parameters such as pH and reagent concentration ratios must be controlled, in order to enhance the efficiency of the degradation process. The optimum pH range for the Fenton and photo-Fenton processes is 2.5–3.0 [16, 17]. The use of an excess amount of H_2O_2 can reduce the efficiency, since hydrogen peroxide can scavenge $\cdot\text{OH}$, generating $\cdot\text{HO}_2$ which has a lower reducing potential than the hydroxyl radical [18, 19].

Fenton and photo-Fenton processes have been successfully employed to treat a variety of effluents containing compounds such as dyes [20], antibiotics [21, 22], landfill leachates [23], and emerging contaminants [24].

The Federal University of Itajubá (Universidade Federal de Itajubá) is located in one of the major strawberry cultivation areas of Brazil. The objective of the present paper was to investigate the degradation efficiency of abamectin using the photo-Fenton process with UV irradiation.

2. Experimental

2.1. Pesticide Solutions. Abamectin solutions were prepared from the commercially available pesticide, in distilled water at a concentration of 9 mg L^{-1} (400 mg L^{-1} TOC). This concentration is the same as that used by farmers during strawberry cultivation.

2.2. Photo-Fenton Process. Iron nitrate (0.5 mmol L^{-1}) was added to the abamectin solution, and the pH was adjusted to 2.5 using $1.0 \text{ mol L}^{-1} \text{ H}_2\text{SO}_4$. The photoreactor consisted of an UV lamp (Hg, 125 W, $\lambda_{\text{max}} = 365 \text{ nm}$), inserted into a double jacket whereby the system could be cooled by water recirculation, and was immersed in the reaction solution. 6.0 mmol L^{-1} of H_2O_2 was added to the abamectin solution, and the lamp was turned on to start the reaction (17 mW cm^{-2} , as measured by a Cole-Parmer radiometer, series 9811). Samples were withdrawn at predetermined intervals, over periods of 60 or 180 minutes. To halt the Fenton reaction, the pH was raised to pH 10 using $6.0 \text{ mol L}^{-1} \text{ NaOH}$, in order to precipitate iron hydroxide. The supernatant was separated by centrifugation and used for the different chemical analyses. The choice of pH value and the H_2O_2 and Fe^{3+} concentrations was based on previous work that used the Fenton reaction to treat another herbicide [25–27].

Natural water samples from the José Pereira stream ($22^\circ 24' 50'' \text{ S}$ and $45^\circ 24' 02'' \text{ W}$, in WGS 84 datum) were also spiked with the same concentration of abamectin and irradiated under the conditions already described. The objective of these tests was to study the efficiency of the Fenton reaction under conditions more representative of those arising from agricultural contamination.

Experiments were also performed without irradiation (Fenton process), using the $\text{H}_2\text{O}_2/\text{UV}$ advanced oxidative process. Control experiments using UV alone (direct photolysis), H_2O_2 alone, and iron alone with UV were conducted in order to evaluate the influence of each parameter on the degradation process.

2.3. Abamectin Quantification. Abamectin was quantified by GC/FID using a Varian Model CP 3380 instrument equipped with an AB-5 column ($25 \text{ m} \times 0.25 \text{ mm} \times 0.25 \mu\text{m}$). Aliquots ($1 \mu\text{L}$) of the eluted samples were injected into the GC. The operating conditions of the oven were an initial temperature of 50°C for 1 minute, a ramp to 200°C at $15^\circ \text{C min}^{-1}$, and a final hold at 200°C for 1 minute. The injector temperature was 240°C , and the FID detector temperature was 300°C . All samples were injected 4 times, and the results were calculated as averages. All experiments were performed in triplicate.

Analytical grade abamectin (Sigma-Aldrich) was used to generate the calibration curve. The detection limit (DL) and quantification limit (QL) were calculated using the ratio of the standard deviation (s) and the slope (S) of the calibration curve (3) and (4) [28]:

$$\text{DL} = 3.3 \times (s/S), \quad (3)$$

$$\text{QL} = 10 \times (s/S) \quad (4)$$

Since the abamectin solution used for the degradation experiments was prepared from a commercially available pesticide that contained other compounds, it was necessary to separate the abamectin from the aqueous solutions prior to the chromatographic analyses. This was achieved by solid phase extraction using Waters Sep-Pak C_{18} cartridges [29]. After the degradation process, the samples were centrifuged in order to separate out the iron precipitate. The supernatant (50 mL) was passed through the Sep-Pak cartridge at a flow rate of 1.66 mL min^{-1} , using a glass syringe. The abamectin retained in the cartridge was then eluted with an aqueous solution containing 85% methanol. This extract was used for abamectin quantification using GC.

2.4. Statistical Analysis. The statistical analysis employed R software and its complement Tinn-R [30] and considered the data to be randomly distributed. The residuals of the data were determined, together with the homogeneity of the variances. The multiple comparison analysis used the Tukey test (at a 5% significance level).

2.5. Hydrogen Peroxide Determination. The hydrogen peroxide concentration was monitored spectrophotometrically using the metavanadate method [31].

2.6. Total Organic Carbon (TOC). The mineralization of organic material in the solution during the photodegradation was monitored by quantifying total organic carbon (TOC) using a carbon analyser (TOC 5000A, Shimadzu). These analyses were performed in the laboratory of the LAPOA

group, at the Institute of Chemistry, UNESP (Araraquara, São Paulo, Brazil).

3. Results and Discussion

Determination of abamectin is usually performed by liquid chromatography [32–35]. At present there are no reports in the literature concerning analysis of the compound by gas chromatography, so that a new method therefore needed to be developed. Injection of a methanolic solution of abamectin showed that it eluted at a retention time of 5.7 minutes. Validation of an analytical method involving a separation technique (such as GC) requires determination of parameters including the linearity of the analytical curve, the DL, and the QL [28]. The calibration curve obtained here showed good linearity, with a high correlation coefficient (0.9988). The calculated detection and quantification limits were 0.0168 mg L^{-1} and 0.0511 mg L^{-1} , respectively, which are low compared to the initial pesticide concentration. Repeatable quantification of abamectin was achieved after separation using Sep-Pak cartridges, showing that the method was also selective. These results demonstrated that the technique used to quantify abamectin met the requirements of the present paper, which were to identify abamectin and monitor its concentration with precision during the photo-Fenton treatment process.

3.1. Control Experiments. In order to understand the influence of the different experimental variables on the degradation of abamectin, experiments were performed using each variable individually. Combinations of variables (such as iron and UV) were also employed. Figure 1 shows the comparative results obtained for these tests.

Abamectin was destroyed by direct photolysis, with 39% removal after 1 hour of irradiation (Figure 1). This result indicates that the pesticide could be photodegraded if present in surface water within the photic zone. Mushtaq et al. [36] showed that avermectin, the chemical group to which abamectin belongs, was also degraded by direct photolysis in natural water after 22 days of solar irradiation. Nevertheless, direct photolysis will not occur in the natural environment when the compound is absorbed in the sediment, or when it is present below the photic zone.

Kamel et al. [37] studied the degradation of abamectin in Saudi Arabian soil. Removal rates of 66% and 88% were observed after 7 and 14 days of solar irradiation, respectively. However, the residual concentration remained higher than that permitted by legislation.

When iron was used alone, together with UV, there was 45% abamectin removal after 60 minutes of irradiation. This probably indicates that photoactive complexes formed between iron and other compounds present in the original pesticide sample, and/or their intermediates, were generated during the degradation process [25, 38]. Similar behaviour was observed by Park et al. [39] using the dye Acid Orange 7, by Silva et al. [25] during photo-Fenton degradation of the herbicide tebuthiuron using solar irradiation, and by Sun

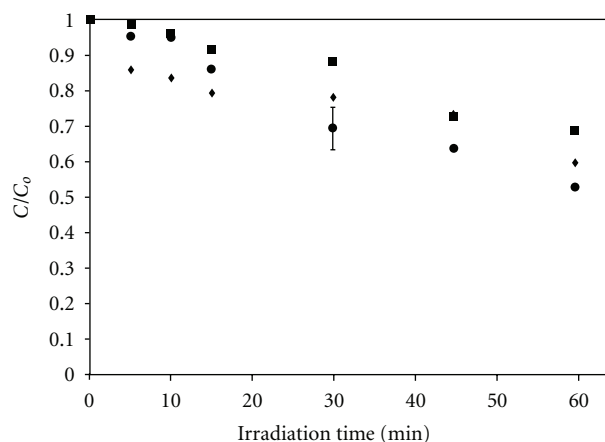


FIGURE 1: Comparison of the efficiency of degradation of abamectin using different treatments: —◆— direct photolysis; —■— H_2O_2 ; —●— $\text{Fe} + \text{UV}$. Initial conditions: $[\text{H}_2\text{O}_2] = 6.0 \text{ mmol L}^{-1}$; $[\text{Fe}^{3+}] = 0.5 \text{ mmol L}^{-1}$; abamectin = 9.0 mg L^{-1} , $\lambda = 365 \text{ nm}$; $\text{pH} = 2.5$.

and Pignatello [40], who attributed the second stage of 2,4-D degradation to iron complex photolysis in the presence of pesticide degradation intermediates. The relatively high degradation efficiency obtained here is interesting since there was no use of H_2O_2 , which could reduce the costs of treatment.

For more than 30 years, the use of H_2O_2 , a strong oxidant, has been commonplace in treatments involving oxidation of organic and inorganic pollutants [41, 42]. In the present paper, use of H_2O_2 alone (in the absence of irradiation) resulted in 30% removal of abamectin after 60 minutes (Figure 1).

3.2. Degradation Studies. Considering that in the control experiments abamectin removal was in the region of only 30% to 45%, the efficiency of degradation of the compound was also investigated using three different AOPs. Figure 2 shows the results of abamectin degradation using Fenton and photo-Fenton reactions, and the $\text{H}_2\text{O}_2/\text{UV}$ system.

In the experiments using the Fenton reaction, there was 40% abamectin removal after 1 hour of irradiation. Similar degradation efficiency was observed after the same time interval using $\text{H}_2\text{O}_2/\text{UV}$. Due to the radiation source used, which had a wavelength limit of $\lambda_{\text{max}} = 365 \text{ nm}$, the UV radiation was not able to cause H_2O_2 decomposition, which requires a wavelength near 254 nm [43]. In the present study, the UV radiation probably only acted to remove abamectin by direct photolysis.

Use of the photo-Fenton system improved abamectin degradation, with up to 55% removal after 30 minutes of reaction, and 80% removal after 60 minutes of irradiation. Similar results were obtained by Pignatello [16], who showed that the photo-Fenton process was more efficient than the Fenton process for degradation of 2,4-dichlorophenoxyacetic acid, since photo-reduction of Fe^{3+} ions to Fe^{2+} increased the catalytic effect. The Fe^{2+} ions can react again with H_2O_2 , and continue the Fenton reaction. The results obtained in

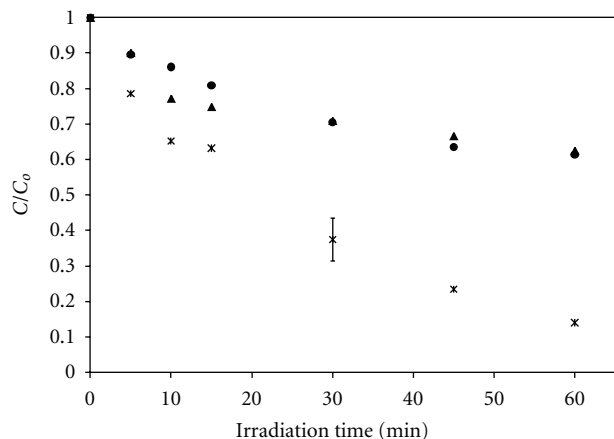


FIGURE 2: Comparison of degradation efficiency of abamectin using different AOPs: —▲— H₂O₂/UV; —●— Fenton reaction; —×— photo-Fenton reaction. Initial conditions: [H₂O₂] = 6.0 mmol L⁻¹; [Fe³⁺] = 5.0 mmol L⁻¹; abamectin = 9.0 mg L⁻¹; λ = 365 nm; pH = 2.5.

the present paper indicate that the photo-Fenton process is effective for the treatment of water and effluents contaminated with abamectin, with a high removal rate within a short irradiation period of up to 60 minutes.

The hydrogen peroxide concentration is an important parameter influencing Fenton and photo-Fenton processes. At high concentrations it can be detrimental to the degradation of organic compounds in water, since excess H₂O₂ can act as radical scavenger [44]. On the other hand, a lack of H₂O₂ interrupts the Fenton reaction, because its absence can halt hydroxyl radical production and, consequently, destruction of organic compounds. Therefore, monitoring the H₂O₂ concentration can help in adjustment of its initial concentration, and identify any need for further addition during the Fenton process.

Monitoring H₂O₂ levels showed that after 60 minutes there was a residual concentration of at least 10% of the initial concentration, and that there was therefore no need to add more H₂O₂ during the period of irradiation.

Figure 3 shows the outcome of the multiple comparison tests (Tukey's test at 5% level of significance) applied to the results of the degradation experiments. The photo-Fenton reaction (a) presented higher abamectin degradation efficiency than the other treatments. The Fe/UV treatment (b) showed better degradation efficiency compared to the H₂O₂ and H₂O₂/UV treatments (c). The results using UV alone and the Fenton process were statistically similar to the results obtained for Fe/UV, H₂O₂ alone, and H₂O₂/UV. These results indicated that each individual process could degrade abamectin to some extent; however, the best results were obtained using the photo-Fenton process.

3.3. Photo-Fenton Degradation of Abamectin in Natural Aquatic Samples. Abamectin removal by the photo-Fenton process reached 80% using solutions prepared in distilled water. In order to investigate removal of the pesticide under more natural conditions, the influences of the different

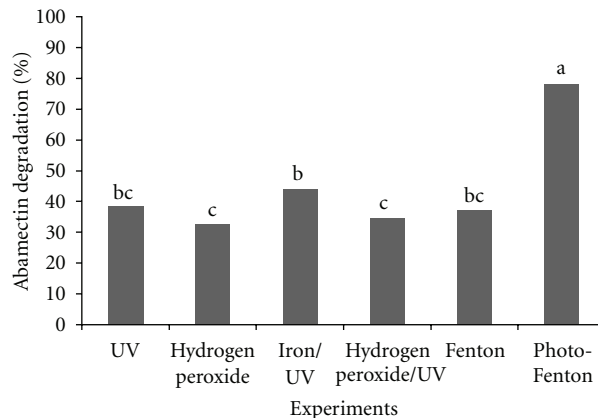


FIGURE 3: Multiple comparison tests for the different processes applied to abamectin removal. The same letters above the means for the different procedures indicates that statistically there were no differences between the procedures, using Tukey's test at a 5% level of significance. Conditions: [H₂O₂] = 6.0 mmol L⁻¹; [Fe³⁺] = 0.5 mmol L⁻¹; abamectin = 9.0 mg L⁻¹; λ = 365 nm; initial pH = 2.5.

physical and chemical parameters were investigated using water samples collected from the José Pereira stream, which were spiked with abamectin. Samples were collected on rainy and dry days. The water collected on a dry day showed values of 120 mg L⁻¹ of total solids and 2 mg L⁻¹ of BOD, while the sample collected during precipitation showed values of 307 mg L⁻¹ of total solids and 4 mg L⁻¹ of BOD. A comparison of abamectin degradation using either distilled water or the natural water samples is shown in Figure 4. It has been reported that organic compound degradation decreases in the presence of natural organic matter and solids, due to reduced penetration of UV radiation. The organic material can compete with the target compound for hydroxyl radicals and/or form complexes with iron, which reduces the efficiency of Fenton degradation [45]. However, even given the possible interferences, abamectin degradation under these conditions reached 70% after 60 minutes of reaction. No difference was observed between degradation of the pesticide in natural water samples collected on rainy or dry days.

3.4. TOC Analysis. Although the results showed that abamectin could be degraded, there was no significant difference in the TOC values after 60 minutes of irradiation. This suggests that abamectin was not mineralised, but that intermediates were generated during the reaction. In a similar study, Fallmann et al. [46] used the photo-Fenton process to treat an aqueous solution containing 100 ppm (TOC) of Vertimec, and observed 20% mineralization after 50 minutes of irradiation, achieving 90% after 150 minutes. However, the authors used a smaller quantity of initial TOC compared to the amount used in the present work (400 ppm). In another study, Bauer et al. [43] used the photo-Fenton reaction to treat a liquid effluent containing a mixture of 10 different pesticides, including Vertimec. The authors used an initial TOC concentration of 10 ppm of each

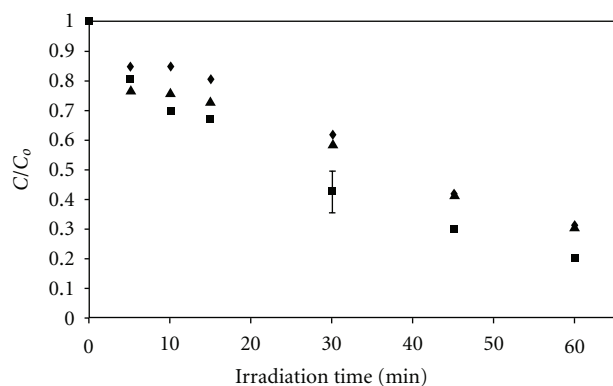


FIGURE 4: Comparison of abamectin degradation using the photo-Fenton process for: —▲— natural water; —◆— natural water (rainy day); —■— distilled water. Conditions: $[H_2O_2] = 6.0 \text{ mmol L}^{-1}$; $[Fe^{3+}] = 0.5 \text{ mmol L}^{-1}$; abamectin = 9.0 mg L^{-1} ; $\lambda = 365 \text{ nm}$; initial pH = 2.5.

pesticide in distilled water, which was treated in a solar UV reactor (300–400 nm). For the photo-Fenton process they used a concentration of $10^{-3} \text{ mmol L}^{-1} \text{ FeSO}_4 \cdot 7H_2O$ and 33 wt % of H_2O_2 , which was added in five portions. TOC removal was in excess of 80% after 3 hours of irradiation using the solar photo-Fenton process. The results of these two earlier studies suggest that in the present work, where the Vertimec solution contained an initial 400 ppm of TOC, the irradiation time and the amount of H_2O_2 were probably not sufficient to achieve pesticide mineralization.

Additional experiments were therefore performed in order to try to improve removal of TOC. In an attempt to reproduce the results obtained by Fallmann et al. [46], the initial concentration of TOC was decreased from 400 ppm to 100 ppm of Vertimec, the H_2O_2 concentration was raised to 20 mmol L^{-1} , with an iron concentration of 0.5 mmol L^{-1} . The exposure time was increased to 180 minutes, in line with that employed by Fallmann et al. [46]. The results of these studies, with a ratio Fe/H_2O_2 of 0.0833, showed that 60% of TOC was removed after 180 minutes. This result is very similar to those reported by Bauer et al. [43] and Fallmann et al. [46].

The possibility of reducing treatment costs was studied by decreasing the Fe/H_2O_2 ratio used for mineralization of 400 ppm (TOC) of Vertimec. Using iron and H_2O_2 concentrations of 1.0 mmol L^{-1} and 80 mmol L^{-1} , respectively (Fe/H_2O_2 ratio of 0.0125), there was 60% TOC removal after 180 minutes of irradiation. A further experiment was performed employing 0.5 mmol L^{-1} of iron and 80 mmol L^{-1} of H_2O_2 (Fe/H_2O_2 ratio of 0.00625); however, there was no observable removal of TOC. These results showed that there was a limiting amount of reagents required to achieve TOC removal. Abamectin could be degraded using Fe/H_2O_2 ratios smaller than 0.0125; however, there was no change in the TOC value, indicating that both the original organic compound and TOC should be monitored in order to ensure detoxification of the solution.

Studies of the toxicity and biodegradability of the possible reaction intermediates will be essential in order to

establish the optimum concentrations of the photo-Fenton reagents. Future investigations should provide information that addresses the need to effectively mineralize the pesticide, or at least degrade it to a nontoxic intermediate. Additional work is also needed to investigate the possibility of combining a biological process with the photo-Fenton treatment described in the present work.

4. Conclusions

Determination of abamectin by gas chromatography was successfully used to assess the efficiency of degradation of the pesticide by the photo-Fenton process.

The photo-Fenton process was shown to be an effective treatment for water and effluents contaminated with abamectin, achieving a high removal rate of 70% of the chemical after 60 minutes of UV irradiation. Increasing the concentrations of Fe^{2+} and H_2O_2 enabled attainment of at least 60% pesticide mineralization after 180 minutes of irradiation.

Acknowledgments

The authors would like to thank CNPq, CAPES/REUNI, and FAPEMIG for financial support; Dr. José Roberto Guimarães (UNICAMP); Dr. Raquel F. Pupo Nogueira (UNESP) for assistance with the analytical procedures.

References

- [1] Z. Huang, Y. Li, B. Chen, and S. Yao, "Simultaneous determination of 102 pesticide residues in Chinese teas by gas chromatography-mass spectrometry," *Journal of Chromatography B*, vol. 853, no. 1-2, pp. 154–162, 2007.
- [2] I. K. Konstantinou, D. G. Hela, and T. A. Albanis, "The status of pesticide pollution in surface waters (rivers and lakes) of Greece. Part I. Review on occurrence and levels," *Environmental Pollution*, vol. 141, no. 3, pp. 555–570, 2006.
- [3] A. J. Dos Santos Neto and M. E. P. B. De Siqueira, "Analysis of organophosphorus pesticides in water using SPE C18 disks and gas chromatography: evaluation of Furnas dam contamination," *Química Nova*, vol. 28, no. 5, pp. 747–750, 2005.
- [4] M. J. Cerejeira, P. Viana, S. Batista et al., "Pesticides in Portuguese surface and ground waters," *Water Research*, vol. 37, no. 5, pp. 1055–1063, 2003.
- [5] E. Maloschik, A. Ernst, G. Hegedus, B. Darvas, and A. Székács, "Monitoring water-polluting pesticides in Hungary," *Microchemical Journal*, vol. 85, no. 1, pp. 88–97, 2007.
- [6] F. P. Carvalho, "Agriculture, pesticides, food security and food safety," *Environmental Science and Policy*, vol. 9, no. 7-8, pp. 685–692, 2006.
- [7] N. D. Uri, "A note on the development and use of pesticides," *Science of the Total Environment*, vol. 204, no. 1, pp. 57–74, 1997.
- [8] Joint FAO/WHO Food Standards Program, Codex Committee on Pesticide Residues, CX/PR 97/9 pp. 159, 1997.
- [9] M. B. Kralj, P. Trebše, and M. Franko, "Applications of bioanalytical techniques in evaluating advanced oxidation processes in pesticide degradation," *Trends in Analytical Chemistry*, vol. 26, no. 11, pp. 1020–1031, 2007.

- [10] R. Andreozzi, V. Caprio, A. Insola, and R. Marotta, "Advanced oxidation processes (AOP) for water purification and recovery," *Catalysis Today*, vol. 53, no. 1, pp. 51–59, 1999.
- [11] V. Claret Dos Santos and M. M. Kondo, "TiO₂ immobilized onto concrete: chloroform and phenol photodegradation," *Química Nova*, vol. 29, no. 2, pp. 251–255, 2006.
- [12] M. Klavarioti, D. Mantzavinos, and D. Kassinos, "Removal of residual pharmaceuticals from aqueous systems by advanced oxidation processes," *Environment International*, vol. 35, no. 2, pp. 402–417, 2009.
- [13] D. Hermosilla, M. Cortijo, and C. P. Huang, "Optimizing the treatment of landfill leachate by conventional Fenton and photo-Fenton processes," *Science of the Total Environment*, vol. 407, no. 11, pp. 3473–3481, 2009.
- [14] J. J. Pignatello, E. Oliveros, and A. MacKay, "Advanced oxidation processes for organic contaminant destruction based on the fenton reaction and related chemistry," *Critical Reviews in Environmental Science and Technology*, vol. 36, no. 1, pp. 1–84, 2006.
- [15] R. F. Pupo Nogueira, A. G. Trovó, M. R. A. Da Silva, R. D. Villa, and M. C. De Oliveira, "Fundamentals and environmental applications of Fenton and photo-Fenton processes," *Química Nova*, vol. 30, no. 2, pp. 400–408, 2007.
- [16] J. J. Pignatello, "Dark and photoassisted Fe³⁺-catalyzed degradation of chlorophenoxy herbicides by hydrogen peroxide," *Environmental Science and Technology*, vol. 26, no. 5, pp. 944–951, 1992.
- [17] R. F. Pupo Nogueira and J. R. Guimarães, "Photodegradation of dichloroacetic acid and 2,4-dichlorophenol by ferrioxalate/H₂O₂ system," *Water Research*, vol. 34, no. 3, pp. 895–901, 2000.
- [18] J. A. Herrera-Melián, E. Tello Rendón, J. M. Doña Rodríguez et al., "Incidence of pretreatment by potassium permanganate on hazardous laboratory wastes photodegradability," *Water Research*, vol. 34, no. 16, pp. 3967–3976, 2000.
- [19] E. Balanosky, F. Herrera, A. Lopez, and J. Kiwi, "Oxidative degradation of textile waste water. Modeling reactor performance," *Water Research*, vol. 34, no. 2, pp. 582–596, 2000.
- [20] T. Maezono, M. Tokumura, M. Sekine, and Y. Kawase, "Hydroxyl radical concentration profile in photo-Fenton oxidation process: generation and consumption of hydroxyl radicals during the discoloration of azo-dye Orange II," *Chemosphere*, vol. 82, pp. 1422–1430, 2010.
- [21] M. Pérez-Moya, M. Graells, G. Castells et al., "Characterization of the degradation performance of the sulfamethazine antibiotic by photo-Fenton process," *Water Research*, vol. 44, no. 8, pp. 2533–2540, 2010.
- [22] O. Rozas, D. Contreras, M. A. Mondaca, M. Pérez-Moya, and H. D. Mansilla, "Experimental design of Fenton and photo-Fenton reactions for the treatment of ampicillin solutions," *Journal of Hazardous Materials*, vol. 177, no. 1–3, pp. 1025–1030, 2010.
- [23] V. J. P. Vilar, E. M. R. Rocha, F. S. Mota, A. Fonseca, I. Saraiva, and R. A. R. Boaventura, "Treatment of a sanitary landfill leachate using combined solar photo-Fenton and biological immobilized biomass reactor at a pilot scale," *Water Research*, vol. 45, no. 8, pp. 2647–2658, 2011.
- [24] N. Klammerth, L. Rizzo, S. Malato, M. I. Maldonado, A. Agüera, and A. R. Fernández-Alba, "Degradation of fifteen emerging contaminants at µg L⁻¹ initial concentrations by mild solar photo-Fenton in MWTP effluents," *Water Research*, vol. 44, no. 2, pp. 545–554, 2010.
- [25] M. R. A. Silva, A. G. Trovó, and R. F. P. Nogueira, "Degradation of the herbicide tebuthiuron using solar photo-Fenton process and ferric citrate complex at circumneutral pH," *Journal of Photochemistry and Photobiology A*, vol. 191, no. 2–3, pp. 187–192, 2007.
- [26] M. R. A. Silva, W. Vilegas, M. V. B. Zanoni, and R. F. Pupo Nogueira, "Photo-Fenton degradation of the herbicide tebuthiuron under solar irradiation: iron complexation and initial intermediates," *Water Research*, vol. 44, no. 12, pp. 3745–3753, 2010.
- [27] M. M. Kondo, K. U. C. G. Leite, M. R. A. Silva, and A. D. P. Reis, "Fenton and photo-fenton processes coupled to uasb to treat coffee pulping wastewater," *Separation Science and Technology*, vol. 45, no. 11, pp. 1506–1511, 2010.
- [28] M. Ribani, C. B. Grespan Bottoli, C. H. Collins, I. C. S. Fontes Jardim, and L. F. Costa Melo, "Validation for chromatographic and electrophoretic methods," *Química Nova*, vol. 27, no. 5, pp. 771–780, 2004.
- [29] J. Hernández-Borges, L. M. Ravelo-Pérez, E. M. Hernández-Suárez, A. Carnero, and M. A. Rodríguez-Delgado, "Analysis of abamectin residues in avocados by high-performance liquid chromatography with fluorescence detection," *Journal of Chromatography A*, vol. 1165, no. 1–2, pp. 52–57, 2007.
- [30] R Development Core Team, *R: A Language and Environment for Statistical Computing*, R Foundation for Statistical Computing, Vienna, Austria, 2009.
- [31] R. F. P. Nogueira, M. C. Oliveira, and W. C. Paterlini, "Simple and fast spectrophotometric determination of H₂O₂ in photo-Fenton reactions using metavanadate," *Talanta*, vol. 66, no. 1, pp. 86–91, 2005.
- [32] H. Diserens and M. Henzelin, "Determination of abamectin residues in fruits and vegetables by high-performance liquid chromatography," *Journal of Chromatography A*, vol. 833, no. 1, pp. 13–18, 1999.
- [33] A. I. Valenzuela, D. S. Popa, M. J. Redondo, and J. Mañes, "Comparison of various liquid chromatographic methods for the analysis of avermectin residues in citrus fruits," *Journal of Chromatography A*, vol. 918, no. 1, pp. 59–65, 2001.
- [34] M. Danaher, L. C. Howells, S. R. H. Crooks, V. Cerkvenik-Flajs, and M. O'Keeffe, "Review of methodology for the determination of macrocyclic lactone residues in biological matrices," *Journal of Chromatography B*, vol. 844, no. 2, pp. 175–203, 2006.
- [35] M. D. Hernando, J. M. Suárez-Barcena, M. J. M. Bueno, J. F. García-Reyes, and A. R. Fernández-Alba, "Fast separation liquid chromatography-tandem mass spectrometry for the confirmation and quantitative analysis of avermectin residues in food," *Journal of Chromatography A*, vol. 1155, no. 1, pp. 62–73, 2007.
- [36] M. Mushtaq, A. C. Chukwudebe, C. Wrzesinski, L. R. S. Allen, D. Luffer-Atlas, and B. H. Arison, "Photodegradation of emamectin benzoate in aqueous solution," *Journal of Agricultural and Food Chemistry*, vol. 46, no. 3, pp. 1181–1191, 1998.
- [37] A. Kamel, S. Al-Dosary, S. Ibrahim, and M. Asif Ahmed, "Degradation of the acaricides abamectin, flufenoxuron and amitraz on Saudi Arabian dates," *Food Chemistry*, vol. 100, no. 4, pp. 1590–1593, 2007.
- [38] R. F. P. Nogueira, M. R. A. Silva, and A. G. Trovó, "Influence of the iron source on the solar photo-Fenton degradation of different classes of organic compounds," *Solar Energy*, vol. 79, no. 4, pp. 384–392, 2005.
- [39] J. S. Park, K. H. Kim, G. J. Kwon et al., "Development of small and efficient ozone generation using corona discharge," *Korus-Physics*, vol. 1, pp. 282–284, 2001.

- [40] Y. Sun and J. J. Pignatello, "Photochemical reactions involved in the total mineralization of 2,4-D by $\text{Fe}^{3+}/\text{H}_2\text{O}_2/\text{UV}$," *Environmental Science and Technology*, vol. 27, no. 2, pp. 304–310, 1993.
- [41] E. Neyens and J. Baeyens, "A review of classic Fenton's peroxidation as an advanced oxidation technique," *Journal of Hazardous Materials*, vol. 98, no. 1–3, pp. 33–50, 2003.
- [42] R. Venkatadri and R. W. Peters, "Chemical oxidation technologies: ultraviolet light/hydrogen peroxide, Fenton's reagent, and titanium dioxide-assisted photocatalysis," *Hazardous Waste and Hazardous Materials*, vol. 10, no. 2, pp. 107–149, 1993.
- [43] R. Bauer, G. Waldner, H. Fallmann et al., "The photo-fenton reaction and the TiO_2/UV process for waste water treatment—novel developments," *Catalysis Today*, vol. 53, no. 1, pp. 131–144, 1999.
- [44] W. C. Paterlini and R. F. P. Nogueira, "Multivariate analysis of photo-Fenton degradation of the herbicides tebuthiuron, diuron and 2,4-D," *Chemosphere*, vol. 58, no. 8, pp. 1107–1116, 2005.
- [45] R. G. Zepp, B. C. Faust, and J. Holgné, "Hydroxyl radical formation in aqueous reactions (pH 3–8) of iron(II) with hydrogen peroxide: the photo-fenton reaction," *Environmental Science and Technology*, vol. 26, no. 2, pp. 313–319, 1992.
- [46] H. Fallmann, T. Krutzler, R. Bauer, S. Malato, and J. Blanco, "Applicability of the Photo-Fenton method for treating water containing pesticides," *Catalysis Today*, vol. 54, no. 2–3, pp. 309–319, 1999.